Bite or flight: stable isotope analysis of teeth to reconstruct hominin prey lifeways in the Middle Pleistocene of France and Israel.

Marian Bailey

BA Archaeology

A thesis submitted in partial requirements for the degree of Master of Archaeology and Heritage Management, Department of Archaeology, Faculty of Education, Humanities and Law, Flinders University, July 2018

Declaration

I certify that this thesis does not incorporate without acknowledgment any material previously submitted for a degree or diploma in any university; and that to the best of my knowledge and belief it does not contain any material previously published or written by another person except where due reference is made in the text.

Name: Marian Bailey

Signature: ______________________________

Date: _28/10/18_________________________________

Abstract

Hominin predation behaviour is explored in this thesis through the isotope analysis of hominin prey teeth. The Middle Palaeolithic sites of Holon and Payre are the two sites of focus in this research. Payre is located in the Ardèche region of France and dates from MIS 5 to 7 (Moncel and Condemi 2007) and has *Homo neanderthalensis* remains associated with several of the layers. Holon is in Israel and has been dated to ca. 200,000 BP (MIS 7) (Porat et al. 1999). The site has been identified as a palimpsest open air site and has multiple scavenging events associated with it. While no *Homo erectus* remains have been found at the site, the timing, location and site formation are all indicative of a *H. erectus* site.

The use of stable isotopes to identify behaviours of hominins has often focused on the tissues of the hominins themselves. These are unfortunately quite rare, and analysis is not always a feasible option. Another increasingly popular approach is the analysis of the tissues of hominins' prey. In this study the enamel and dentine of 14 *Bos primigenius* teeth from the site of Payre and 4 *Palaeoloxodon* sp., 3 *Dama Dama* and 3 *Bos primigenius* teeth from Holon were analysed for strontium, oxygen and carbon isotope concentrations.

The results of the analysis indicated a far greater level of mobility for the Payre animals when compared to the Holon animals from the same period. Overall the mobility of prey at Payre were variable, with the distance changing alongside the climate. The results of the diet analysis indicated a diet primarily composed of C4 vegetation. The prey at Holon showed a far lower range of mobility and remained almost entirely within 1.2km of the site. Like the animals at Payre, the prey ate C4 vegetation. The results and interpretations drawn from the results are similar to the commonly held views about *H. neanderthalensis* or *H. erectus* hunting behaviours. The more mobile prey at Payre, which were reactive to climate were hunted. The more sessile prey at Holon were more likely

scavenged, although due to the location of the site the hominins there likely chose the site for its strategic scavenging potential, rather than choosing to scavenge because they could not hunt.

Contents

List of Figures

List of Tables

Acknowledgments

I must first thank my supervisor Dr Ian Moffat, for always being incredibly supportive and for all his help during the writing (and often lack of writing) of this thesis. Ian – you were ridiculously generous with your time, teaching me new skills and giving me numerous fun and interesting opportunities during my masters – I am so appreciative of this.

Thank you to my collaborators, without whom the project for this thesis would never have existed; Dr Marie-Hélène Moncel and Dr Liora Kolska – who were always ready to give me advice and send words of encouragement. Thank you also to Dr Anthony Dosseto and Mark Rollog for all their help with the chemistry side of things, Dr Antigone Uzunidis for identifying the Payre teeth, and Dr Mick Morrison for being so generous with extensions. Thank you also to Apostolos Sarris and the IMS-FORTH lab in Rethymno, Crete who gave me an amazing space to finish the writing of this thesis.

Thank you to my friends and family who supported me through numerous health issues and existential crises, especially my parents who always answered the phone to listen to me stress about the same exact thing over, and over again.

Special mentions go to the whole Archaeometry team for always reading my drafts, Chelsea Wiseman who was somehow always awake at 2am ready to chat, Belinda Duke for tea, hugs and comfort, Jarrad Kowlessar for his thoughtful and levelheaded analysis of problems, Kleanthis Simyrdanis for all his advice, hugs, and cooking and of course Jessie Farrer-Smith and James Cassidy, who I miss dearly but were always there for me when I needed them. I am also extremely grateful to the Australian Federation of University Women (AFUW) for their generous Diamond Jubilee Bursary, which alleviated much financial hardship while I was writing this thesis.

Chapter One: Introduction

1.1 Introduction and Aims

The behaviours of early hominins such as *Homo neanderthalensis* and *Homo erectus* have been a matter of debate for many decades. Gaining fame with the seminal 'Man the Hunter' symposium in 1966, many new models and theories were developed in order to explain how these early hominins behaved (Isaac 1978; 1983; Binford 1981; Brain 1981; Blumenschine et al. 1994; Mitchell and Lane 2013). Most of these studies and the subsequent debates surrounding them have focused on using zooarchaeology and lithic technology as the primary source of analysis. However, in a more recent research (Britton 2009, Rivals et al. 2009) determining the behaviours of these hominins' prey has become a greater focus. The identification and analysis of prey behaviours (such as their diet and mobility) adds nuance to understanding how hominin predations behaviours may change in reflection to prey behaviours.

The use of stable isotopes in archaeological research provides alternative insights into the behaviours of archaeological prey. Fauna is a major component of archaeological sites, yet it can only be partially understood by zooarchaeology techniques. While knowledge about the diet and mobility of the modern counterparts of prey species is sometimes known, the descendants of many ancient species are now domesticated and so have completely different mobility or dietary patterns. Some species are extinct completely. The climate and vegetation during the lifetimes of these archaeological specimens was often different from the current climate, which may have changed the distance and vector of mobility and diet for many individuals (Britton et al. 2012). Considering this, the analysis of stable isotopes such as strontium, oxygen and carbon can be used together to create a detailed image of an individual animal's behaviour, where zooarchaeological analysis on its own could not (Britton et al. 2009).

Most commonly, the material used in analyses are bioapatites. Dental tissue is one such example – it forms incrementally and remains resistant to chemical and structural alteration, although the dentine is more vulnerable than enamel to post burial diagenesis (Lee-Thorp and Sponheimer 2003). Teeth often survive in the archaeological record due to this resistance to alteration and as such are a good candidate for stable isotope analysis. The analysis of the $^{87}Sr/^{86}Sr$ ratio in dental tissue can provide a detailed reflection of an individuals' geographic origin, mobility during amelogenesis and demonstrate whether the individual is local or non-local to that area (Lee-Thorp and Sponheimer 2003; Montogemery 2010; Widgar, Walker and Stockli 2010; Britton et al. 2011). Oxygen isotope analysis can determine the local palaeoclimatic conditions of an area, and the analysis of carbon can aid in determining the diet of an individual (Bryant, Lutz and Froelich 1994; Kohn et al. 1998; Tewari 2004; Britton et al 2009). Using this approach, the life histories of fauna can be more readily examined and insights into their ecology gained.

This research focuses on the Middle Palaeolithic sites of Payre (Ardèche, France) and Holon (Israel). Strontium, oxygen and carbon isotope analysis was undertaken on aurochs (*Bos Primigenius*), fallow deer (*Dama cf. mesoptamica*) and straight-tusked elephants (*Palaeoloxodon sp.*). The thesis aims to determine the diet, range and level of mobility of each individual, as well as further investigate the palaeoclimate during their lives. The two sites are very different, but both contain *Bos Primigenius* which are compared to investigate the impacts of climate on their mobility. Changes in climate over time and its impact on animal mobility are also investigated at the site of Payre, which contains several layers all containing remains of *Bos.*

Specifically, it will address the following questions:

1. To what extent are the prey at Holon and Payre local or non-local, and what is their distance and vector of mobility during amelogenesis?
2. Are there variations in mobility on an intra-species or inter-species level and are these differences the same between the two sites?

3. Do changes in mobility reflect changes in the paleoclimate over time? and
4. What inferences can be made about the potential predation behaviours of early hominins.

To answer these questions, stable isotope analysis was undertaken on 4 *Dama cf. mesoptamica*, 4 *Palaeoloxodon sp* and 3 *Bos Primigenius* specimens from Holon, and 14 *Bos Primigenius* (collected over multiple layers) from Payre. A review of the archaeological literature regarding hunting behaviours of hominins was synthesised and gaps in information that isotope analysis could fill were identified.

Figure 1. 1: Payre location in France.

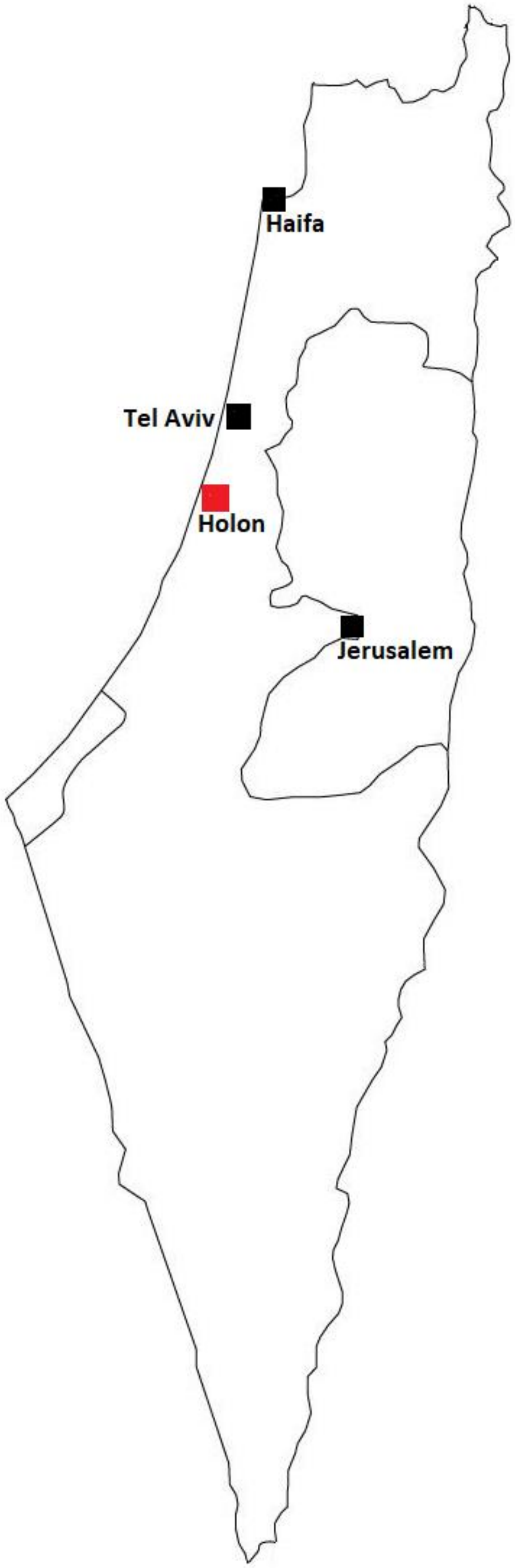

Figure 1. 2: Holon location in Israel.

1.1 Significance of Study

This study is significant because it is the first systematic investigation of the hunting capabilities of two different hominins (other than Moffat 2013), using isotope analysis on prey teeth. It is also the first longitudinal study of *Bos* mobility through time at the site of Payre. Isotope analysis has been undertaken at both Payre and Holon (Aubert et al. 2011; Benson et al. 2013; Moffat 2013; Bocherens et al. 2016), however neither site has had oxygen, carbon and strontium isotope analyses performed and compared on the same teeth. This thesis extends the research beyond a purely isotopic study and combines the archaeological models and theories of early hominin predation behaviours, with the isotope results from their prey. A novel approach for the samples at both Holon and Payre.

1.2 Thesis Outline

Chapter One outlines the aims, research questions and significance of thesis to the field of study.

Chapter Two provides background to the formation and function of both sites and reviews the geology and palaeoenvironments in both areas.

Chapter Three provides a comprehensive overview of the relevant literature surrounding *H. erectus* and *H. Neanderthalensis* who were associated with the sites and the theories that are surround them. This chapter also provides a background to isotope analysis and a review of palaeo-mobility and dietary studies pertinent to the research.

Chapter Four outlines the methodology used during the preparation of samples, the laboratory analysis and the subsequent processing of data.

Chapter Five summarises the results of the analysis using tables and graphs, further detail can be found in Appendix One.

Chapter Six is the discussion chapter and explains the strontium isotope analysis results. It compares the mobility of the different animals and compares species with species. It also examines how the palaeoclimate at the time would have impacted mobility and diet. Inferences about hominin hunting behaviours are made and a comparison of the archaeological sites is undertaken.

Chapter Seven provides a conclusion to the thesis, re-examining the research question and aims, considering the conclusions made from the results.

Chapter Two: Background

2.1 The archaeological site: Holon

Holon is an open-air site located on the coastal plain of Israel, south of Tel Aviv. Holon is late lower Palaeolithic site which has been dated to ca. 200,000 BP (MIS 7) (Porat et al. 1999). The site was excavated over a single period and has being dated and analysed in detail (Horwitz and Chazan 2007:181). Holon is unique in that it is currently the only site of this period and region which contains faunal remains and lithics in association with each other.

Holon is located approximately 2 km south of Tel Aviv, and 6 km east of the present-day coastline. It was discovered first in 1951 and was excavated in preparation for an industrial development. Today, the site is covered by a factory and a parking lot. The excavation of Holon was undertaken over three excavation seasons, in 1963, 1964 and 1971, by Dr Tamar (Yisraeli) Noy. The estimated area of the excavation area varies slightly between publications (Chazan 2007; Noy and Isaar 1971; Porat 1999 and Yizraeli 1967). The site is found within the Pleistocene aged sedimentary sequences of the coastal plain of Israel (Malinsky-Buller 2014), and these sequences are composed of "alternating layers of unconsolidated sands, cemented carbonate-rich aeolianites (kurkar) and mature, non-calcereous red Mediterranean sandy loam soil (hamra)" (Malinsky-Buller 2014:485). The site itself was formed in a light grey clay matrix, which was created when the Ayalon River was blocked by incursive dunes, and a marsh developed along its outlet (Chazan and Horwitz 2006; Nester and Chazan 2007). According to Gvirtzman et al. (1984; 1996) the cyclic hamra and kurkar units are correlated with sea level or climatic changes. The excavation by Noy (Yizraeli 1967) revealed a sequence of beds of variable thicknesses, and in total was comprised of five distinct geological strata. Only one stratum (C) contained archaeological material, which included lithic remains and animal bones (Chazan et al. 2001; Yizraeli 1967). This artefact bearing deposit is characterised as a light grey, sandy clay layer (Chazan et al. 2001), reaching a maximum thickness of 1.70 m and lays horizontal, at an elevation of just over 38 m above sea level (Horwitz and Chazan 2016). The other layers, from bottom to top are as follows; Stratum E, the base of the sequence is a kurkar (cemented sand) deposit and was only partially exposed. Stratum D is a hamra (red sandy loam soil) and approximately c. 0.5 m thick, Stratum B is a dark clay layer reaching a maximum thickness of 0.5 m, and the sequence is capped by Stratum A, another hamra deposit, but reaching up to 2m in thickness (Chazan et al. 2001, Yizraeli 1967; Porat et al. 1999 and Malinsky-Buller 2014). Stratum C was further divided into three sub-layers. These sub-layers were identified by Yizraeli (1967) as being; Top: containing many chalk incrustations; Middle: very clayey with fewer chalk incrustations but a high density of archaeological material, and Bottom: sandier, with few archaeological remains (Yizraeli 1967; Horwitz and Chazan 2016). Although questions have been raised over whether the site contains more than the single archaeological level (Bar Yosef 1994; 1998), differences between the faunal and lithic materials from all the excavation seasons were tested (Horwitz and Chazan 2016) and variance mean ratio tests were undertaken, demonstrating that the lithic and bone remains were not randomly distributed, but spatially associated (Horwitz and Chazan 2016).

2.1.1 Chronology

Optically stimulated luminescence dating was undertaken on sediments taken from two pits excavated near the original excavation sites (Porat et al. 1999). These pits were correlated to the site based on their geology, shown in figure 2.1. The following sequence goes from the top of the section to the base: top palaeosol was given an age of 81±8 kyr and the lower palaeosol 150±13 kyr. The archaeological horizon was aged 198±22 kyr and the lower kurkar level was 240±17 ka (Porat et al. 1999; 2002; Porat 2007). ESR dating was also performed on two auroch (*Bos primigenius*) teeth from the site providing dates of 197±11 and 210±17 kyr, respectively (Porat 2007*).* Consequently, the ESR and OLS methods both provided an age for the occupation of Holon, falling within the end of Marine Isotope Stage (MIS) 7, ~200 kyr (Porat et al. 2002; Porat 2007).

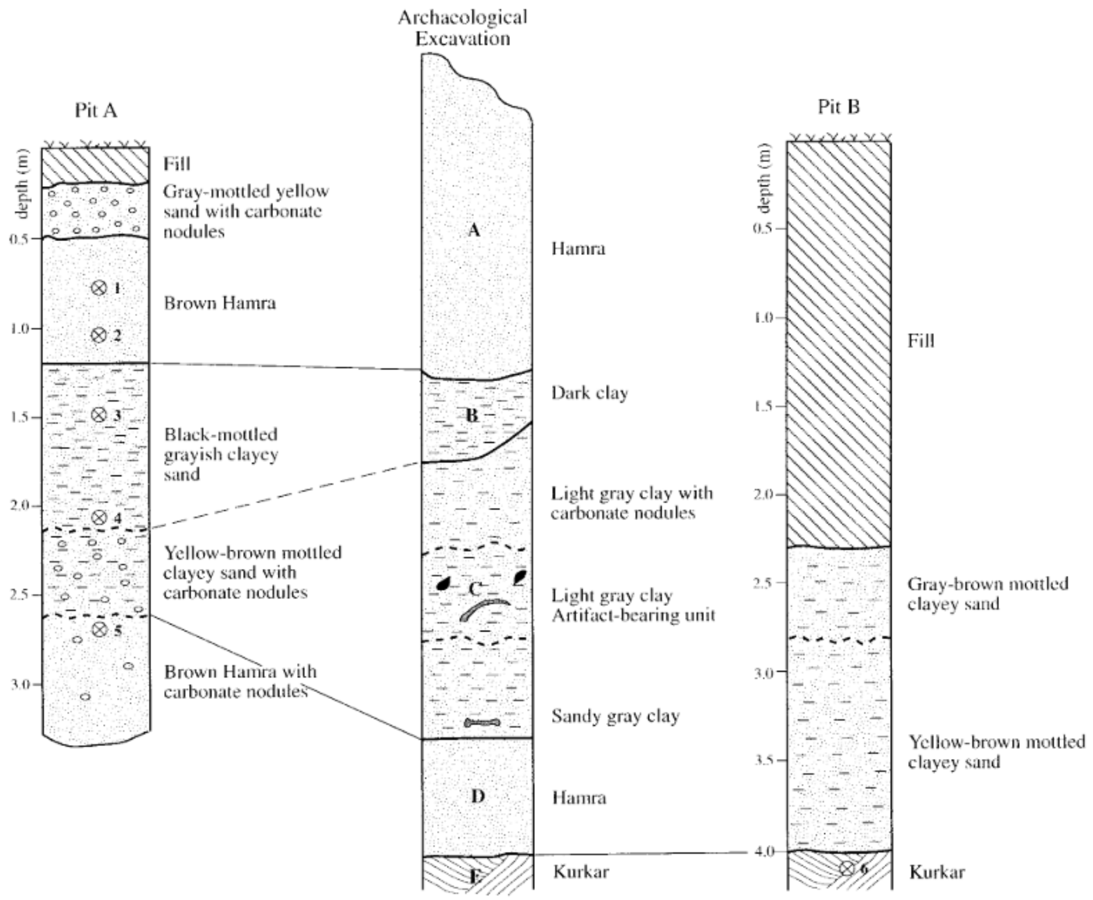

Figure 2. 1: Correlating sections of the excavation with the two test pits (Porat et al. 1999:331).

2.1.2 Fauna

There were 1,569 bones recovered during excavations at Holon, however less than half (573 or 36.5%) were able to be identified to a species level (Horwitz and Chazan 2016). The fauna that could be identified included a wide spectrum of Holarctic taxa, including fallow deer ,*Dama dama cf. meopotamica* (NISP = 247, MNI = 5), aurochs, *Bos Primigenius*, (NISP = 162, MNI = 3*)* and straight-tusked elephant, *palaeoloxodon antiquus* (NISP = 120, MNI = 6). Smaller numbers of hippopotamus, gazelle, red deer, wild boar and fresh water turtle were also found (Chazan and Horwitz 2006). While the data on mortality for *Dama* and *Bos* are restricted due to the limited number of bones and teeth that could be aged, *Palaeoloxodon* was able to show a mortality curve resulting from natural death (Chazan and Horwitz 2006).

The Holon assemblage has been interpreted as a palimpsest site, caused by repeated hunting events (Chazan and Horwitz 2006; 2007) – although the possibility remains that the lithic and faunal assemblage pattern could have been created through 'repeated scavenging or carnivore-prey activities' (Monchot et al 2012:36). This interpretation was drawn from evidence including the cut marks, chop marks and conchoidal flake scars on 3.6% of bones in the assemblage (Horwitz and Monchot 2002; Chazan and Horwitz 2006; Horwitz and Chazan 2016). Another 3% of the bones showed evidence of gnaw marks, pits and puncture holes, likely the result of carnivore and rodent damage, and no bones were found showing evidence of burning (Horwitz and Chazan 2016). Utility indices were calculated for *Bos* and *Dama* by Lyman (1994) and both showed a negative utility curve, with the majority of skeletal elements having a moderate to low utility value, meaning the skeletal elements with high utility values had been removed (Horwitz and Chazan 2016). This is indicative of a kill or scavenge site. Correspondence analysis was also undertaken on the faunal taxa and skeletal elements (Chazan et al 2007; Monchot et al 2012), and the results are indicative of 'discrete scavenge/kill locations within the site' (Horwitz and Chazan 2016).

Considering the wide variety of taxa found, as well as the high MNI count compared to the small size of assemblage (that was identifiable), Chazan and Horwitz (2006) acknowledge Holon could have potentially been a multiple mortality or scavenging location, rather than a hunted assemblage (Chazan and Horwitz 2006). As they point out however, this interpretation does not explain the concentration of multiple carcasses around the site.

2.1.3 Lithics

The three excavation seasons at Holon revealed 1468 lithic items, including 792 unretouched flakes, 387 retouched flakes, 100 handaxes, and 39 choppers (Monchot et al. 2012). Research by Chazan (2007c) indicates that the knapping of flakes occurred onsite, but the handaxes and choppers were produced offsite. The assemblage contains very few flakes that are smaller than 2cm, and Chazan and Horwitz (2006) suggest this is most likely due to selective retrieval during the excavation. There was retouch on approximately 50% of the flakes, with both sidescrapers and Nahr Ibrahim truncations being identified. Nahr Ibrahim truncations are truncated-faceted pieces, and their frequency in the Holon assemblage is considered unique (Horwitz and Chazan 2016). Correspondence analysis was also undertaken on the lithic assemblage, and it showed that the lithics were highly associated, except for bifaces (Horwitz and Chazan 2016; Chazan et al 2007; Monchot et al 2012).

2.1.4 Site Function

The site of Holon has been interpreted to be a palimpsest site, where multiple discreet events would have taken place in adjacent areas, or even superimposed over earlier activities. These events or activities could have included hunting or scavenging, or a mixture of both (Chazan and Horwitz 2006; Horwitz and Chazan 2007). The focus of hominin activity at Holon appears associated with an ephemeral fresh water marsh. Horwitz and Chazan (2016) suggest that apart from the obvious evidence of activities such as hunting, collecting plants and collecting raw material for knapping that occur near to the site, there is evidence of a linkage between Holon and other sites that were the location of biface manufacture (Horwitz and Chazan 2016). The location of Holon, laying near to a river system, suggests its location would have been a resource focus for not only hominins, but a variety of animal species. It is for this reason that Monchot and Horwitz (2007a,b) suggest that some of the bones found at the site, despite their association with the lithics, may not have been culturally deposited but instead the result of carnivore activity.

2.2 The archaeological site: Payre

Payre is located in the southeast of France, opening to the southeast on a cliff approximately 60m above the Payre river, which is a tributary of the large Rhône river (Moncel and Condemi 2007). It is situated in the Jurassic and Cretaceous formations found on the western bank of the Middle Rhône Valley (Valladas et al. 2009) and is a part of the karstic complex (Debard 1988). Payre has a long sequence, dating from MIS 5 to 8, which is unusual for that part of France, where sites dating to MIS 5 and 8 are rarely found (Moncel and Condemi 2007). The long continuous occupation of this valley has been suggested as being a result of it being further from glaciated areas (Moncel and Condemi 2007). The site of Payre has been studied extensively, with excavations of 30-70m^2 of the 80m^2 site starting in 1990 (Combier 1967; Moncel *et al.* 2002; Moncel 2003, Moncel 2004; Moncel and Condemi 1996, 1997).

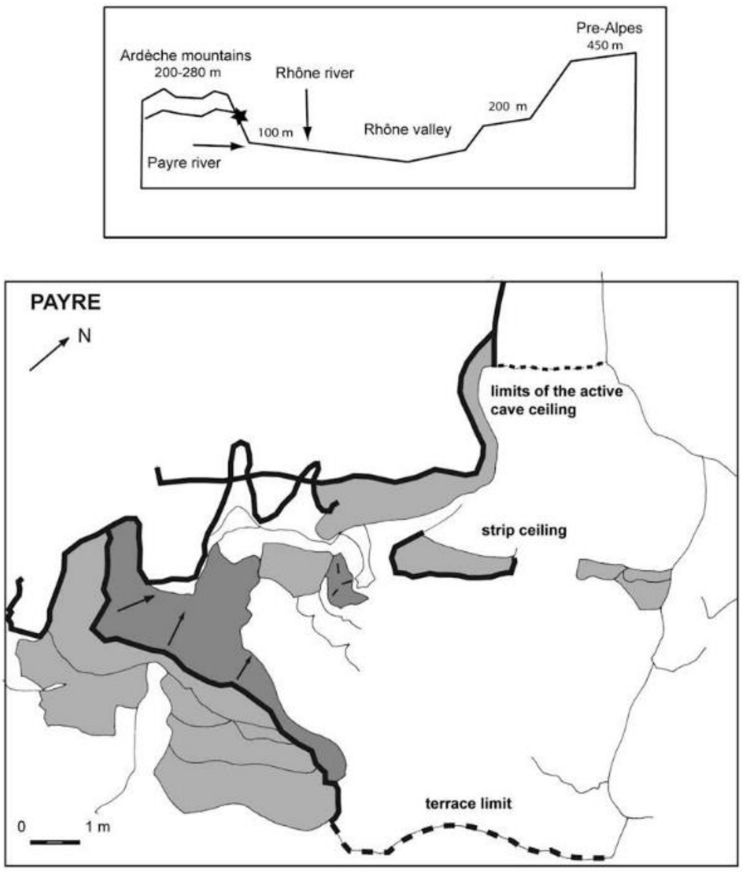

Figure 2. 2: Morphology of Payre (Moncel et al. 2009: 1895).

2.2.1 Site sequence

The site is composed of a 5-m thick sequence, which is broken into 5 main layers (from bottom to top – G, F, E, D-C and B-A), and further divided into sub-layers – see Fig 2.3 (Moncel et al. 2009:1894).

The absolute chronology is the site is uncertain as there are large errors on the dates (Valladas et al. 2008). The sequence summarised from Moncel and Condemi (2007) is as follows:

Base – stalagmite floor formed during MIS 8 -7, on both sides of the cave.

Level G – 80cm thickness divided into 6 stages. Primarily composed of an orange clay, with large numbers of stones and slabs, becoming brecchia. Level G yielded the majority of the human remains, corresponding to two occupations. TL dates give an average age of 232 ± 15 ka and U/Th and ESR ages between 235 ± 18 ka and 169 ± 13 ka (Valladas et al. 2008; Moncel et al. 2009).

Level F – 100cm thickness, with 7 stages composing of grey sediment and beds of rubble and clay. There are alternating occupations of human and carnivores (mainly bear) in the layers. TL dates give an age of 231 ± 27 ka and U/Th and ESR ages between 235 ± 18 ka and 169 ± 13 ka (Valladas et al 2008; Moncel et al. 2009).

Level E – It is rich in stones and large blocks and appears to be the result of the cave ceiling collapse. The collapse opened a cavity and ESR and U/TH dates suggest it occurred at the end of MIS 6 or start of MIS 5 (Moncel et al 2009:1895)

Levels C and D – the last period of sedimentation after the cave ceiling collapse. At this point the cave was now more like small open air shelters. The deposits of level D were given an average age of 144 ± 11 ka, or the end of MIS 6/ start of MIS 5 (Valladas et al 2008; Moncel et al. 2009).

Levels A and B – these are the surface levels and do not contain any archaeological remains. They are formed from the sediment from the local and active karst (Moncel et al. 2009).

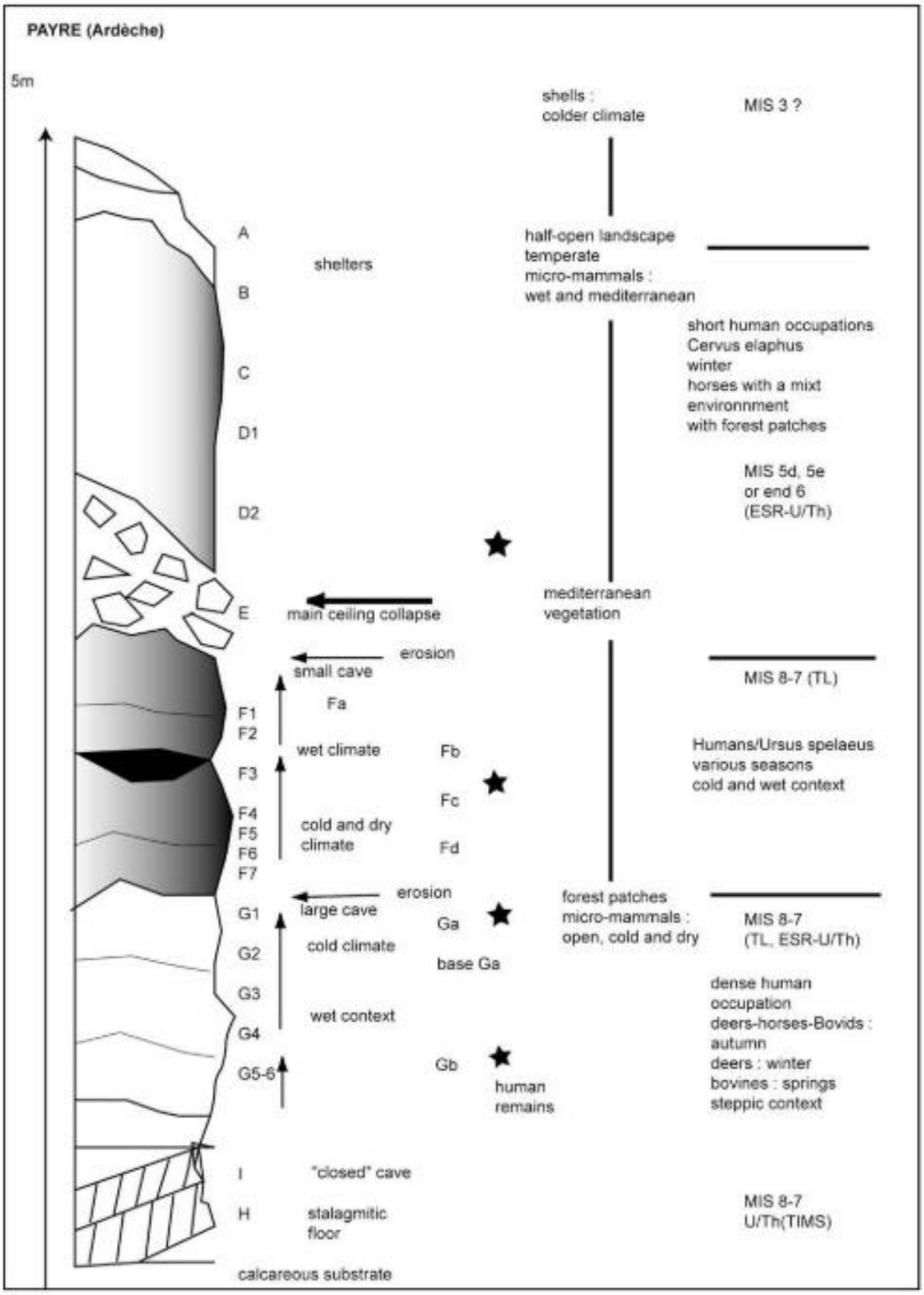

Figure 2. 3: “Synthesis of the Payre sequence with palynological, faunal, and radiometric data related to the type of human occupation” (Moncel et al. 2009:1895).

2.2.2 Hominins

The hominin remains at Payre were identified as Neanderthal. Neanderthal populations appeared to regularly inhabit this site during MIS 8-7 to MIS 5 (Rivals et al. 2009: 1070). Evidence of hominin occupation was identified in level G, F, D and C. Charcoal and evidence of hearth emptying was found in layers G, F and D (Moncel and Chacon 2007). Rivals et al (2009) suggest that the Neanderthals were coming back to the site regularly during the temperate climate periods (MIS 7 and 5) and even when the aspect of the site changed (the rock fall) they still returned, indicating the location was more important than the general morphology of the cave (Rivals et al. 2009: 1071).

2.2.3 Fauna

There was an abundance of different faunal types found through the various levels at Payre including horse (*Equus ferus)*, bovid (*Bos Primigenius, Hemitragus bonali*), cervid (*cervus elaphus, Capreolus* capreolus), rhinoceros (*Dicerorhinus hemitoechus, D.* kirchbergensis), cave bears (*Ursus* spelaeus) and elephant. According to Bocherens et al (2016:227) the list of fauna suggests a climate that is mildly cold and has different biotypes (forests, wooded prairie and open-steppe) environments. Equids, cervids and bovines were hunted, with equids not being hunted during the summer, and cervids and bovines not being hunted during the winter (Rivals et al. 2009:1072). Levels G and F appear to have a positive correlation to short or annual occupations focused on species specific hunting, as seen in level D and the hunting of *C. elaphus* (Rivals et al. 2009:1072).

2.2.4 Lithics

350 lithics were excavated from several archaeological levels at Payre – these layers also contained human skeletal remains (Moncel et al. 2009). The types of lithics commonly found at Neanderthal sites are convergent tools, which Bordes (1961) describes as points and convergent scrapers. Payre contains a diverse range of tools, primarily pseudo-Levallois flakes, and these tools fall into the classification of points, convergent scrapers and *de´jete´* convergent scrapers, as well as tools that are retouched or partially retouched on the tip point or retouched to make a tool thinner (Moncel et al. 2009: 1895). It is believed that the convergent tools could have been mounted on the shafts of wooden spears using haftings (Callow and Cornford 1986; Hardy 2004; Villa et al. 2009). The use of these tools appears to be primarily related to hunting strategies, as studies show the importance of meat in the Neanderthal diet (Bocherens et al. 1999) and evidence of butchering has been

discovered (Lumley et al. 2004). The lithic material, the identified location of materials, and the various types of tools across the levels suggest that the subsistence behaviour was diversified between levels.

2.3 Palaeoenvironment

The Marine Isotope Stages (MIS) is a timescale that represents glacial or interglacial periods in the Earth's palaeoclimate. The MIS were originally based on the glacial record in the Alps and then confirmed by deep sea cores (Langway et al. 1985; Johnsen et al. 1992; Grootes et al. 1993). Some stages are subdivided, with stages within a MIS being warmer or cooler. Pollen records can also be used to determine patterns of vegetation across a spatial scale. As the pollen data is a record of the vegetation, it is also sensitive to factors that affect vegetation such as the climate (Webb and Bartlein 1992).

2.3.1 Holon

The artefact baring horizon at Holon has been placed at the end of MIS 7, 198±22 kyr by Porat et al. (2002). During the MIS 7 Israel had a variable climate. Analysis of sapropels by Cheddadi and Rossignol-Strick (1995) showed a transition from a warm humid climate, to a more arid climate, with the Mediterranean forest being replaced by semi-desert vegetation. Speleothem studies indicate humidity and higher rainfalls before the transition to a more arid environment (Vaks et al. 2006).

2.3.2 Payre

The different levels have all been associated with particular environmental conditions, either through pollen analysis, through analysis of the abundance of fauna that characterise specific ecological niches or through knowledge of the characteristics of the MIS stage they fall within. The three main occupation levels (G, F, and D) fall within MIS 8-7 and MIS 5d/5e or end of MIS 6. These are considered temperate and humid interstadial phases and the MIS 5e was the warmest period in 730 ka (Gamble 1992, Moncel et al. 2009: 1895). The environment across the study period broadly would have included temperate forested areas as well as open spaces (Laville et al. 1980). The correlation of MIS and vegetation based on cores from the Massif Central (Reille et al. 1998; Reille and de Beaulieu 1990) indicate that MIS 7e was primarily deciduous forest, 7d was steppe with some shrub, 7c was Montane/*Pinus* forest, 7b was steppe, 7a was open mixed oak forest, 6 was steppe, 5e was dense woodland and 5d was steppe. There was dense human occupation in these layers (G, F and D) as well as an abundance of herbivores, including deer (*Cervus elaphus*), horses (*Equus* sp.) and bovids (*Bos primegenius*). The carnivores are most abundant in level F, particularly bears (*Ursus spelaeus*) (Moncel et al. 2009: 1895). In level D, there are rodents and avian remains which are indicative of a humid environment and an open, rocky landscape with a temperate climate (Moncel et al. 2009: 1895).

2.4 Geology

2.4.1 Holon

Israel is broadly broken into topographic zones which correspond to geological provinces; the coastal plain (young, unconsolidated sediment), the Judean Hills (Cretaceous carbonates), the Jordan Rift Valley and the Golan Heights (basalts) (Goldreich 1995). These zones run north-south. More specifically the geological provinces can be broken into the Southern Igneous Province, the Southern-Central Clastic Province, the Central Carbonate Province, the Northern Volcanic Province, and Coastal Sediments (Sneh et al. 1998). The coastal plain around where Holon is situated is primarily composed of sand and hamra (red soil) deposits, or kurkar (parallel calcareous aeolian sandstone ridges), with clay and silt running through it all (Zviely et al. 2009). The site of Holon itself is situated on Quaternary red sand and loam hamra (clay, silt and sand) sediment.

2.4.2 Payre

France, like Israel is also divided into a number of provinces; the Massif Central, the Aquitaine Basin (sedimentary rocks), the Rhône Valley (exposed sedimentary rocks) and the coastal sediments. The Massif Central is primarily granites and basalts (Duthou et al. 1984) with some poorly preserved carbonates (Pomeral 1980). The Aquitaine Basin is a large sedimentary basin that forms a triangular shape (Laborde 1961). Several different events have shaped the specific geologies within the basin which range from carbonate sediments (Pomeral 1980) to dolomitic marlstone and limestone (El Albani et al. 2005). The Rhône Valley was subject to change during the end of the Miocene. As such, there are sediments from a number of eras, such as Oligocene sediments, Middle and Late Miocene sandstones, Pliocene lacustrine marls and silt, pebbles and loess during the Quaternary (Bles and Gros 1991; Moffat 2013). The coastal sediments are primarily comprised of Lower Miocene carbonate and lacustrine sediments and Quaternary clastic sediments. The site of Payre is situated in the Middle Rhône Valley on an Upper Jurassic, marl, limestone and clay geology, and is part of the karstic complex.

Chapter Three: Literature Review

3.1 Hominins in this study: *Homo erectus*

There is a dearth of knowledge based on archaeological evidence surrounding *H. erectus* behaviour patterns. While their morphology, origins, and migration are well researched, researchers still can only theorise about their social behaviours and group dynamics. Undoubtedly the most debated aspect of Homo erectus are their hunting behaviours. Much has been postulated about hunting v scavenging, with a long history of paradigm shifts and evolving models (Isaac 1978; 1983; Binford 1981; Brain 1981; Blumenschine et al. 1994; Mitchell and Lane 2013) which will be explored later.

Homo erectus lived through the Pleistocene geological epoch, with fossil evidence dating to 1.9million years ago, to as recently as 35,000 years ago (Dennell 2003). The most commonly agreed upon origin and migration route, is from Africa, migrating through Eurasia, as far as Indonesia (Antón 2003; Dennell and Roebroeks 2005). According to the fossil record, *Homo erectus* was widely distributed, with fossils found originally in Africa, as well as Georgia, Indonesia, Vietnam, China and India (Haviland et al. 2007). While this may be agreed upon, the classification of *Homo erectus* is still in debate. Two main theories persist; the first is that *Homo erectus* and *Homo ergaster* are the same species (Dennell 2003; Klein 1999), therefore a direct ancestor of the hominins *Homo heidelbergensis,* Neanderthals, and *Homo sapiens*. Conversely, *Homo erectus* has been considered a separate, Asian species (Dennell and Roebroeks 2005; Klein 1999). A more recent debate, although quite controversial, began with the Dmanisi skulls in 2013 (Lordkipanidze et al. 2013), where some researchers suggesting that Homo erectus should also include *Homo ergaster*, *Homo rudolfensis*, as well as *Homo habilis* (Lordkipanidze et al. 2013). This theory came about as their occupation of the Dmanisi site has been dated to the same time, or slightly earlier than the fossil records in Africa (Ferring et al. 2011). This led to suggestions of their evolution in Eurasia, and migrating into Africa instead of the commonly accepted, other way round. Regardless the main debate still surrounds whether *Homo erectus* and *Homo ergaster* should be regarded as separate species (Frayer et al. 1993; Jelinek 1978; Weidenreich 1943).

According to Boehm (1999), *H. erectus* probably lived in similar social structures to some modern 'hunter-gatherer' societies, and likely hunted together. More recent data, analysed by Hatala et al. (2016:6) demonstrate that *Homo erectus* individuals were walking together at times in groups, and this is:

> *at the very least consistent with the hypotheses that Homo erectus had group composition and dynamic that could have supported the emergence of human-like social behaviors such as patterns of increased cooperation and sexually-divided foraging behavior* (Hatala et al. 2016:6)

This knowledge comes in light of decades of debate surrounding hominin hunting behaviours with the ideas of scavenging and hunting being argued furiously. The section 3.3 'theories and models related to hunting or scavenging behaviour' will outline the main arguments and models that makeup the debates.

3.2 Hominins in this study: Neanderthals

Homo neanderthalensis were a subspecies of ancient humans. *H. neanderthalensis* lived throughout Europe and moved into southwest and central Asia between 430,000 (Callaway 2016) to 35,000 – 40,000 years ago. (Higham et al.2014, Pinhase et al. 2011). *H. neanderthalensis* were found in Western Europe (below 55°N latitude), to Israel in the south and east to Southern Siberia (Hublin 2009). It is mostly agreed upon that *H. neanderthalensis* shared a common ancestor with *Homo sapiens* that is, *H*. *erectus* There is suggestion that of a *Homo heidelbergensis* being a transitional species (Mounier et al. 2009) however this is still debated (Hublin 2009, Leakey et al. 2012). Mellars (1996) describes *H. neanderthalensis* as having distinctive heavy, enlarged brow ridges, a flattened cranial vault and a large cranial capacity. In depth description of the biological features have been summarized by Stringer and Gamble (1993). *H. neanderthalensis* lived in primarily cool or cold environments (Hublin 2009) but their mobility is debated with suggestions they may have moved long distances during their lives, stayed within a limited area for hunting purposes, or that they stayed in one small area their whole life (Richards et al. 2008). *H. neanderthalensis* behaviour is debated, from their diet to their ability to have complex thought which is discussed primarily in section 3.3.

3.3 Theories and models related to hunting or scavenging behaviours

This research analyses faunal mobility in the Palaeolithic, focusing on how the movement of fauna across the landscape may have been a factor in the hunting behaviours of ancient hominins, particularly *H. neanderthalensis* and *H. erectus*. These hunting behaviours have been the focus of an significant amount of debate, and the question of hunting or scavenging primarily seeks to determine the order of access to food resources (specifically carcasses) by hominins (Dominguez-Rodrigo, Egeland and Barba 2007). Scavenging is broken up into primary or passive scavenging. If access to resources occur before another predatory carnivore or scavenging species, the access is primary and suggests a confrontational form of scavenging or hunting (Bunn 1995, 1996). If access is secondary, it is more likely the hominins engaged in 'passive scavenging' (Dominguez-Rodrigo, Egeland and Barba 2007). The hunting-versus-scavenging debate has major implications for agreement on site formation, classification and usage as well as the socio-economic functions of the sites. There is generally consensus on the formation of hominin sites, with many researchers agreeing that hominins would have selected and moved carcass remains and stones to a chosen area in a repeated fashion (Bunn 1982; Potts 1988; Isaac 1983; Blumenschine 1988; Schick and Toth 1993; Dominguez-Rodrigo 1994; Selvaggio 1994; Capaldo 1995; Rose and Marshall 1996; Cavallo 1998). The use of sites and their function from a socioeconomic and cultural perspective is one of the leading divisive questions arising from the hunting-versus-scavenging debate, as it leads into questions about cognitive abilities and the representation of social behaviours in a site. (Isaac 1978; Potts 1982; Schick and Toth 1993; Blumenschine et al. 1994; Rose and Marshall 1996). One of the other main questions arising from the debate is the involvement that hominins had with the carcasses (Bunn and Kroll 1986; Selvaggio 1994; Blumenschine et al. 1994; Capaldo 1995; Cavallo 1998).

More modern studies of hominin predation behaviours began using isotopic studies instead of purely zooarchaeological studies and butchery mark analysis as isotopic analysis can provide information that more conventional analysis cannot. These studies have added to the debate by providing evidence of the types of food hominins were eating apart from the remains of carcasses found on sites, and evidence for systematic or seasonal exploitation of fauna (Richards et al. 2000; Patau-Mathis 2000; Bar-Yosef 2004; Bocherens et al 2005; Richards et al. 2008; Richards and Trikaus 2009; Villa and Lenoir 2006). What became apparent prior to the involvement of isotope analysis, was that as research into diet and predation behaviours of hominins continued, a wider approach to the debate was needed. Isotopic analysis on its own or zooarchaeological analysis alone will not provide an accurate representation of diet or predation behaviours. They must be used in combination with different methods such as lithic residue and use wear-analysis (Hardy and Moncel 2011) or analysis of dental calculus (Blasco and Fernandez 2012). Importantly an understanding of the different theories that have directed the hunting-versus-scavenging debate over the years must be examined, in order to understand through which theoretical lens interpretations or conclusions are being drawn.

Historically, the early theories within the hunting-versus-scavenging debate were very much influenced by Darwin’s 'Descent of Man and Selection in Relation to Sex' (1871). Darwin’s research applied evolutionary theory not only to human evolution but to society, suggesting that ‘hominisation’, or the ‘dawn of culture’ truly started “when our ancestors abandoned trees, adopted a bipedal gait, and used their free hands to make and use tools" (Dominguez-Rodrigo 2002:1). These traits were what then allowed these hominins to go forth and hunt. Interpretations made by Darwin suggested that it was the eating of meat that led to an increase in brain size, and following on, the superiority of men to women in regards to mental capacity (Darwin 1871). Perhaps unsurprisingly due to the era, this paradigm was extremely popular in academic circles, and to this day has managed to still subtly shape how we project interpretations of hunting-versus-scavenging onto hominins such as *H. neanderthalensis* and *H. erectus*. Darwin's combination of the inevitability of the aggressive nature of humans and cognitive differences between genders became a defining feature in hypotheses surrounding hunting behaviours and their sociobiological implications (Binford 1981; Binford 1985; 1988; Gamble 1999; Kuper 1994). In a wider sense, as pointed out by Dominguez-Rodrigo (2002:2), the combination of the hunting hypothesis, social implications (such as aggression and gender differences), and the idea of 'survival of the fittest' were major justifiers for human evolutionary achievements and modern human behaviours, to the point where "hunting became the most diagnostic behavioural trait to distinguish what was human or not" (Dominguez-Rodrigo 2002:2). This hypothesis maintained popularity for many years, producing often sensationalised books such as African Genesis and The Hunting Hypothesis (Ardrey 1961; 1976), which while entertaining, consisted mainly of wild exaggerations, doing more harm than good to the state of research into hunting behaviours of ancient hominins and early modern humans. This hypothesis also led to researchers employing it as the main reason behind the rise of bipedalism (Fisher 1982) as well as adaptation to savanna landscapes (Washburn 1950). The Man the Hunter conference in 1966 was a major moment in the hunting debate. Cultural progression was dismissed as a reason for the development of hunter-gatherer societies (instead adaptation to extreme environments was posited), and the concept of hunting as a male specific role re-emerged, and with it the idea that men shaped human evolution (Dominguez-Rodrigo 2002). The early interpretation of sites and theories about *H. neanderthalensis* and *H. erectus* site formation and the socio-economic functions of the site were heavily influenced by the perceived gender roles of the time. A change in perspective arose with Goodall (1963; 1986), where it was suggested the changing hunting strategies and increasingly complex nature of those strategies was what had helped shape human evolution, and it had not, as previously suggested, arisen simultaneously with the emergence of hominins.

There are a number of specific theories and models that were produced mainly in the 1970s to 1990s that had (and continue to have) major influence of the state of debate and helped research move away from the original hunting hypothesis. These include Brain's 1981 research suggesting that bone accumulations associated with stone tools do not automatically mean hunting was taking place, Binford's 'Obligate Marginal Scavenger' model (1981), and Isaac's 'Home-Base/Food-Sharing' model (1978), and 'Central-Place Foraging' model (1983). The 'Stone Cache' model was later developed (Blumenschine et al. 1994), which then evolved into the 'Refuge' model (Mitchell and Lane 2013).

Home-Base/Food-Sharing model: where regardless of if the food was hunted or scavenged, places being established as "foci of activity" and cooperation between hominins were what Isaac believed should be used to model early human behaviour (Isaac 1978).

Obligate Marginal Scavenger model: Binford (1981) suggested scavenging was the logical reasoning for the bone accumulations and developed the "obligate scavenger model". It was based on the analysis of carnivore dens and modern hunter-gatherers bone refuse, finding that the formation of these sites was due to the actions of carnivores, not the hominins.

Central-Place Foraging model: After Binford's (1981) OMS model entered the research sphere, Isaac reworked his model, where it became the "central-place foraging model" (Isaac 1983). The cooperation and socioeconomic basis of the initial model gave way to a more simplistic foundation-hominins were coming to the same location to consume food, with no requirement for there to be suggestions of sharing, sexual division of labour, or socioeconomic constructs (Dominguez-Rodrigo 2002).

Stone Cache model: Potts (1982) developed the model where the sites were representative of strategic locations for stone to be brought and stored, so any newly obtained carcass could be brought to the nearest cache for butchering and consumption.

Refuge model: sites were created as temporary 'refuges' near, but safe from carnivore competition and predation, where hominins could eat (Mitchell and Lane 2013).

According to Dominguez-Rodrigo (2002:8), the main interpretive positions in the hunting/scavenging debate are:

1. ‘Hominids hunted
2. Hominids used confrontational scavenging to have access to fleshed carcasses
3. Hominids scavenged carcasses that were undistributed by carnivores
4. Hominids passively scavenged defleshed carcasses at carnivores' kills
5. Hominids used a combination of these four strategies’

'Central-place foraging' is the framework most widely accepted for interpreting early archaeological sites (Dominguez-Rodrigo, Egido and Egeland 2007:7) however O'Connell et al. (2002) argues for a 'Male-display’ model, which is based on ethnographic analogy as well as archaeological data. This has had some criticism levelled at it due to its reliance on ethnography (Dominguez-Rodrigo, Egido and Egeland 2007:8).

Regarding *H. neanderthalensis* subsistence strategies specifically, more evidence is showing that *H. neanderthalensis* were likely hunting as well as eating a more varied diet (Richards et al. 2000; Patau-Mathis 2000; Bar-Yosef 2004; Bocherens et al 2005; Richards et al. 2008; Richards and Trikaus 2009; Villa and Lenoir 2006). While some early research suggested that *H. neanderthalensis* were simply ‘opportunistic scavengers’ (Binford 1984; 1988), there is more evidence that suggests otherwise. A great amount of the debate surrounding *H. neanderthalensis* predation behaviours has been influenced by a perceived inferiority of *H. neanderthalensis* cognition when compared to early modern humans. Cognition in hominin species is usually informed through the material remains left behind by the species, and the lack of visual or material art (Pettit 2000), language (Lieberman 1994), recognised burial practices and lack of older individuals (Trinkaus 1995) is considered by some scholars as evidence of a society lacking much cognitive ability.

Other researchers argue the opposite: that the stone tool knapping, and creation of bone and wooden tools (Patau-Mathis 2000), along with apparent special burials accorded to specific individuals (Leroi-Gourhan 1975), symbolic modification of shell using pigment (Zilhao et al 2010; Roebroeks et al 2012) are all symptomatic of intelligence. Some go so far as to suggest the cognitive abilities of *H. neanderthalensis* were similar to those of early modern humans (Dusseldorp 2009). The reason that cognition is so important in understanding how theories about *H. neanderthalensis* hunting behaviours were developed, is that it is commonly perceived that scavenging requires lower cognition levels and that there would have been little ability by *H. neanderthalensis* to hunt or exploit any sources of food other than those left behind by carnivores (Richards et al 2000; Richards and Trinkaus 2009). One of the common suggestions by proponents of theories that posit *H. neanderthalensis* as lacking cognitive abilities are that they simply scavenged for meat (Binford 1981) or that they hunted easy prey of a small or medium size (Marean and Assefa 1999; Stiner 1994). The other perspective is that *H. neanderthalensis* did have cognitive abilities equaling early modern humans and had the same ability to introduce a variety of resources into their diet (Chase 1989; Henry et al 2010; Stringer et al 2008). Researchers arguing the two sides tend to focus their evidence from faunal (zooarchaeological studies and taphonomic analysis) and isotopic data. Analysis of faunal assemblages can provide data on diet, and to a lesser extent inform whether assemblages were created through the process of scavenging or active predation. However these methods have several problems, when specifically profiling diet. Primarily the assemblage may not be true representations of what was being eaten, with larger animals being butchered with smaller pieces being brought back, and animals that were smaller being brought back whole (Sorenson 2009). A specific example of this is Sorenson's (2009) investigation into mammoth hunting, where they determined that the enormous size of the mammoth would have required preservation, through drying over fire in order to bring back to the site without it rotting over summer periods. The kill site, they suggested would have been the location of butchering activity, which explains the lack of complete body parts at the base settlement. These actions (logical thought, planning, organising) are in contrast to the idea that *H. neanderthalensis* were not cognitively similar to early modern humans. Their actions suggest that they were cognitively at least on a similar level to early modern humans. Indeed, a combination of lithic tools analysis, faunal evidence for slaughter, along with isotopic studies indicate an effective and intelligent hominin. Patau-Mathis (2000) concluded from her data analysis of three hundred and thirty three sites across Europe that *H. neanderthalensis* were undertaking deliberate, selective hunting of species during migrations, and using the landscape to their advantage in order to cull numerous animals at a time. This was also suggested by Jelinek et al (1989) who also found evidence of deliberate mass culls of herd animals using geomorphological features. In combination with the cut marks of the bones (suggesting processing by hominins) and later analysis by Mellars (1996) showing no other levels of the cliff with concentration of remains, it seems fairly likely these were deliberate and planned actions by *H. neanderthalensis*.

3.4 Geochemistry literature review

3.4.1 Introduction to strontium isotopes

The analysis of strontium isotopes can provide archaeologists with answers surrounding provenance, as well as the mobility of hominins and fauna. Simply put, strontium is absorbed into the body tissues of individuals through the food grown or grazed. The body tissue reflects the ratio of biologically available strontium in the local area during an individual's' early development. It is analysed and ratios of the strontium are compared to the surrounding geological environment (Evans, Chenery and Montgomery 2012). The resulting data can provide insight into mobility, migration patterns, the places where people grew up, or where fauna might have lived before moving to new locations.

Strontium (Sr) is an alkaline earth metal element (Zumdahl 1997) with four naturally occurring isotopes; ^{84}Sr, ^{86}Sr, ^{87}Sr and ^{88}Sr (Faure 1986). Importantly, strontium (2^+) has a similar ionic radii to calcium (2^+), and therefore is often taken up into the biominerals of bone and teeth (Faure and Powell 1972). Within isotope archaeology, the strontium isotopes used most commonly are ^{86}Sr and ^{87}Sr, as according to Beard and Johnson (2000), the similar relative concentrations of these isotopes allow more analytically precise results than ^{84}Sr and ^{88}Sr.

Strontium is distributed widely within geological and biological materials. Within mobility studies using strontium analysis, regolith is critical, as according to Capo et al. (1998), it is the principle source of bioavailable strontium to plant life. Bioavailable strontium is the strontium available for absorption into a biological system, for example faunal body tissue (Evans et al. 2009). Because only a portion of the total strontium in the regolith is bioavailable (Sillen et al. 1998) the $^{87}Sr/^{86}Sr$ ratio may be very different between the biological systems and the original geological system.
Farrand (2001) suggests that considering the strontium values of sediment samples from archaeological sites as representative of local values is problematic, as they have a number of different anthropogenic and taphonomic factors giving an archaeological site its own unique strontium composition (Moffat 2013). However this potentially problematic situation can be offset by using fossil teeth of vertebrates, such as small herbivores (Price et al. 2002, Bentley et al. 2004) as the strontium composition teeth are totally bioavailable (Moffat 2013). Strontium is also not significantly fractionated by natural processes, meaning that the abundance of the strontium isotope is not changed through its transference through bedrock, to soil, vegetation and into the food web (Pollard et al. 2007). The bio-purification of strontium occurs without significant fractionation because of the aforementioned similar ionic radii of strontium (2^+) and calcium (2^+), as the strontium when taken into the biological tissue of animals, substitutes for the calcium (Blum et al. 2000) with between 20 to 40% absorbed (Sips et al. 1996). Strontium therefore, is an excellent marker for the geological environment where the formation of teeth took place (Moffat 2013).

Importantly to this project, strontium isotope composition in teeth is taken up during early tooth development providing a geographic origin of an individual's migration (White and Folkens 2005) and is then preserved throughout the life of the individual (Schweissing and Grupe 2003), and potentially survives post-burial diagenesis. Post-burial diagenesis refers to changes to the strontium isotope composition of bones or teeth once deposited in archaeological sites and the process is summarised by Lee-Thorp (2002). Any changes to the strontium isotope composition can seriously damage attempts to track migration (Lee-Thorp 2002). However, enamel has been demonstrated to show resistance to post-burial alteration (Trickett et al. 2003) and is resistant enough to preserve the isotope composition in material up to the Cretaceous age (Bocherens et al. 1994). This means that the strontium isotope composition of archaeological teeth can be compared, and a regional map can be created providing an estimation of the distance and vector of migration, and whether an individual was born locally.

3.4.2 Introduction to oxygen isotopes

Oxygen-18 is a stable isotope that is used in isotope geochemistry in fields such as palaeoclimatology (Capilla et al. 2012). It is often written as $\delta^{18}O$, which represents the ratio $^{18}O/^{16}O$ (the contents of ^{18}O in water). It is usually reported with reference to Vienna Standard Mean Ocean Water (VSMOW) or the Protein Data Bank (PDB). $\delta18O_w$ refers to meteoric water, while $\delta18O_P$ and $\delta18O_C$ refer to the phosphate and carbonate fractions in bioapatite (Pellegrine et al. 2011). Studies using oxygen isotope analysis, use intra-tooth analysis to provide a path to understanding seasonality, climate and environmental variations, yearly or monthly, throughout time (Pellegrini et al. 2011:71). Combining oxygen isotope analysis with other analyses (such as strontium isotope analysis), the isotopic profiles can be placed into a seasonal context (at moderate and high latitudes) (Britton et al. 2009). Oxygen can be used to determine palaeoclimates, as a distinct research question, but can be combined with other techniques to characterise migratory behaviour in archaeological faunal remains (Britton et al. 2009). hard tissue (such as dentine and enamel and bone) retain the oxygen isotopic signatures (Sharma et al. 2004). The signature will be retained with high fidelity in tooth enamel particularly (Bryant et al. 1994) because in comparison to bone and dentine, it is lower in organic content and has a dense, crystalline apatite structure (Sharma et al. 2004). This dense, crystallised structure means it is more resistant to diagenetic alteration, although may still be subject to some diagenesis (Lee-Thorp and Sponheimer 2003). The composition of a bodies' oxygen sources are from the atmosphere, ingested water, and organic compounds containing oxygen. It is however, ingested water is the primary source that controls the ^{18}O of enamel (Sponheimer and Lee-Thorp 1999). Just as with strontium, the ^{18}O values are closely correlated with local values. In this case, lower ^{18}O values occur during the coolest periods of the year, and high ^{18}O values being associated with warmer periods (Britton et al. 2009; Dansgaard 1984). Seasonal changes are also able to be elucidated from the oxygen isotope ratio within the enamel, along with intra-annual variations (Britton et al. 2009; Kohn et al. 1998).

The archaeological context to which oxygen isotope analysis can be applied are varied. Specific to this project are the applications to reconstructing palaeoenvironments and the migratory behaviours of fauna. According to Britton et al. (2009), when archaeological teeth undergo oxygen isotope analysis in combination with strontium, this approach can provide answers surrounding seasonal movements and patterns of mobility. There has been some successful research in this area, that has provided data showing the movements of wild and domestic fauna through intra-tooth analysis. The use of oxygen isotope analysis in archaeology generally however, is well established (Bryant et al. 1994; Fricke and O'Neil 1996; Kohn 1996; Hoppe et al. 1999; Balasse 2002; Lee-Thorp and Sponheimer 2003; Pellegrini et al. 2008; Bernard et al. 2009).

3.4.3 Introduction to carbon isotopes

Carbon-13 (usually written as ^{13}C) is a stable isotope commonly used in archaeological science to determine the dietary makeup of an individual (hominin or fauna) (Bocherens 2016). The ratio used is $\delta^{13}C$ which represents the ratio of ^{13}C and ^{12}C. The composition of carbon in tooth enamel of fauna correlates with the vegetation ingested, and therefore provides an idea of the type of diet they had or the vegetation available in an area (Faure 1972). There are two particular types of plants that determine the carbon composition. These are C_4 plants and C_3 plants and the difference between them relates to their method of photosynthesis of CO_2 (Yamori et al. 2014). C_3 plants tend to fall within a range of -20 to -37‰ and photosynthesise better in cool, wet climates (Kohn 2010) while C_4 vegetation have a threshold around 19.2% and photosynthesise better in hot sunny climates (Urban 2015). Analysis of $\delta^{13}C$ has the potential to inform about the ecology and resource use of animals, such as with Feranec et al (2010) who determined the diet of *Bos Primigenius* in Spain (grasses in open environments) and was able to determine the differing diets of a number of other species. Britton (2009) also used $\delta^{13}C$ to look at the diet of Reindeer, along with many other studies looking at diet through the enamel of mammals (Bocherens et al. 1996; Kohn 2005; Widga et al. 2010).

3.5 Past Palaeo-mobility, palaeoclimate and dietary studies

The application of strontium isotope analysis on biominerals has been a method of determining distance and vector of mobility, of both prehistoric fauna and human individuals for a number of years but was first suggested in 1985 (Ericson 1985). Strontium isotopes have been used for a great number of palaeo-mobility studies, and have been reviewed in Bentley (2006), Budd et al. (2004), Montgomery (2010) and Price et al. (2002). Specific examples of usage have been in the tracking of variations in African elephants' migration patterns (Koch et al. 1995), caribou migration (Britton et al. 2009) and also as a method of provenance, such as the source of elephant bone (Vogel et al.

1990) and white-tailed deer antlers (Beard and Johnson 2000). Further examples of studies using strontium isotope analysis to interpret migration of fauna include Arppe et al. (2009), Hoppe et al. (1999), Hoppe and Koch (2007), Julien et al. (2012), Pellegrini et al. (2008) and Widga et al. (2010). Mobility can be determined through a number of applications of strontium isotopes. There is the straightforward method, for example Bentley et al. (2007) compared the isotopic signature of the enamel of their specimen to the background value taken from the associated archaeological site, to determine that their specimen was local. Other authors, for example Richards et al. (2008) and Britton et al. (2011) inferred mobility patterns, based on the strontium isotope composition of the surrounding areas. Another approach is to map the surrounding area and develop bioavailable strontium maps for the regions of interest, such as the IHRUM strontium database (this project will employ the use of a bioavailable strontium map, with data accessed from the IRHUM strontium database (Willmes et al. 2014). There are problems associated with the strontium isotope technique, including an increase in radiogenic strontium from individuals who had a high seafood diet (Slovak et al. 2009:163) , a lack of contrast between the background bioavailable strontium compared with the post-burial diagenesis (Moffat 2013: 41), and issues relating to the use of laser ablation (Horstwood et al. 2008). Moffat (2013:42) suggests that a potential problem that can arise in applying strontium isotope composition to mobility mapping, is that the bioavailable strontium composition of regolith changes due to changing climatic conditions and little thought has been given to reconstruction of these changes.

Oxygen, carbon and nitrogen isotopic analysis on Neanderthal teeth (in collaboration with taphonomic studies) has had much success in examining the diet and predation of Neanderthals. Many studies have focused on carbon and/or nitrogen in the bone collagen of individuals to measure the average of protein consumed in the last years of their life (Richards et al 2000; Bar-Yosef 2004). The source of the protein could then be determined, by comparing the isotope values to the mammals from the same site or region (Richards and Trinkaus 2009). There are problems associated with this method, mainly in a marine setting, where the many trophic levels for fauna mean increases in the carbon and nitrogen ratios each level resulting in marine fauna with higher carbon and nitrogen values (Tykot 2006).These studies have been very successful in identifying the species of animal consumed, and suggests that Neanderthals were eating a diet consisting of large herbivores through to small ungulates over large geographical and chronological zones (Villa and Lenoir 2006; Patau-Mathis 2000). Through isotopic studies, such as those by Richards et al (2000), Bocherens et al (2005) and Richards et al (2008) the role of Neanderthals as hunters is now mostly accepted.

The isotopic record in combination with faunal analysis does not show variation in diet, however if Neanderthals were as adept hunters as they seem to be, it is highly unlikely they were eating a diet only consisting of meat (Hardy 2010). The evidence for this is shown in a number of sites including Payre, where Hardy and Moncel (2011) were able to demonstrate through lithic residue and use-wear analysis, that plant starch and fish residues were present. The site of Shanidar cave, Iraq, and Spy Cave, Belgium (Henry et al 2010) also showed evidence that Neanderthals were consuming a variety of plant foods such as date palms and legumes, through analysis of dental calculus.

Hominin predation behaviours have been discussed by many people, often framed within debates surrounding subsistence behaviours (e.g. Binford 1981, 1983; Conard and Prindiville 2000; Daujeard and Moncel 2010; d'Errico et al. 1998; Rendu 2009; Shea 1998). Isotope analysis in this context is more often applied to the hominin remains themselves. The applications of isotope analysis to faunal remains that are associated with early hominin sites in order to examine faunal mobility, and draw inferences for hominin hunting behaviour by proxy is rarer. Britton (2009) and Moffat (2013) were both successful to different extents in this aim. Britton (2009) successfully used multi-element isotope (strontium $^{87}Sr/^{86}Sr$ and Oxygen $\delta^{18}O$) analysis on reindeer and bison teeth from the Quina Mousterian bone bed at Jonzac, France (a late Pleistocene site) to determine migratory behaviour in the fauna. This research was the first to use these techniques to demonstrate migration in

Pleistocene reindeer. By doing so, Britton (2009) was able to develop a greater insight then ever previously available into the palaeoenvironment of Neanderthals in this area. Some of the conclusions Britton (2009:224) reached, were that the isotope data demonstrated “hunting events in which Neanderthals targeted the same reindeer herd” and that it also indicated “the exploitation of these animals (by Neanderthals) during their annual migrations” (2009:225). The site, Britton goes on to suggest, may have been selected by the Quina Neanderthals, in order to exploit “the seasonally abundant and predictable resources” (2009:237), and that the accumulation of faunal deposits at the Jonzac site was “the result of intensive seasonal exploitation of this species during their annual migration” (2009:236).

Britton et al (2011) continued the research undertaken by Britton (2009) in order to better understand subsistence choices of Palaeolithic hunter–gatherers, by examining the palaeoecology of reindeer and bison from the Jonzac site. The results were able to give insight into Neanderthal predation, suggesting that the Reindeer were killed during their seasonal migration through the site, and were the product of either “a single hunting event of a small number of successive hunting events” (Britton et al. 2011:176).

Kelly (2007) also undertook strontium isotope studies, as part of an ongoing study surrounding Neanderthal migration and predation at the Upper Pleistocene site of Les Pradelles (France). The resulting strontium isotope ranges were far closer to the local strontium values of soil and plant, suggesting that the *Bison/Bos* were available year round, as they did not appear to migrate through different geological terrain during their development. This was a similar result to Britton (2009) who also found lower $^{87}Sr/^{86}Sr$ values in the analysis of *Bison/Bos* also suggesting a lower range of movement, as suggested by the large values of local strontium found in the tooth. Kelly et al (2008) as an extension to the 2007 honours thesis, determined that the $^{87}Sr/^{86}Sr$ of reindeer showed a relatively large range of migration, similar to that of Britton (2009). While some difficulty was found in determining the seasonality of migration during tooth formation, Kelly et al (2008:2) indicated this could have been the result of "reservoir effects and complexities in tooth mineralisation".

Moffat (2013) undertook an extensive study into the applications of strontium isotope analysis and LA-MC-ICP-MS, as well as its utility in determining the mobility of that fauna. The PhD focused on 90 faunal teeth from the Lower and Middle Palaeolithic, at archaeological sites within Israel and France. This study was successful in demonstrating the applicability of laser ablation and strontium isotope analysis on faunal teeth to examine migration. Research by Benson (2013) examined laser ablation depth profiling on a Neanderthal tooth, and was successful in obtaining usable $^{87}Sr/^{86}Sr$ data. Benson's research focused on the methods of LA-MC-ICP-MS and was very important in determining appropriate sampling strategies and minimising damage to teeth when using laser ablation. Willmes (2015) also approached the topic of mobility using strontium isotope analysis, with his research covering the mapping of strontium isotopes, and specific techniques for laser-ablation methodology. Hodgkins (2012), Willmes et al. (2016) and Hartman and Richards (2013) have also undertaken similar studies, focusing on the methodology of multi-isotope analysis and LA-MC-ICP-MS, all of which indicates the significant potential benefits associated with using this technology in undertaking faunal mobility studies

Chapter Four: Methodology

4.1 Overview

The procedures undertaken for the preparation, processing and analysis of strontium, oxygen and carbon isotopes will be summarised in this chapter. It will outline how the LA-MC-ICPMS was undertaken using a Thermo Neptune connected to a New Wave UP-193 Excimer laser was used to analyse the $^{87}Sr/^{86}Sr$ data and Nu Horizon GasPrep in line with Nu Instruments IRMS. A Sensitive High Resolution Ion Microprobe (SHRIMP II) was used to analyse the $\delta^{18}O$ and $\delta^{13}C$ data.

4.2 Maps used

Data collected and maps produced by Moffat (2013) were used as the reference for the strontium values of the geologies in each country. In order to match, or identify the range of geology strontium values that the samples fitted into, an algorithm was developed of MatLab. Details of this algorithm can be found in Appendix Two.

4.3 Preparation of samples

The samples Holon and were found in stratum C of the excavation, corresponding to the penultimate interglacial MIS 7. The data set were comprised of 11 teeth total, consisting of 4 fallow deer (*Dama cf. mesopotamica*), 3 aurochs (*Bos primigenius*) and 4 straight-tusked elephant (*Palaeoloxodon sp*.). Refer to Appendix One for sample details. These samples were provided by Dr Liora Kolska, from the National Natural History Collections in the Hebrew University of Jerusalem, Israel.

Samples from the site of Payre in the south-east of France, were taken from layers F1 through to G6 and consisted entirely of 14 teeth from aurochs (*Bos Primigenius*). These layers all fall within MIS 8-7. These samples were provided by Dr Marie-Hélène Moncel, from the Muséum National d'Histoire Naturelle in Paris

All samples were prepared by being placed in an acid wash bath of 10% hydrochloric acid for five minutes, while being gently cleaned with a toothbrush. They were then rinsed with fresh DI (deionised) water. The samples were placed in an oven at 60ºC for 12 hours to dry. The samples were then cut longitudinally with a dremel drill and sanded down with P800 sandpaper for a flat smooth surface, then wiped clean with acetone. The samples were embedded in melted parafilm and placed in a specially designed mount to hold that sample in place (Figure 4.2). All samples were then cleaned with a laser ablation run prior to analysis, which cleaned any contamination that may have remained, or been introduced with the sandpaper or drill.

The preparation for analysis of oxygen and carbon followed on from the newly cleaned samples. The samples were microdrilled, taking one sample from each tooth. Sample 72 and sample G2 N9 821 were incrementally sampled along the length of the tooth. The samples were then taken to the University of Adelaide where they were placed into numbered vials along with standards and put into the GasPrep. The samples were first purged, and then 10 drops of phosphoric acid were added to each vial. The standards used were ANU-P3 – Australian National University Standard, UAC-1 – Adelaide University carbonate and the CO-8 International standard.

4.4 Instrumentation

The instrument used in the conduction of the $^{87}Sr/^{86}Sr$ analysis was a Thermo Neptune + MC-ICPMS connected to a New Wave Research 193 nm Excimer laser. This analysis was conducted at the University of Wollongong with the assistance of Dr Tony Dosseto The analysis of $\delta^{18}O$ and $\delta^{13}C$ were undertaken at the University of Adelaide with Mark Rollog, using a GasPrep with NuHorizon multicollector and analysis was conducted on Sensitive High Resolution Ion Microphone (SHRIMP II), which analyses oxygen isotopes in biogenic and inorganic minerals.

4.5 Strontium analysis

Five runs were undertaken for this analysis, they can be seen in Figures 4.1, 4.2, 4.3, 4.4 and 4.5. The arrows indicate the direction sampling took place, with red and purple denoting enamel and dentine respectively. The parameters were as follows:

Run 1) 80% output; 5hz rep-rate; 150um width; intersite pause 10sec; 30sec dwell time; 500u µm spacing; and a washout of 60 seconds.

Run 2) Parameters the same as Run 1, however the grid space changed to 400 µm; and the washout time changing to 120 seconds.

Run 3) Grid space changed back to 500 µm while the other parameters remained the same as Run 2.

Run 4) Grid space changed back to 400 µm, other parameters remained the same as Run 2

Run 5) remained the same as Run 4.

There were several problems with the runs. Run 2 started overnight but failed early in the morning. It was restarted around 7am. Run 4 also stopped as the laser closed a few hours into the run. It was re-started at 7am but went out again – due to changing of Argon gas by suppliers. The run then dropped out at sample 313 (dentine) but was started up again and continued.

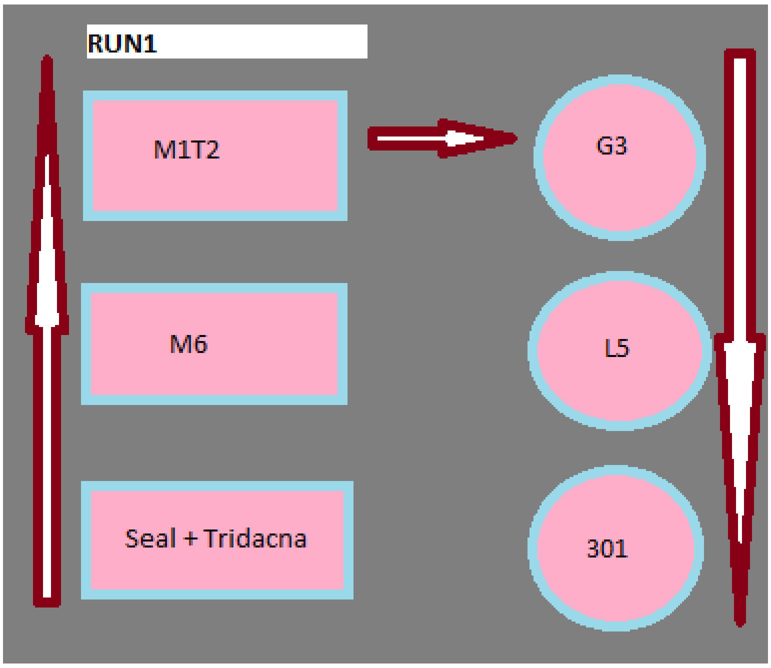

Figure 4. 1: Run 1.

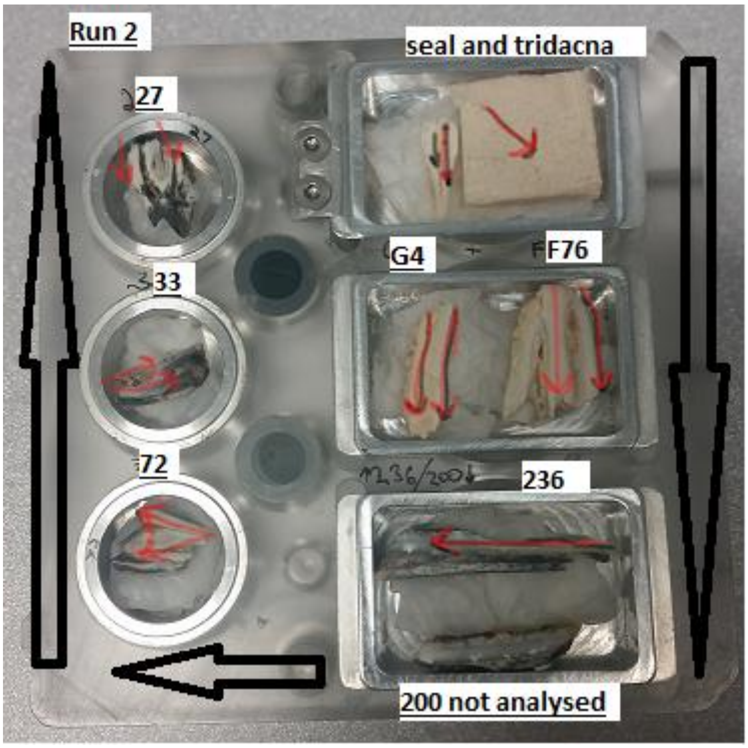

Figure 4. 2: Run 2.

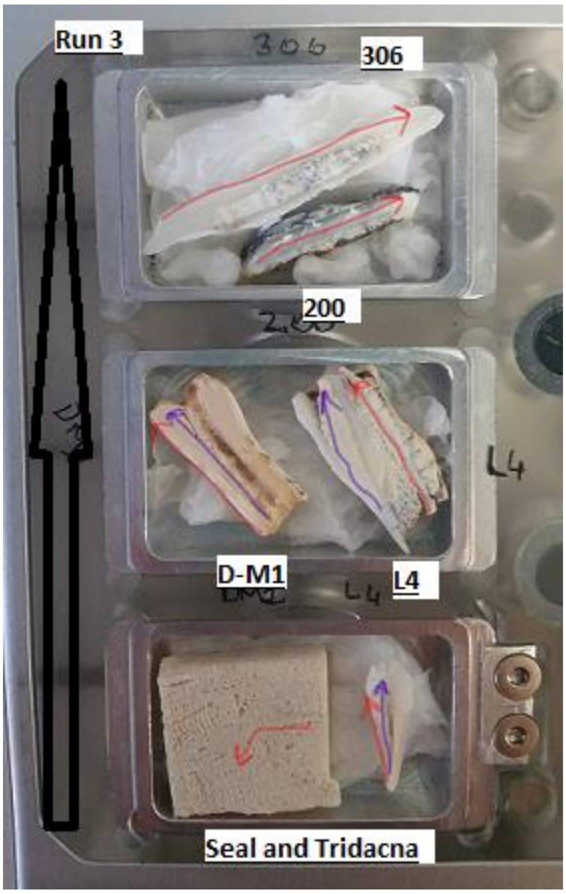

Figure 4. 3: Run 3.

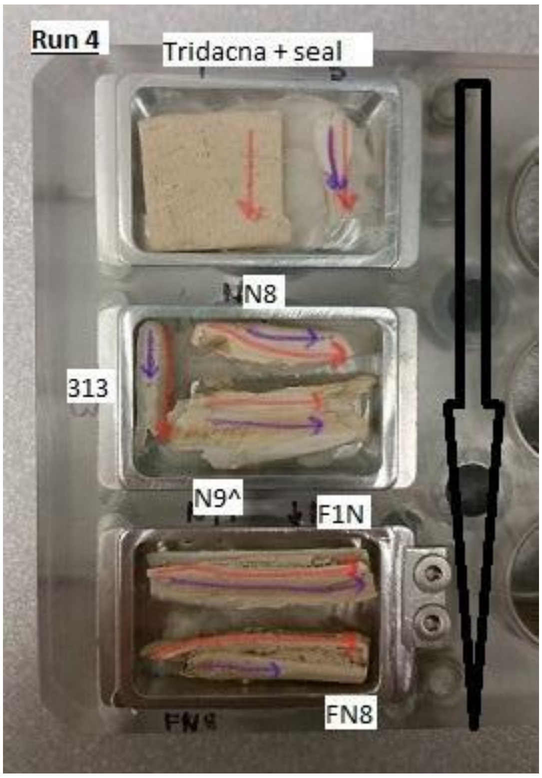

Figure 4. 4: Run 4.

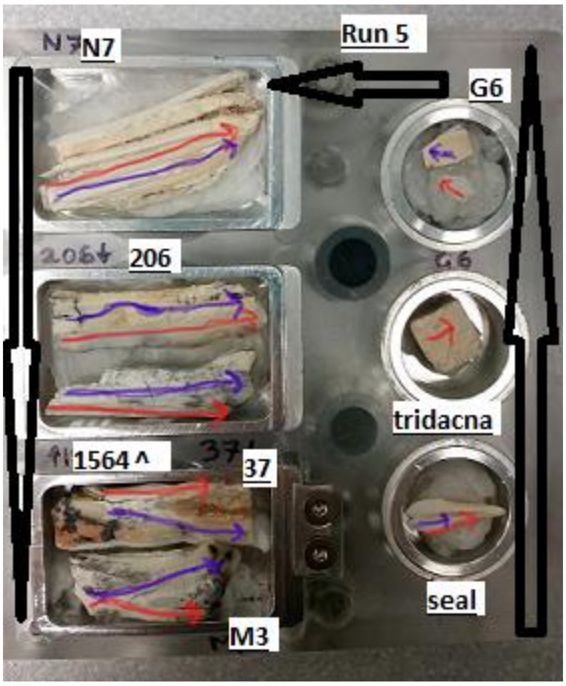

Figure 4. 5: Run 5.

4.6 δ^{18}O and δ^{13}C analysis

The δ^{18}O and δ^{13}C analysis and processing were undertaken by Mark Rollog at the University of Adelaide using a method modified from Spötl and Vennemann (2003). Where Spötl and Vennemann (2003) use a double needle system, which only works for pure carbonates, Adelaide University uses a single needle. The teeth take longer to dissolve than pure carbonates and need at least 18 hours in the acid prior to starting the run.

Considerable discussion exists about whether oxygen isotope analysis of the carbonate or phosphate portion of biominerals is the most appropriate approach for archaeological applications (Bryant et al. 1996, Chenery et al. 2012). We chose to analyse the carbonate fraction based on the more straightforward sample preparation.

The oxygen data were corrected for drift and peak size using 2 point corrections with reference to the ANU P2 and UAC-1 standards. In order to facilitate comparison of our data to other sources, we converted the results from PDB to VSNOW using equation 1 from Lightfoot and O'Connell (2016) and applied equation 3 from D'Angela and Longinelli (1990) based on the reported relationship between bovid ($\delta^{18}O_C$ (VSMOW)) and water ($\delta^{18}O_w$ (VSMOW)) (Podlesak et al. 2008). Clearly there are increased uncertainties associated with these corrections (ie. Pryor et al. 2014, Pollard et al. 2011) it is necessary to enable comparison with the rainfall oxygen isotope record.

4.7 Processing of strontium data

LA-MC-IPCMS data was processed using Iolite software (Paton et al. 2011) with the CaAr data reduction scheme (Woodhead et al. 2005) The following are the steps taken to process this data:

1. Data were imported as a Fin2 file.
2. A baseline subtraction was undertaken. Using the autoselection took, the intensities and time scale of the baselines were identified and selected across the whole sample. Each selection was then visually checked to make sure it was a good fit for each wave separately.
3. Moving to the reference materials tab, the standards were identified first and selected. Two references were used, tridacna and seal tooth.
4. Selection of the samples took place next. The autoselection tool was used again. The data log was imported and overlaid on the waves, which meant each sample corresponded to the time it was sampled in the mass spectrometer. The selections were identified and separated into groups.
5. The DRS (or data reduction scheme) 'Sr_isotopes_CaAr' was chosen and Z_Temora2 was chosen as the reference material. The data was then 'crunched'.
6. Finally the data were exported as a CSV file.

The method followed is outlined in more detail in Paton et al. 2011. The strontium values for both the entire mean for each material, as well as the mean of each laser ablation spot was calculated.

Chapter Five: Results

5.1 Overview

This chapter will summarise the results of strontium, oxygen and carbon isotope analyses undertaken on samples from the sites of Payre and Holon.

5.2 Holon: strontium

A total of 11 teeth from the site of Holon were analysed for their strontium isotope composition. Samples 279, 33, 37, 72, 200, 206, 236, 301, 306, 313, 1564, from the site of Holon were analysed for strontium isotope concentration using LA-MC-ICPMS. The mean strontium values for each sample are outlined in Table 5.1 and Figure 5.1 below:

Sample	Material	$^{87}Sr/^{86}Sr$	$^{87}Sr/^{86}Sr$ error σ^2	Total spots
279	Enamel	0.708528	0.000033	14
279	Dentine	0.708562	0.000024	12
33	Enamel	0.708388	0.000037	20
33	Dentine	0.708568	0.000056	28
37	Enamel	0.708656	0.000033	41
37	Dentine	0.708717	0.000024	52
72	Enamel	0.708518	0.000036	26
72	Dentine	0.708544	0.000024	23
200	Enamel	0.709209	0.00003	40
206	Enamel	0.707999	0.000059	83
206	Dentine	0.70839	0.000016	83
236	Enamel	0.708793	0.000019	67
236	Dentine	0.708675	0.000019	23
301	Enamel	0.708294	0.000048	21
301	Dentine	0.70847	0.000024	14
306	Enamel	0.709342	0.000036	68
313	Enamel	0.709273	0.000029	40
313	Dentine	0.708734	0.00003	18
1564	Enamel	0.708533	0.00004	75
1564	Dentine	0.708527	0.000018	73

Table 5. 1: Summary table of Holon faunal teeth LA-MC-ICPMS Sr isotope results.

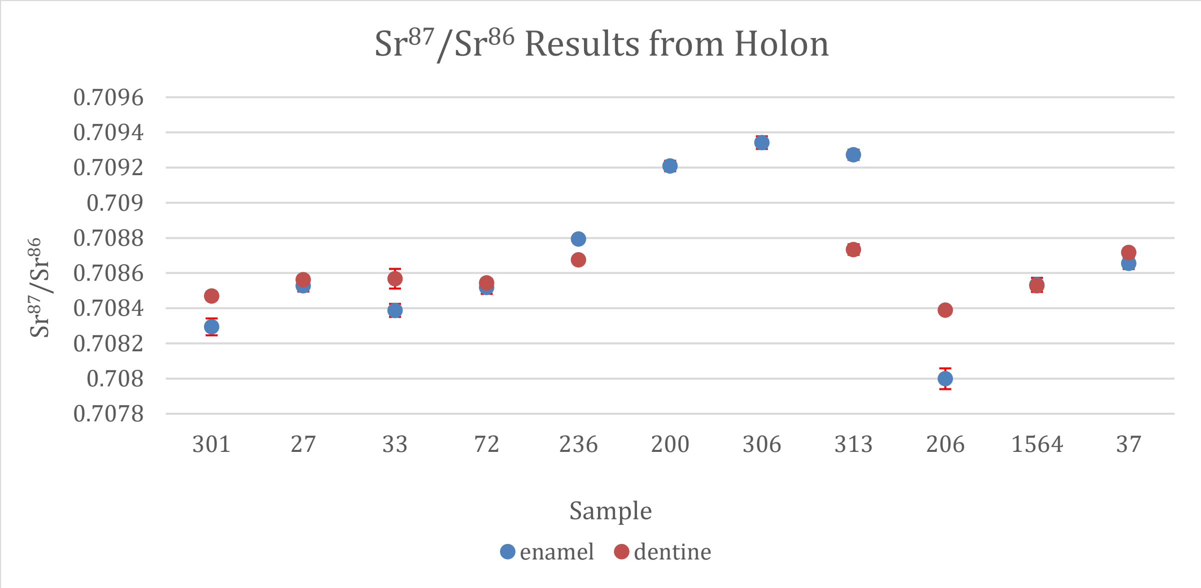

Figure 5. 1: Summary plot of Holon faunal teeth LA-MC-ICPMS Sr^{87}/Sr^{86} isotope results.

Sample 33

Strontium concentrations were collected for 20 spots within the enamel, and 28 spots within the dentine of sample 33.

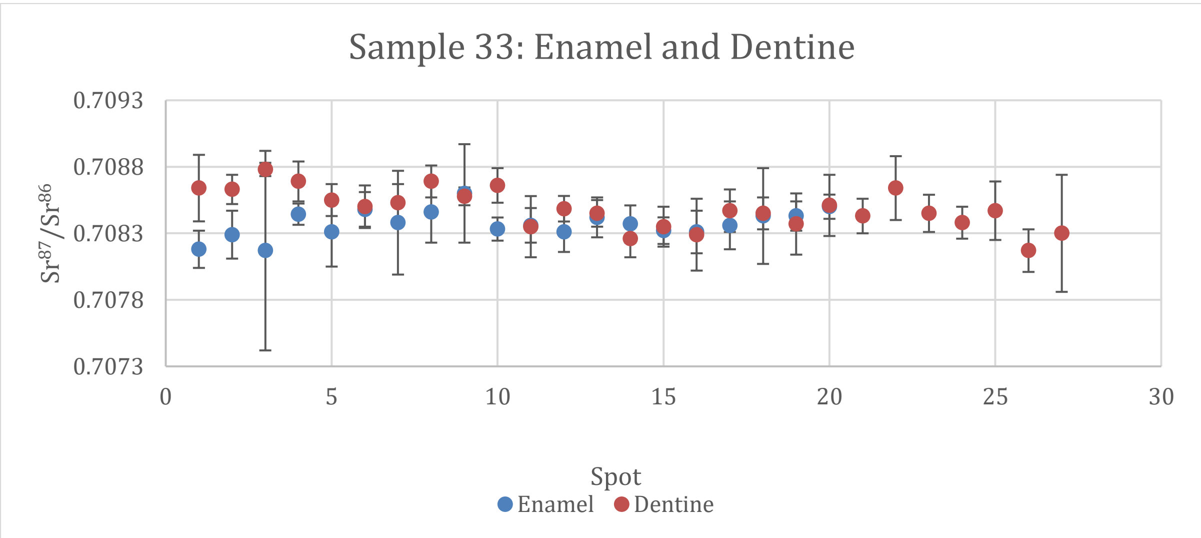

Figure 5. 2: Sample 33 Sr^{87}/Sr^{86} enamel and dentine values.

Sample 37

Strontium concentrations were collected for 41 spots within the enamel, and 52 spots within the dentine of sample 37

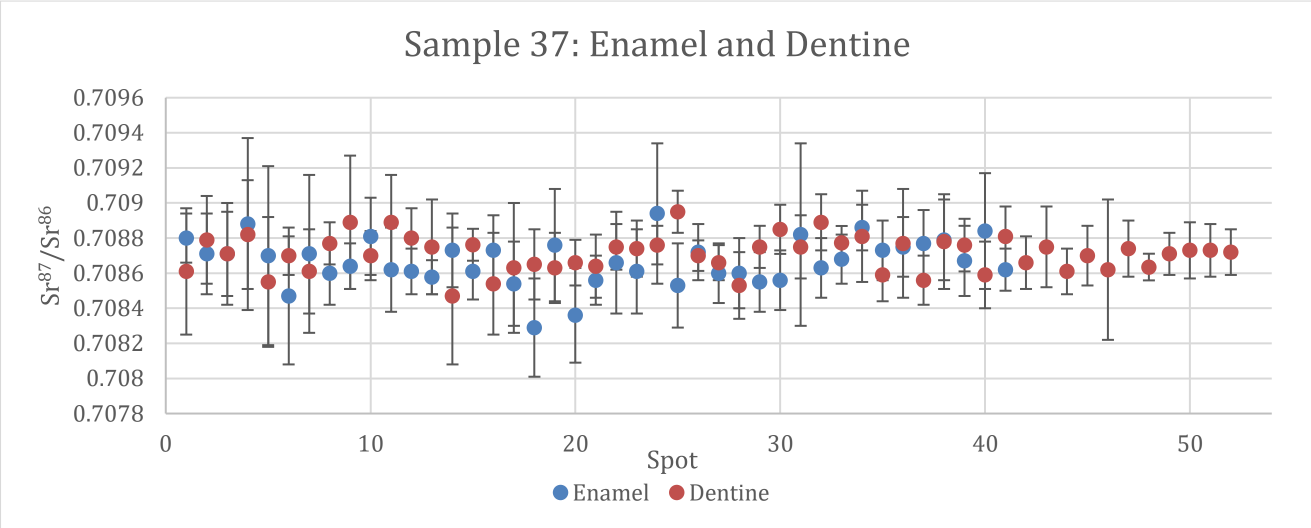

Figure 5. 3: Sample 37 Sr^{87}/Sr^{86} enamel and dentine values.

Sample 279

Strontium concentrations were collected for 14 spots within the enamel, and 12 spots within the dentine of sample 279.

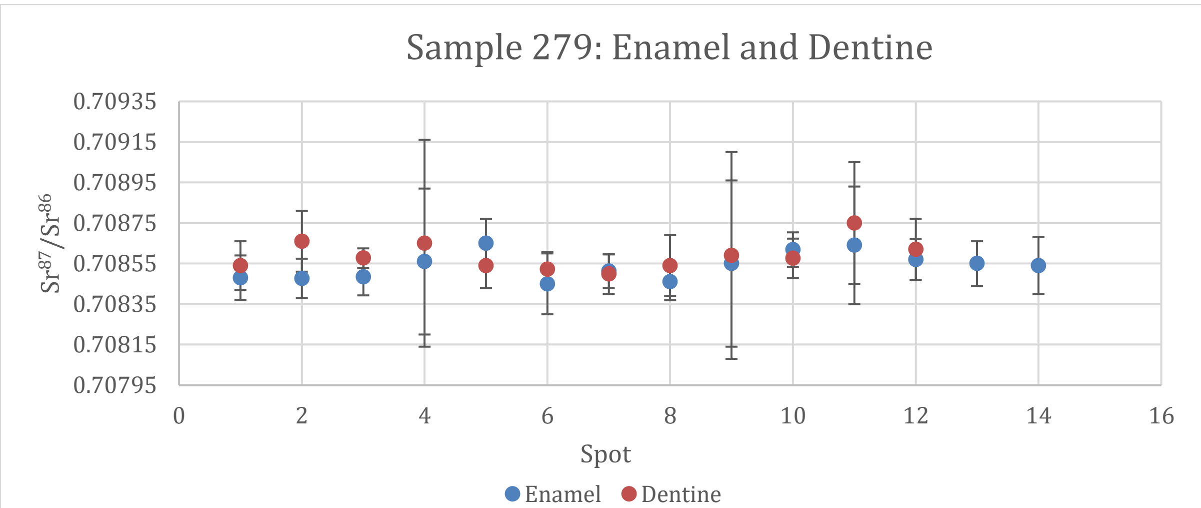

Figure 5. 4: Sample 279 Sr^{87}/Sr^{86} enamel and dentine values.

Sample 72

Strontium concentrations were collected for 26 spots within the enamel, and 23 spots within the dentine of sample 72.

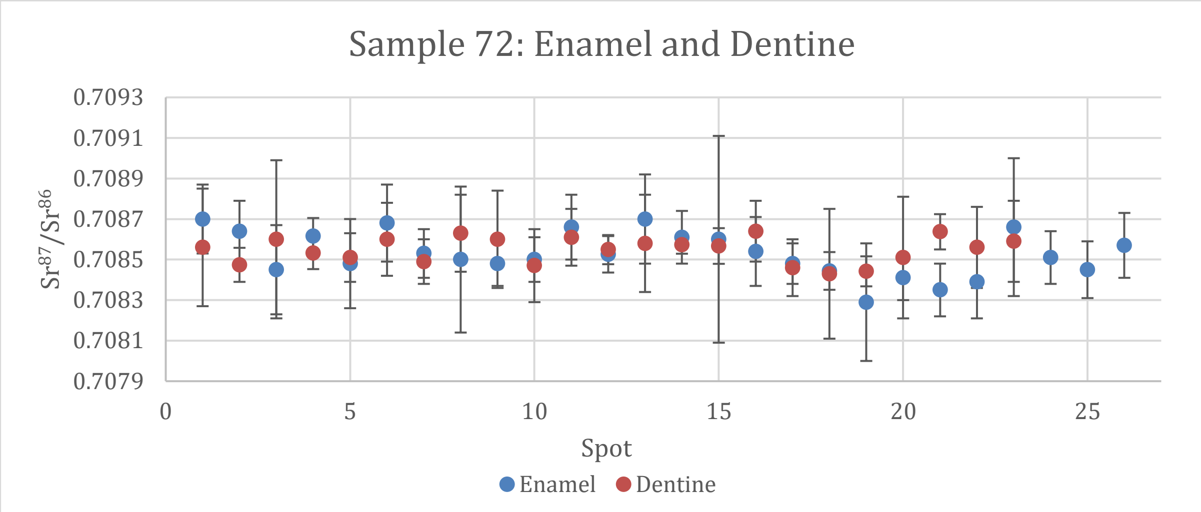

Figure 5. 5: Sample 72 Sr^{87}/Sr^{86} enamel and dentine values.

Sample 200

Strontium concentrations were collected for 40 spots within the enamel, however were unable to sample any dentine from the sample 200.

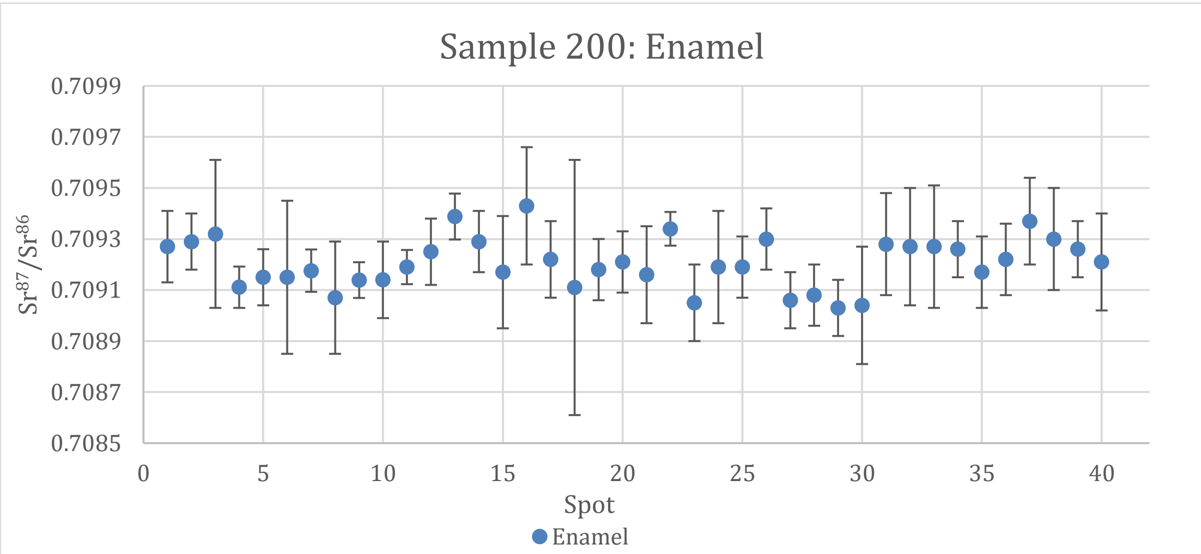

Figure 5. 6: Sample 200 Sr^{87}/Sr^{86} enamel and dentine values.

Sample 206

Strontium concentrations were collected for 83 spots within the enamel, and 83 spots within the dentine of sample 206.

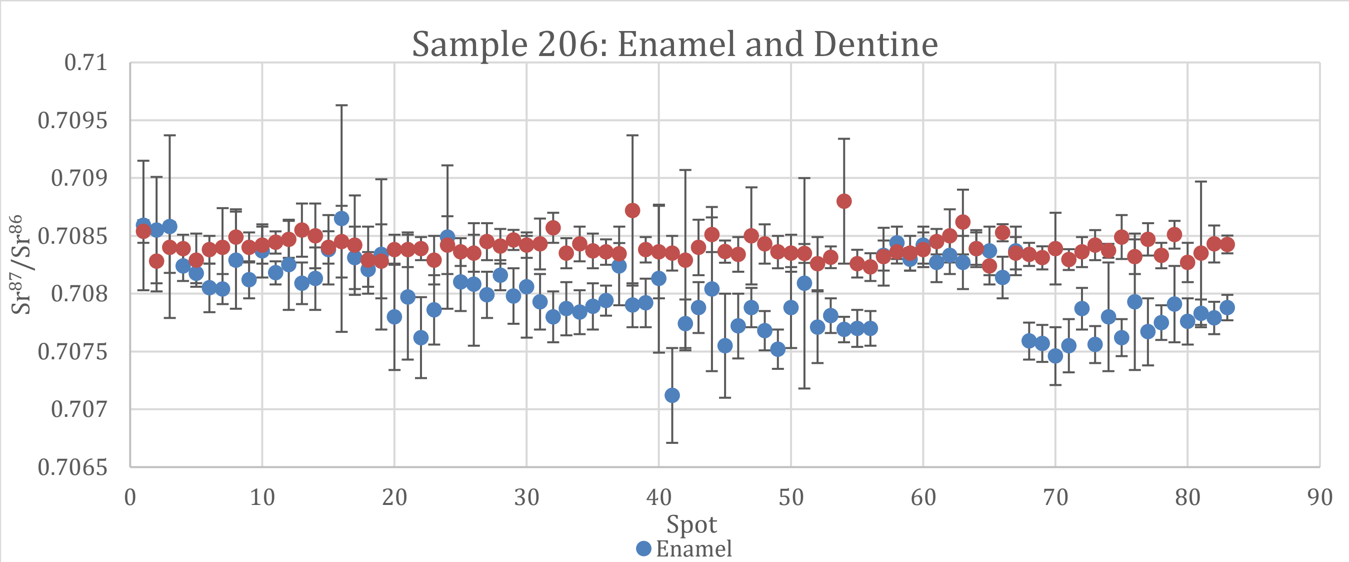

Figure 5. 7: Sample 206 Sr^{87}/Sr^{86} enamel and dentine values.

Sample 236

Strontium concentrations were collected for 67 spots within the enamel, and 23 spots within the dentine of sample 236.

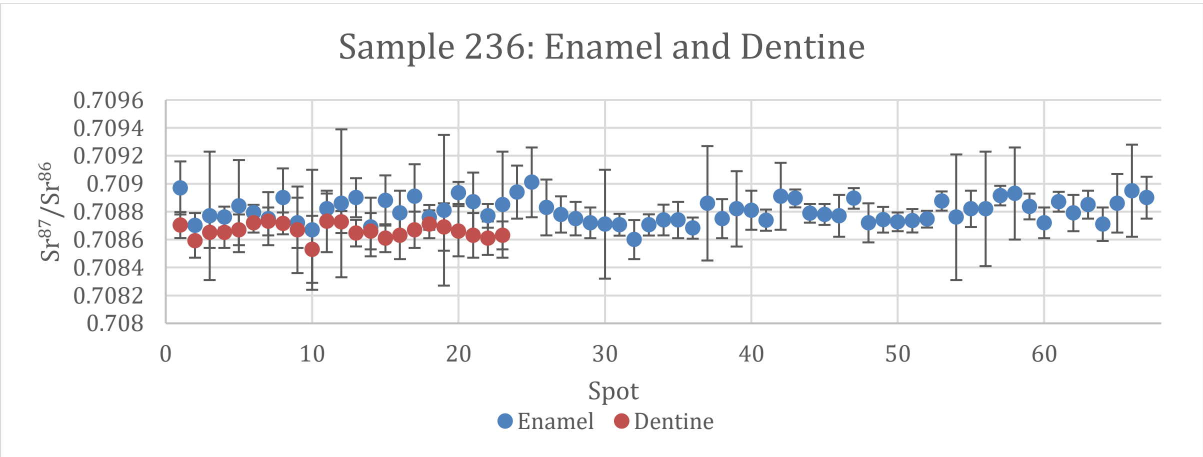

Figure 5. 8: Sample 236 Sr^{87}/Sr^{86} enamel and dentine values.

Sample 301

Strontium concentrations were collected for 21 spots within the enamel, and 14 spots within the dentine of sample 301.

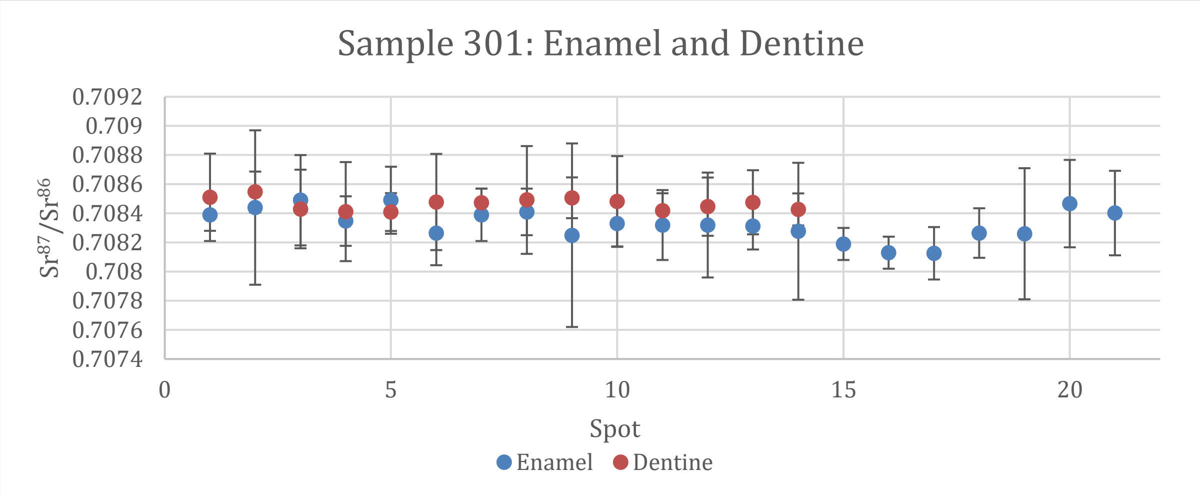

Figure 5. 9: Sample 301 Sr^{87}/Sr^{86} enamel and dentine values.

Sample 306

Strontium concentrations were collected for 68 spots within the enamel, however were unable to sample any dentine from the sample 306.

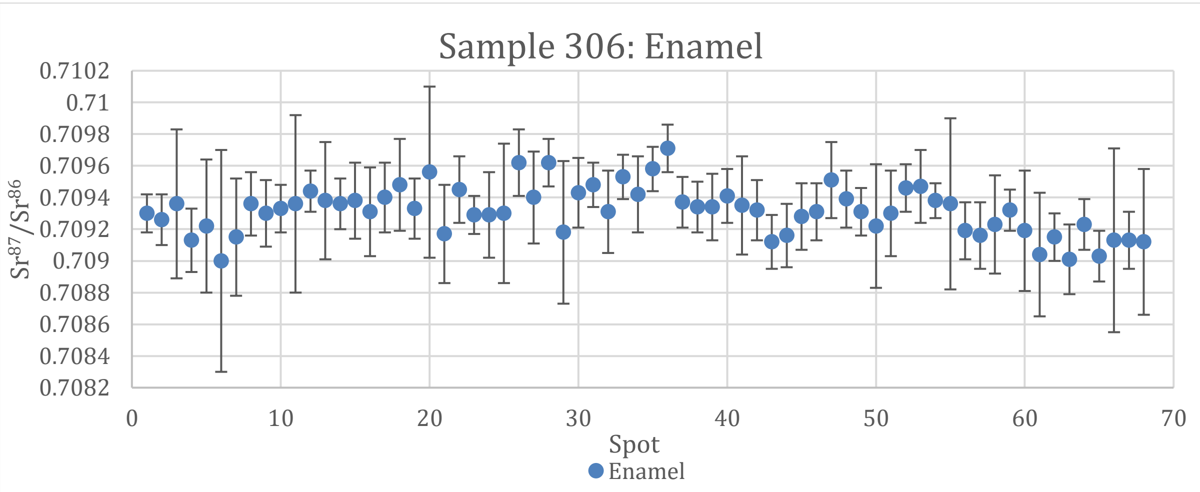

Figure 5. 10: Sample 306 Sr^{87}/Sr^{86} enamel values.

Sample 313

Strontium concentrations were collected for 40 spots within the enamel, and 18 spots within the dentine of sample 313.

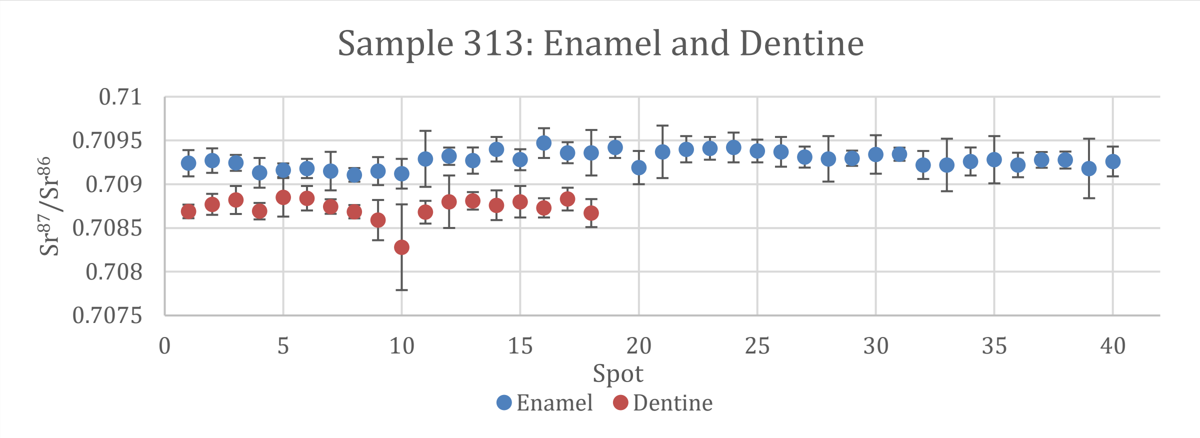

Figure 5. 11: Sample 313 Sr^{87}/Sr^{86} enamel and dentine values.

Sample 1564

Strontium concentrations were collected for 75 spots within the enamel, and 73 spots within the dentine of sample 1564.

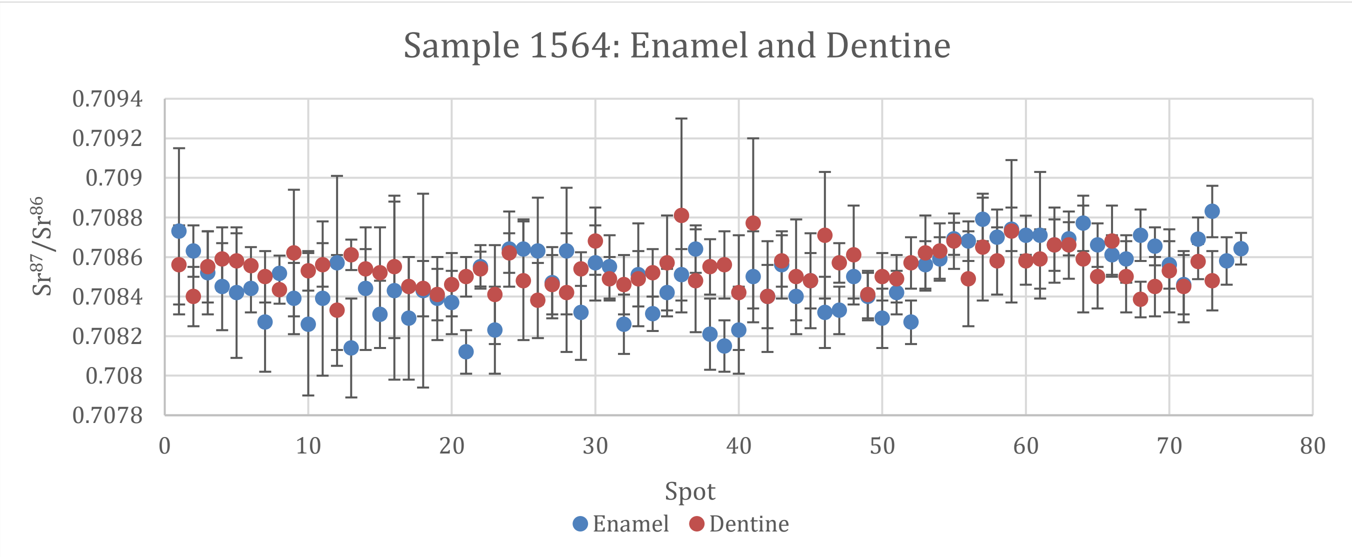

Figure 5. 12: Sample 1564 Sr^{87}/Sr^{86} enamel and dentine values.

5.3 Holon: oxygen and carbon

The following table shows the results after processing, for the oxygen and carbon analysis.

Sample	$\delta^{18}O$	error σ^2	$\delta^{13}C$	error σ^2
33	-2.55	0.09	-11.23	0.19
301	-2.76	0.04	-10.42	0.10
279	-3.56	0.05	-10.33	0.07
200	-4.34	0.05	-10.08	0.05
306	-1.78	0.07	-10.93	0.02
236	-3.31	0.09	-10.92	0.03
148	-0.59	0.09	-9.98	0.07
206	-2.18	0.07	-9.48	0.07
1564	-3.21	0.04	-10.19	0.11
37	-2.91	0.05	-10.30	0.09
313	-3.83	0.05	-10.36	0.08
72 (1)	-3.80	0.02	-11.09	0.05
72 (2)	-3.47	0.03	-10.02	0.12
72 (3)	-2.37	0.07	-11.00	0.09
72 (4)	-1.74	0.05	-10.97	0.10

Table 5. 2: Summary table of δ18O and δ13C results from Holon.

The values were then arranged by species in order to identify trends when comparing individuals within a species, and comparing species against each other.

	Elephas				Bos			Dama			
	236	313	200	1564	206	37	306	279	301	33	72
$\delta^{18}O$	-3.31	-3.83	-4.34	-3.21	-2.18	-2.91	-1.78	-3.56	-2.76	-2.55	-1.74
$\delta^{13}C$	-10.92	-10.36	-10.08	-10.19	-9.48	-10.30	-10.93	-10.33	-10.42	-11.23	-10.97

Table 5. 3: Summary table of δ18O and δ13C results from Holon by species.

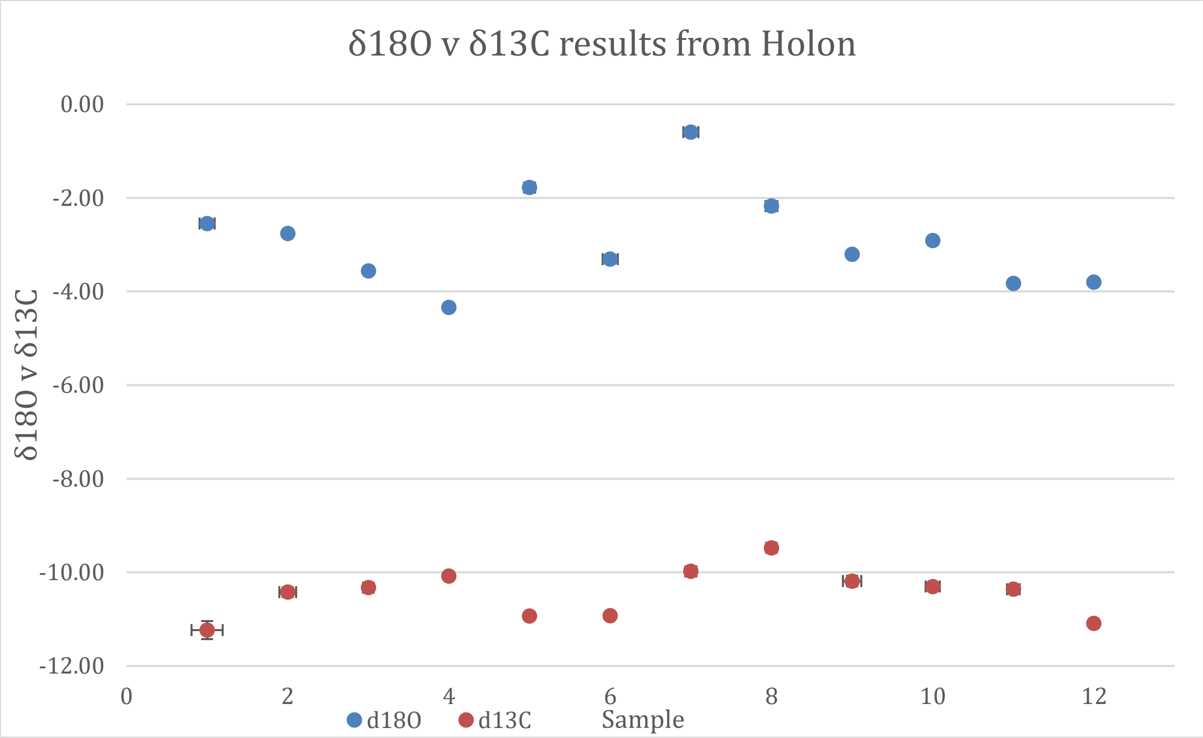

Figure 5. 13: Plotted δ18O and δ13C results from Holon.

Incremental sampling was undertaken on sample 72, a fallow deer.

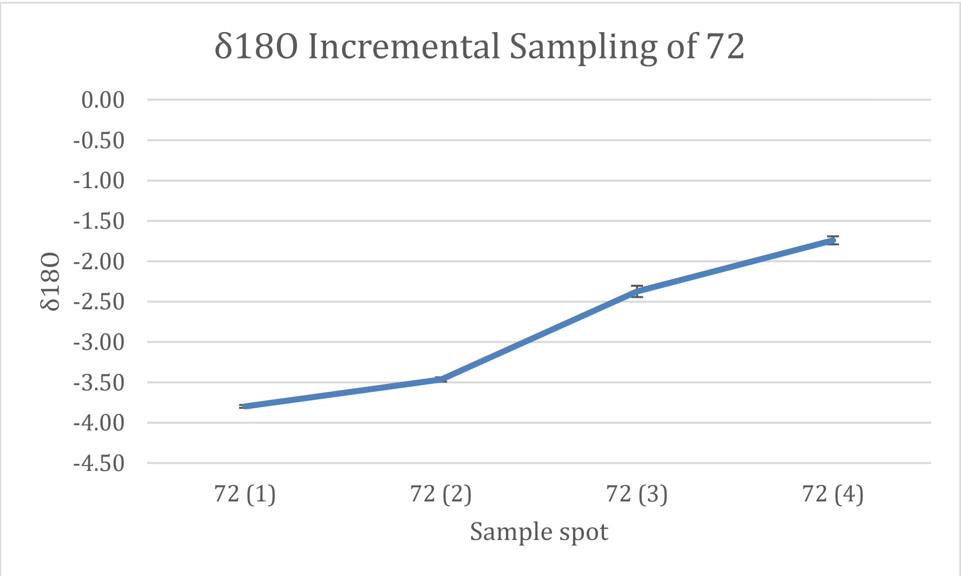

Figure 5. 14: Incremental sampling of sample 72 δ18O values.

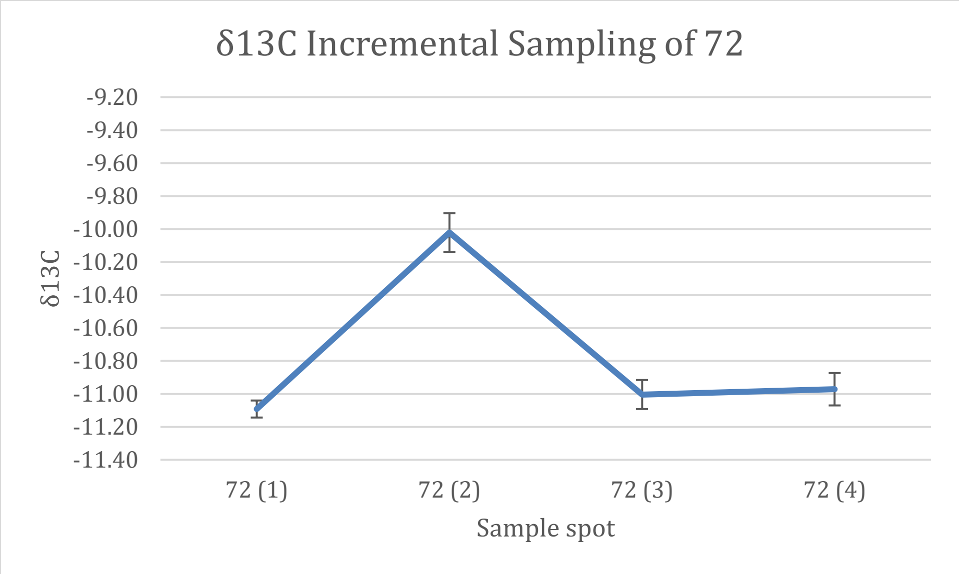

Figure 5. 15: Incremental sampling of sample 72 δ13C values.

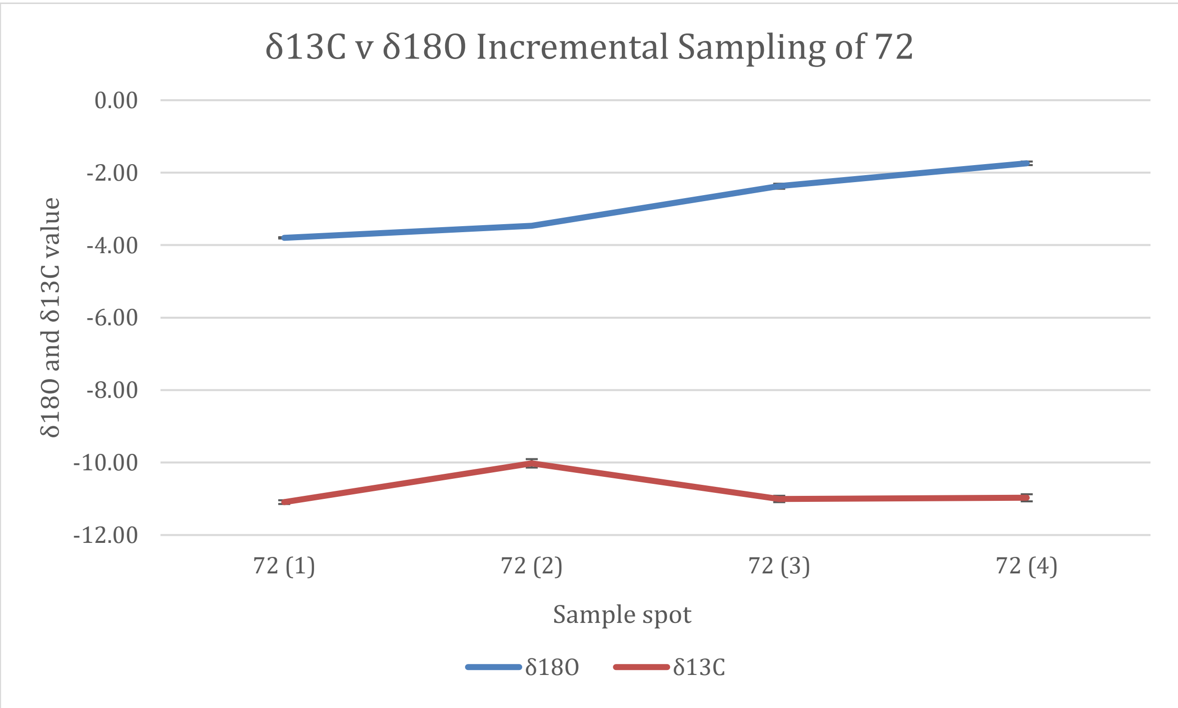

Figure 5. 16: Comparison of δ13C and δ18O of sample 72.

5.4 Payre: strontium

A total of 14 teeth from the site of Payre were analysed for their strontium isotope composition

Samples G6 O5 114, G5 N7 860, G4 O7 271, G4 M6 585, G3 N8 423, G3 N8 420, G2 N9 82, F9 L4 791, F7 L4 662, F6 L5 729, F1 N4 2, F N8 141, D M1 Lower (t1) and D M1 Lower (t2) from the site of Payre were analysed for strontium isotope concentration using LA-MC-ICPMS.

The mean strontium values for each sample are outlined in Table 5.5 and Figure 5.17 below.

Sample	Material	$^{87}Sr/^{86}Sr$	$^{87}Sr/^{86}Sr$ σ^2 error	Total Spots
G6 O5 114	Enamel	0.710737	0.000077	3
G6 O5 114	Dentine	0.70931	0.00026	3
G5 N7 860	Enamel	0.70764	0.00031	84
G5 N7 860	Dentine	0.70752	0.00013	76
G4 O7 271	Enamel	0.710665	0.0001	47
G4 O7 271	Dentine	0.70968	0.00021	41
G4 M6 585	Enamel	0.707734	0.000077	34
G4 M6 585	Dentine	0.70923	0.00017	28
G3 N8 423	Enamel	0.715846	0.000075	58
G3 N8 423	Dentine	0.71434	0.00031	30
G3 N8 420	Enamel	0.71355	0.00011	9
G3 N8 420	Dentine	0.71034	0.00018	19
G2 N9 82	Enamel	0.714352	0.00006	45
G2 N9 82	Dentine	0.710887	0.000054	49
F9 L4 791	Enamel	0.71555	0.00011	37
F7 L4 662	Enamel	0.706327	0.000081	38

F7 L4 662	Dentine	0.706342	0.000053	41
F6 L5 729	Enamel	0.710739	0.000063	28
F6 L5 729	Dentine	0.70958	0.000024	14
F1 N4 2	Enamel	0.708098	0.000032	80
F1 N4 2	Dentine	0.708264	0.000083	66
F N8 141	Enamel	0.709555	0.000042	78
F N8 141	Dentine	0.708885	0.000059	20
D M1 Lower (t1)	Enamel	0.70826	0.00019	38
D M1 Lower (t1)	Dentine	0.70927	0.000097	38
D M1 Lower (t2)	Enamel	0.709153	0.000035	54

Table 5. 4: Summary table of Payre faunal LA-MC-ICPMS Sr^{87}/Sr^{86} isotope results.

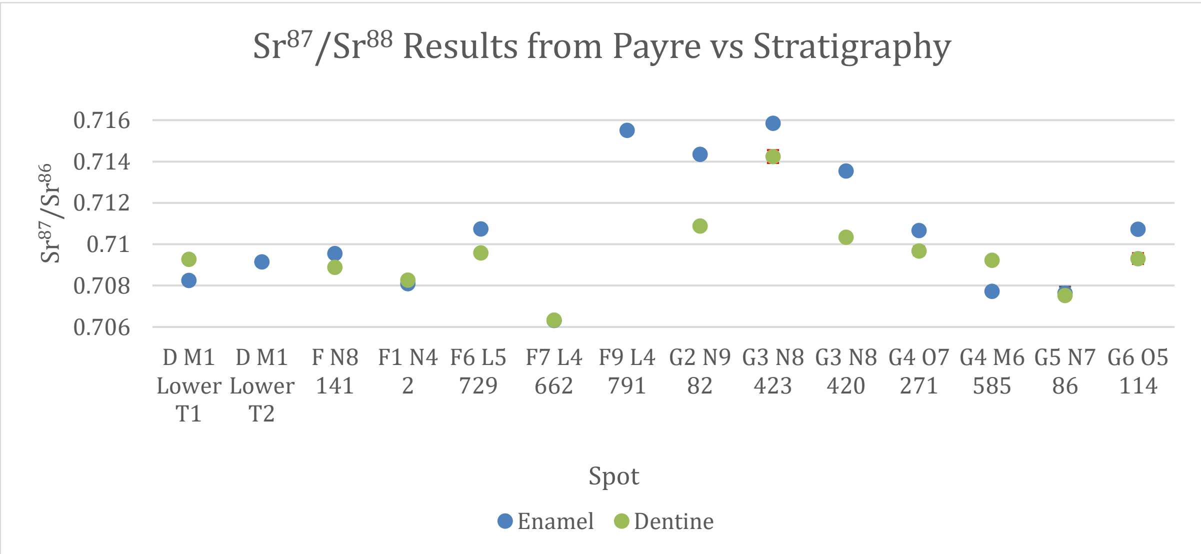

Figure 5. 17: Mean values for Payre LA-MC-ICPMS Sr^{87}/Sr^{86} isotope results.

Sample G6 O5 114

Strontium concentrations were collected for 3 spots within the enamel, and 3 spots within the dentine of sample G6 O5 114.

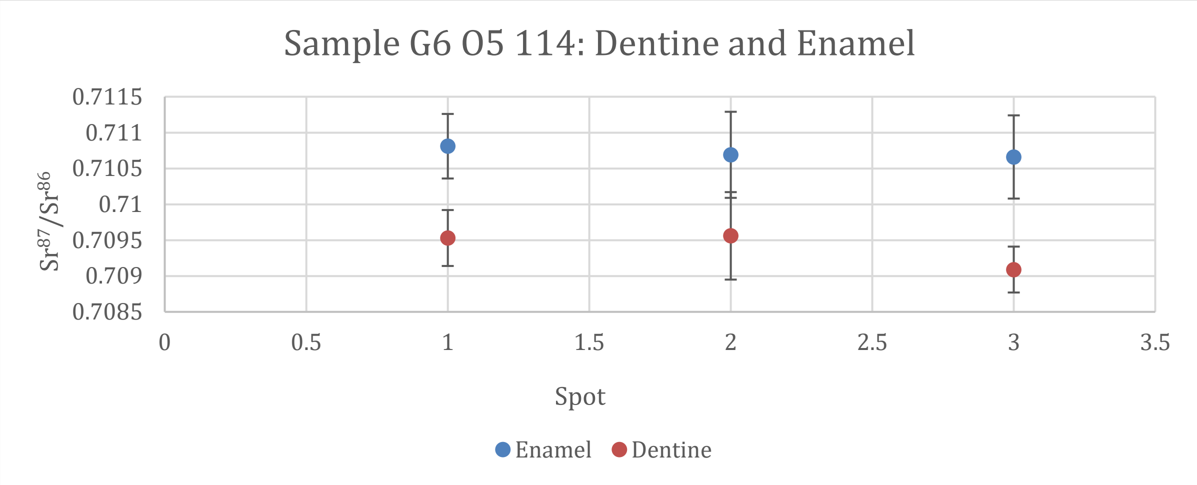

Figure 5. 18: Sample G6O5114 Sr^{87}/Sr^{86} dentine and enamel values.

Sample G5 N7 860

Strontium concentrations were collected for 84 spots within the enamel, and 76 spots within the dentine of sample G5 N7 860.

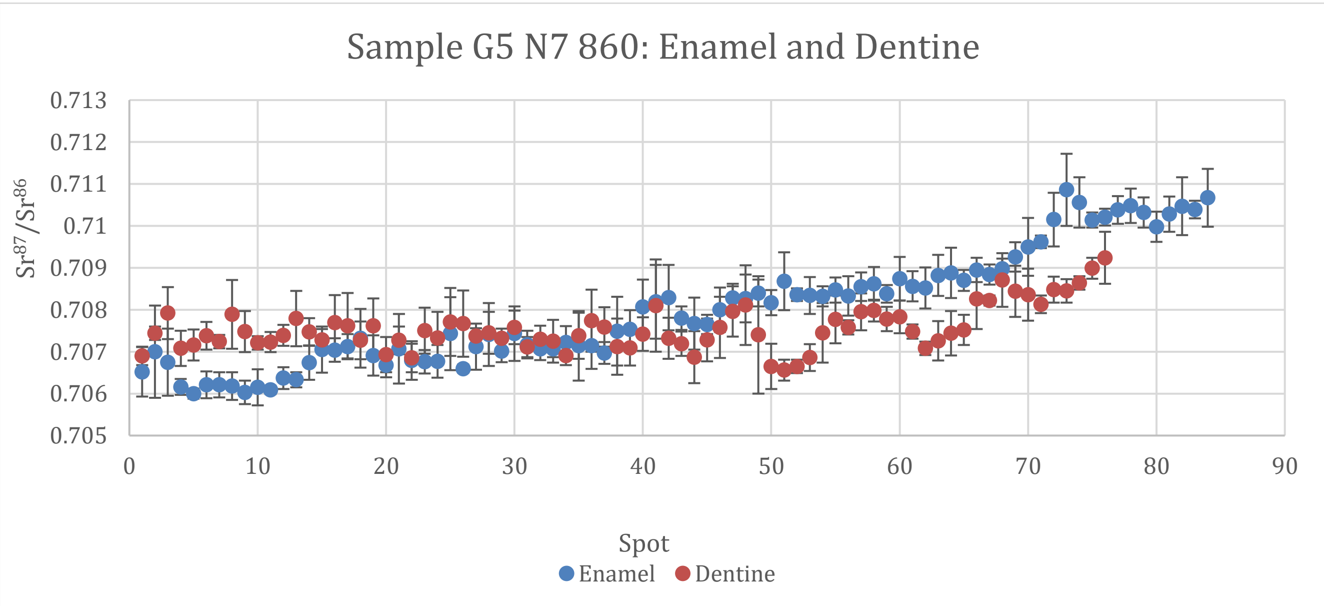

Figure 5. 19: Sample G5N7860 Sr^{87}/Sr^{86} enamel and dentine values.

Sample G4 O7 271

Strontium concentrations were collected for 47 spots within the enamel, and 41 spots within the dentine of sample G4 O7 271.

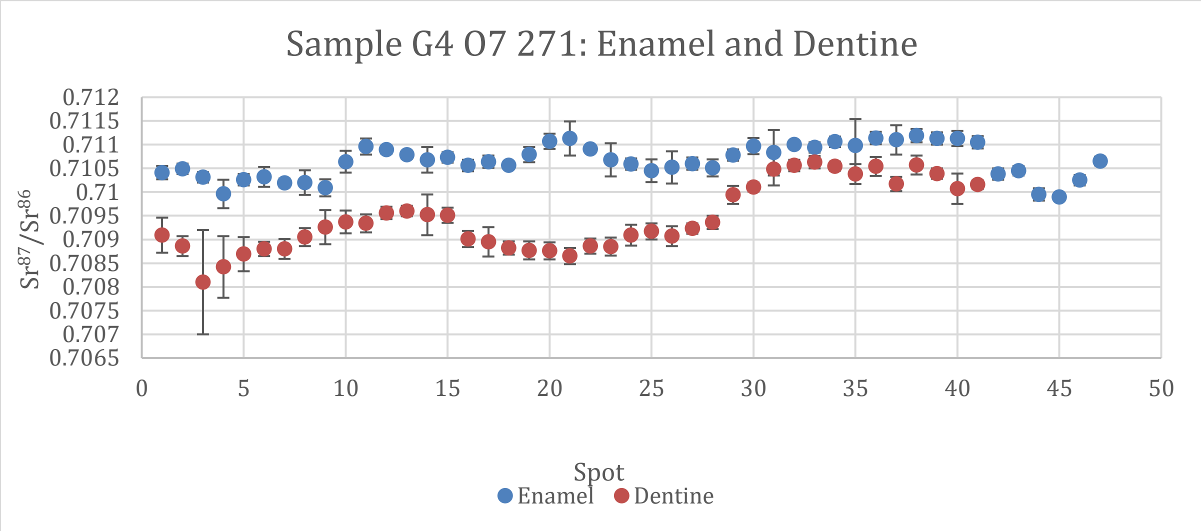

Figure 5. 20: Sample G4O7271 Sr^{87}/Sr^{86} enamel and dentine values.

Sample G4 M6 585:

Strontium concentrations were collected for 34 spots within the enamel, and 28 spots within the dentine of sample G4 M6 585.

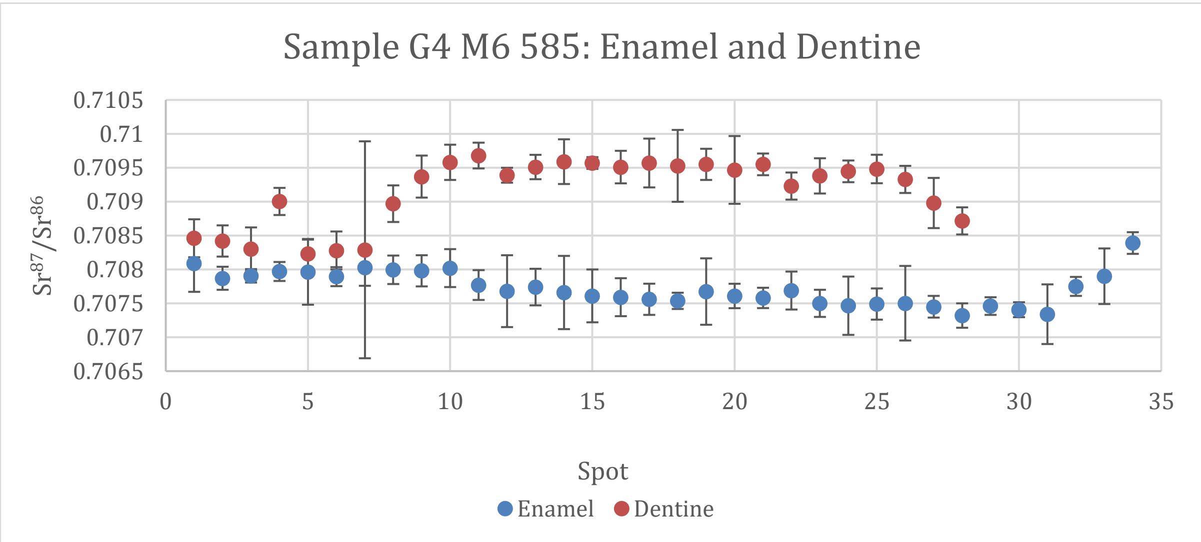

Figure 5. 21: Sample G4M6585 Sr^{87}/Sr^{86} enamel and dentine values.

Sample G3 N8 423

Strontium concentrations were collected for 58 spots within the enamel, and 30 spots within the dentine of sample G3 N8 423.

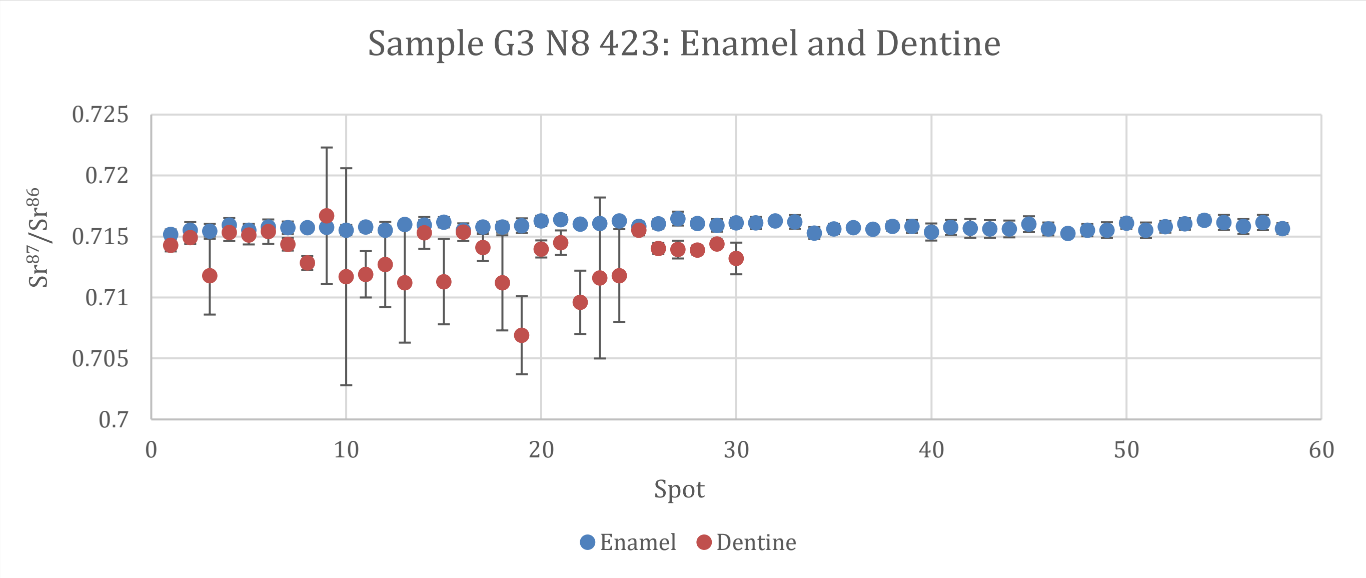

Figure 5. 22: Sample G3N8423 Sr^{87}/Sr^{86} enamel and dentine values.

Sample G3 N8 420

Strontium concentrations were collected for 9 spots within the enamel, and 19 spots within the dentine of sample G3 N8 420.

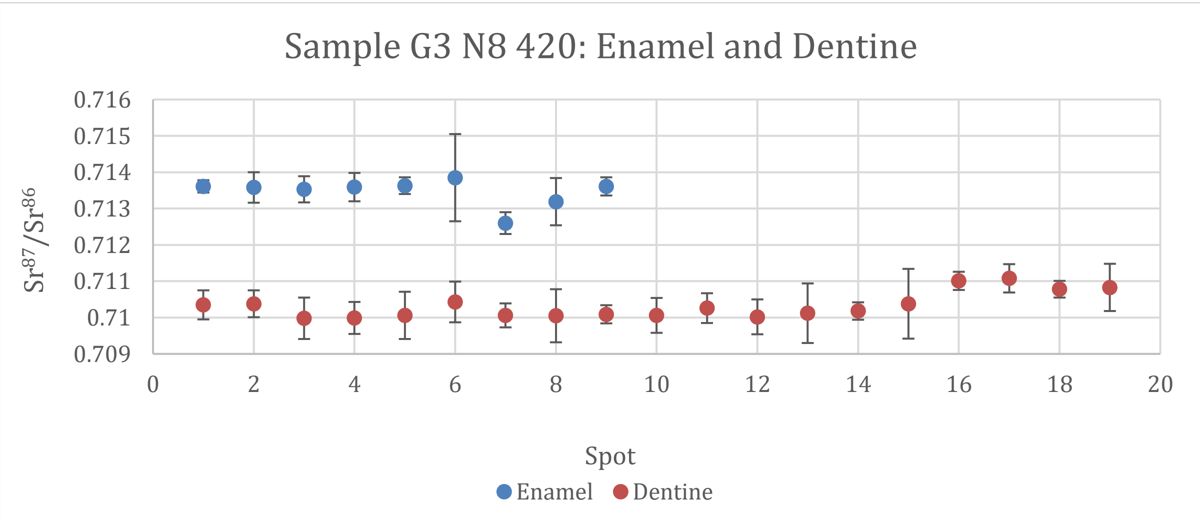

Figure 5. 23: Sample G3N8420 Sr^{87}/Sr^{86} enamel and dentine values.

Sample G2 N9 82

Strontium concentrations were collected for 45 spots within the enamel, and 49 spots within the dentine of sample G2 N9 82.

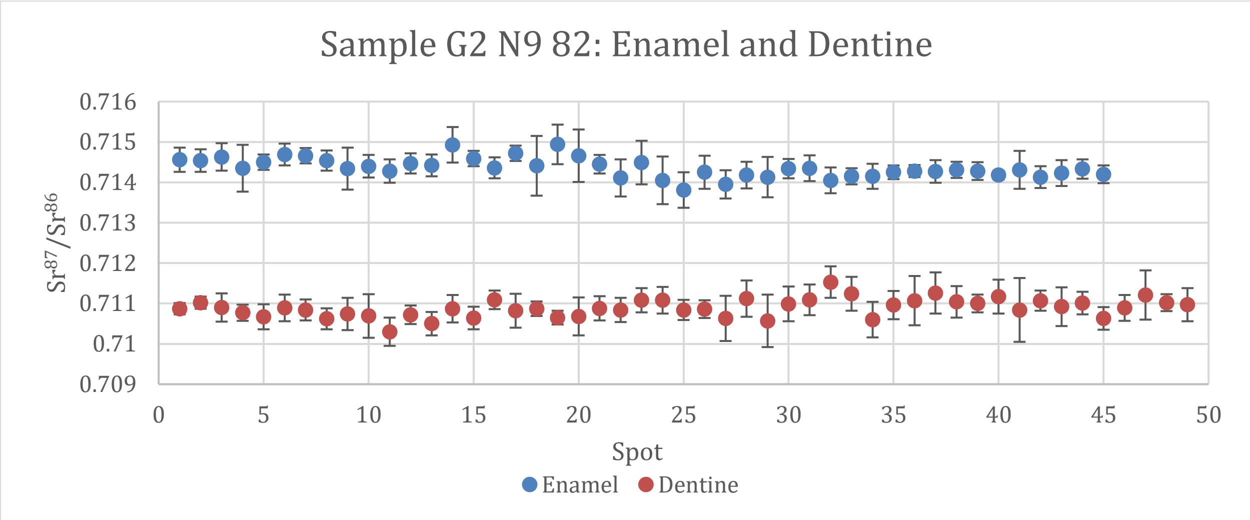

Figure 5. 24: Sample G2N982 Sr^{87}/Sr^{86} enamel and dentine values.

Sample F9 L4 791

Strontium concentrations were collected for 37 spots within the enamel, however were unable to sample any dentine from the sample F9 L4 791.

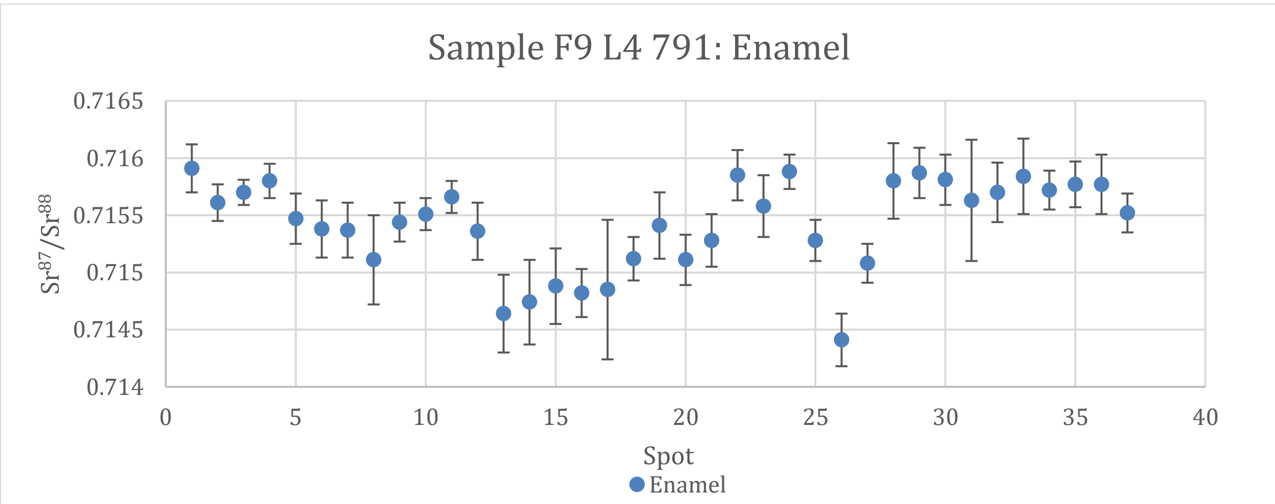

Figure 5. 25: Sample F9L4791 Sr^{87}/Sr^{86} enamel values.

Sample F7 L4 662

Strontium concentrations were collected for 38 spots within the enamel, and 41 spots within the dentine of sample F7 L4 662.

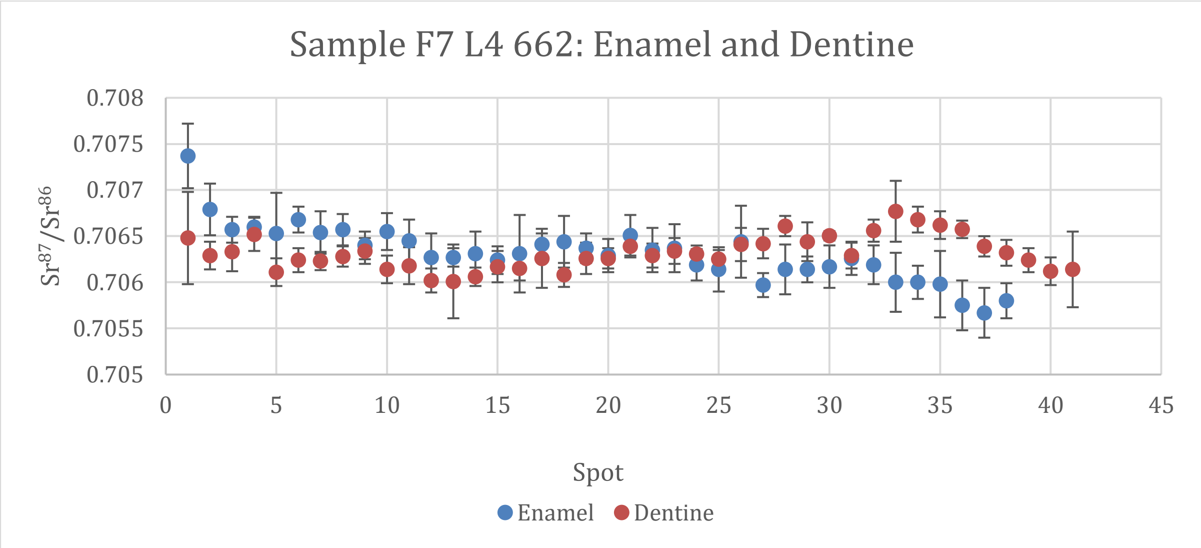

Figure 5. 26: Sample F7L4662 Sr^{87}/Sr^{86} enamel and dentine values.

Sample F6 L5 729

Strontium concentrations were collected for 28 spots within the enamel, and 14 spots within the dentine of sample F6 L5 729.

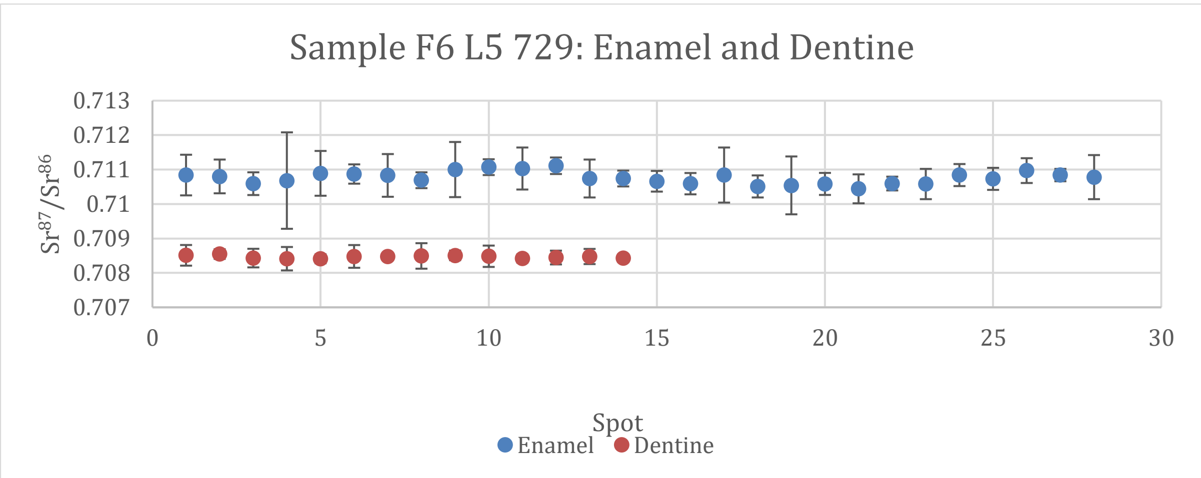

Figure 5. 27: Sample F6L5729 Sr^{87}/Sr^{86} enamel and dentine values.

Sample F1 N4 2

Strontium concentrations were collected for 80 spots within the enamel, and 66 spots within the dentine of sample F1 N4 2.

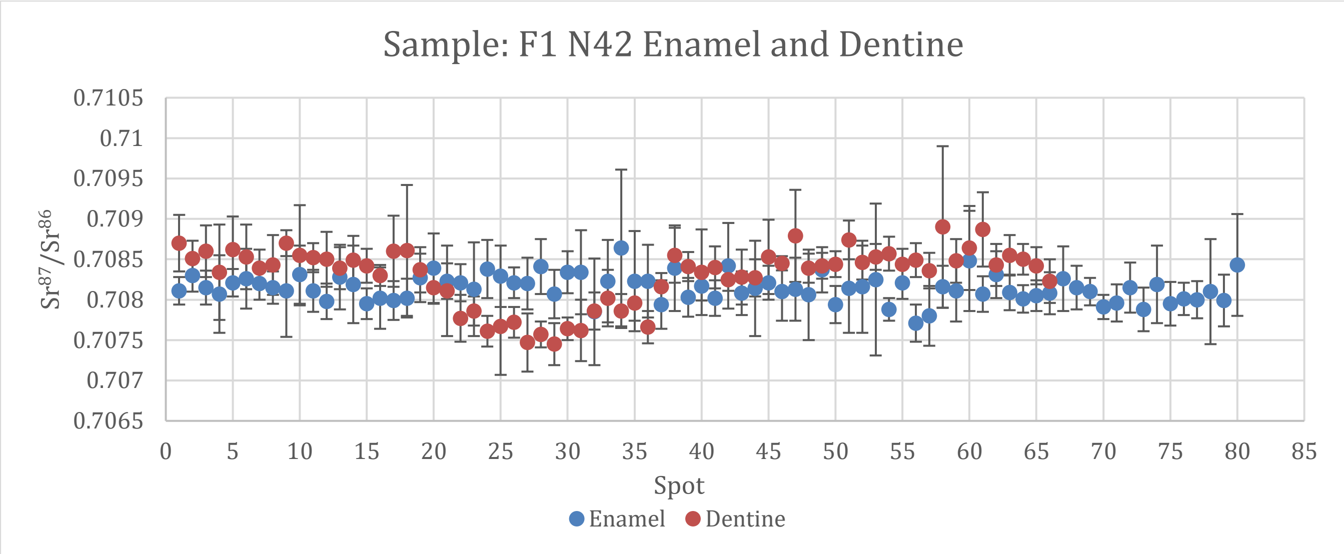

Figure 5. 28: Sample F1N42 Sr^{87}/Sr^{86} enamel and dentine values.

F N8 141

Strontium concentrations were collected for 78 spots within the enamel, and 20 spots within the dentine of sample F N8 141.

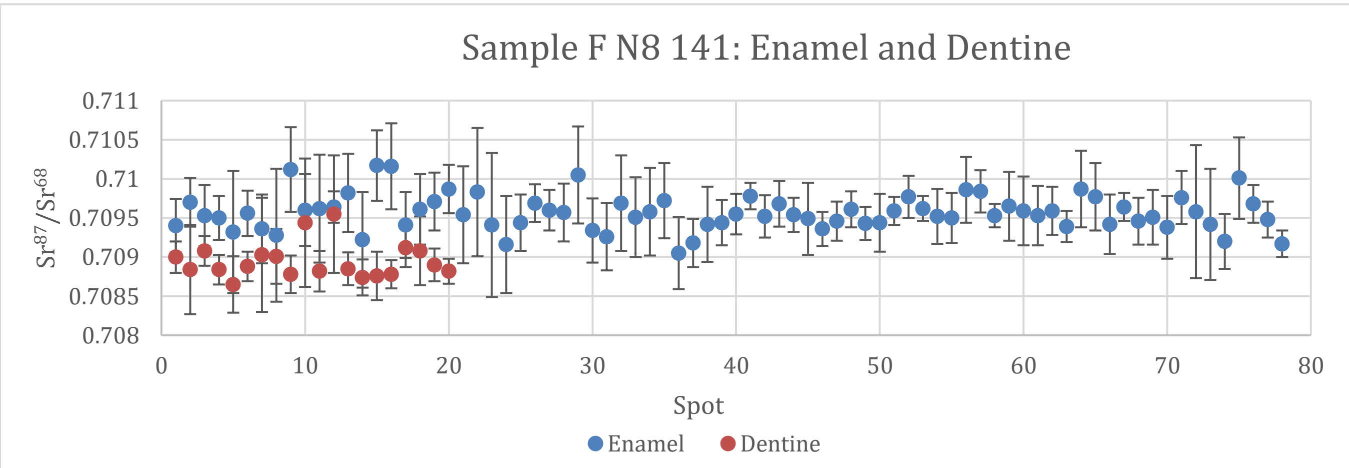

Figure 5. 29: Sample Fn814 Sr^{87}/Sr^{86} enamel and dentine values.

Sample D M1 Lower (t1)

Strontium concentrations were collected for 38 spots within the enamel, and 38 spots within the dentine of sample D M1 Lower (t1).

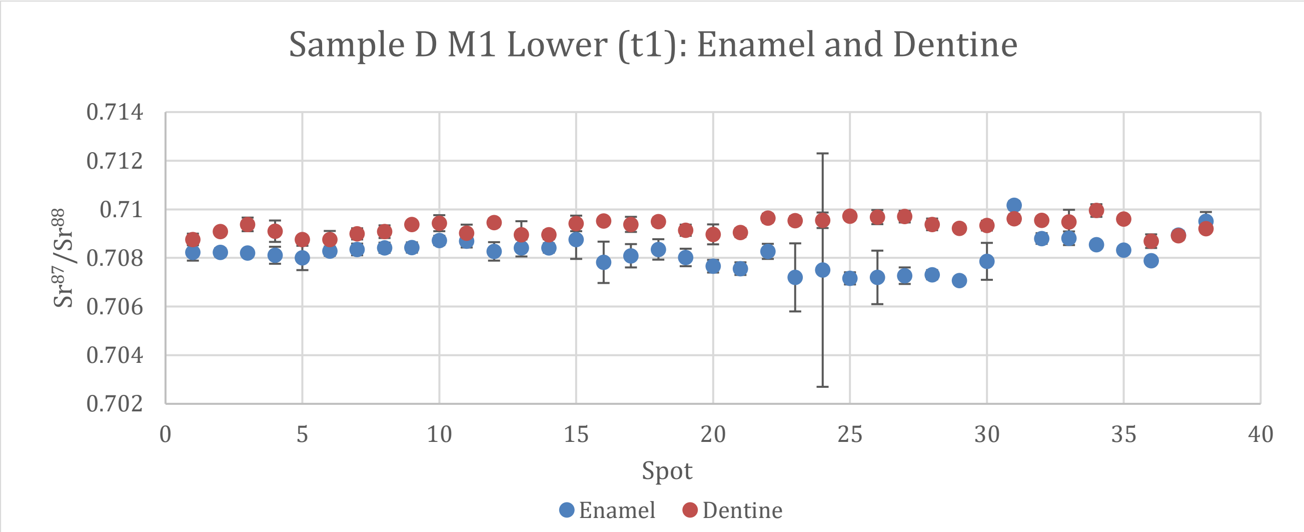

Figure 5. 30: Sample DM2t1 Sr^{87}/Sr^{86} enamel and dentine values.

Sample D M1 Lower (t2)

Strontium concentrations were collected for 54 spots within the enamel, however were unable to sample any dentine from the sample D M1 Lower (t2).

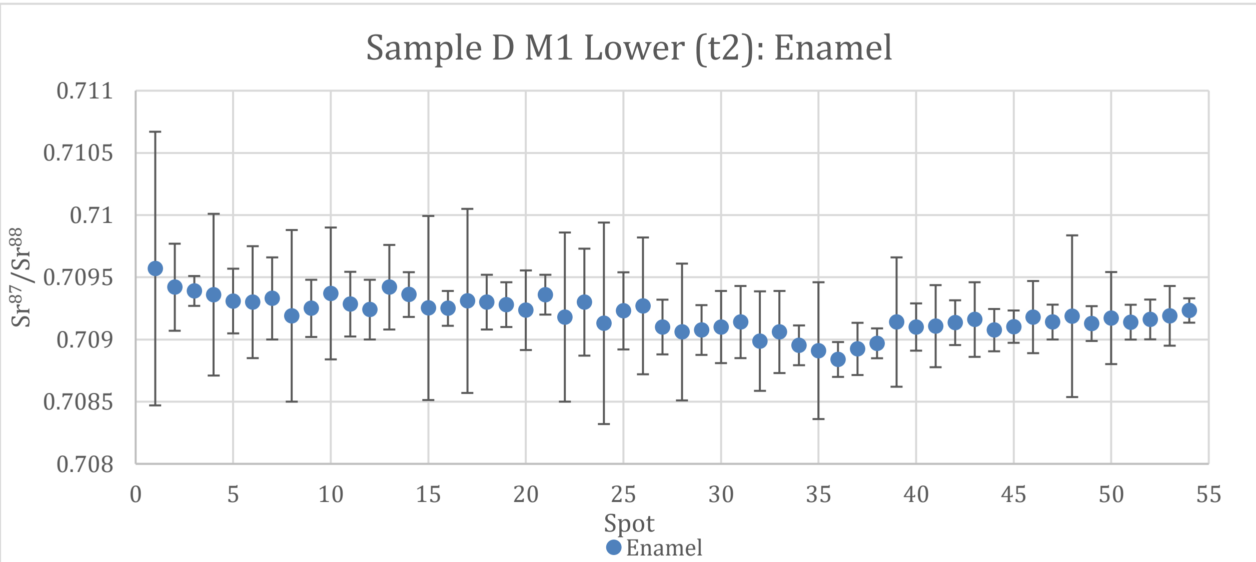

Figure 5. 31: Sample DM1t2 Sr^{87}/Sr^{86} enamel values.

5.5 Payre: oxygen and carbon

The results of the oxygen and carbon analysis are shown here, in descending order from the most recent layer of the site (D) to the oldest (G).

Sample	$\delta^{18}O$	Error σ^2	$\delta^{13}C$	Error σ^2
D-M1-T1	-4.26	0.09	-13.71	0.09
D-M1-T2	-5.11	0.01	-11.58	0.11
F1N42	-4.87	0.07	-13.14	0.08
FM51039	-5.99	0.14	-11.81	0.03
FN8141	-3.77	0.05	-14.54	0.06
F6L5729	-2.96	0.11	-10.45	0.12
F7L4662	-5.34	0.11	-11.17	0.02
F9L4791	-5.52	0.10	-11.61	0.08
G2N982 1	-4.22	0.20	-12.08	0.07
G3N8423	-4.76	0.06	-11.55	0.05
G3N8420	-4.76	0.13	-10.95	0.05
G407271	-5.66	0.11	-10.02	0.03
G4M6585	-4.19	0.09	-13.22	0.22
G5N7860	-7.86	0.15	-9.46	0.06
G605114	-4.68	0.10	-9.20	0.06

Table 5. 5: Payre δ18O and δ13C results.

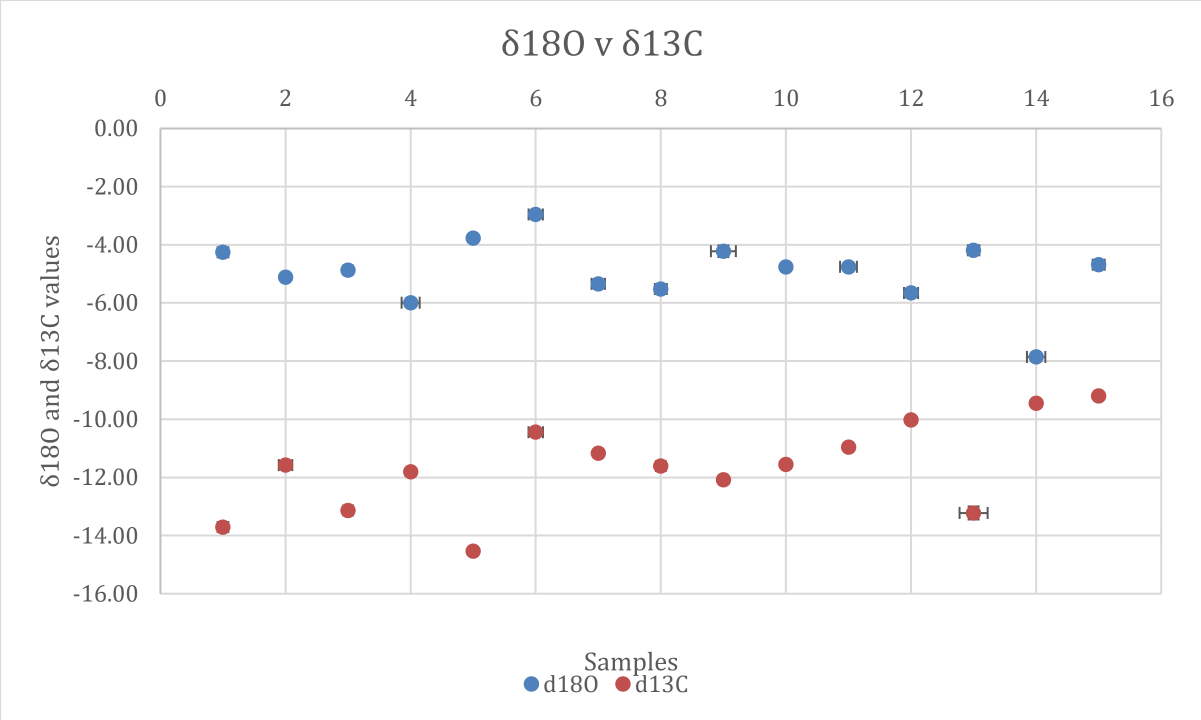

Figure 5. 32: Comparison of δ18O and δ13C results.

Incremental sampling was undertaken of sample G2 N9 821.

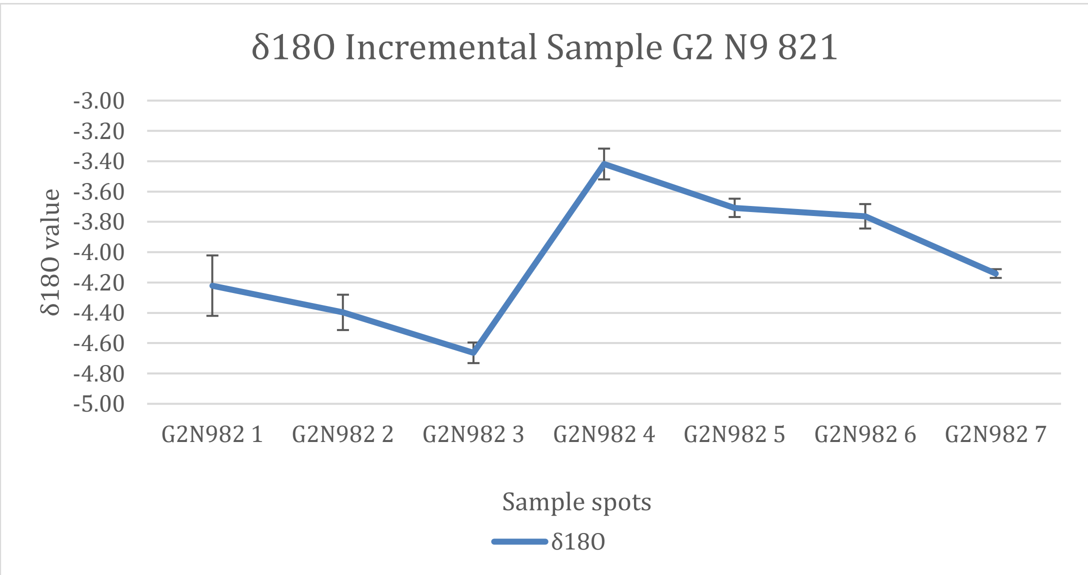

Figure 5. 33: δ18O incremental sampling of G2N9821.

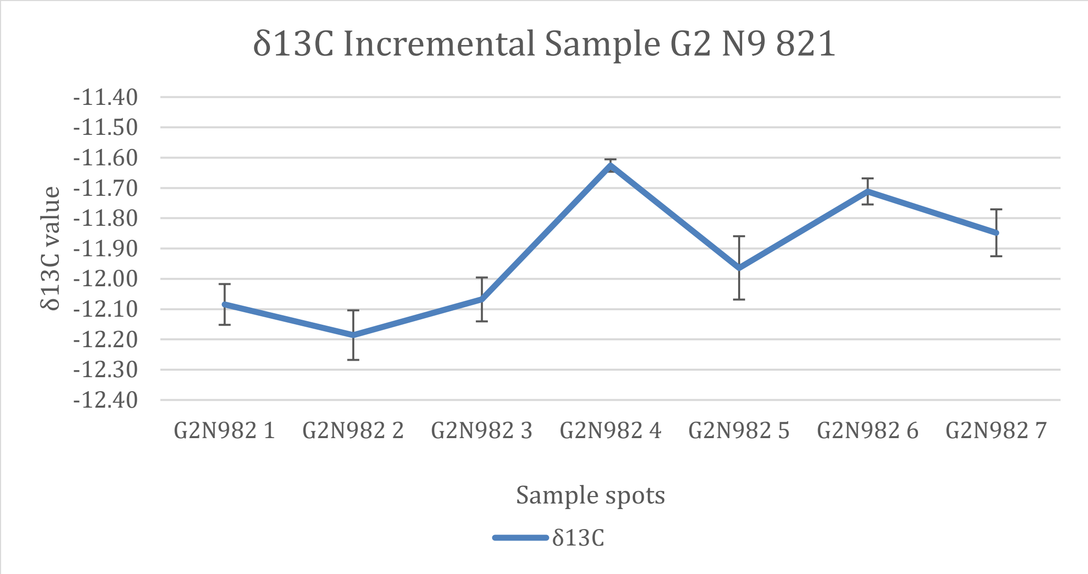

Figure 5. 34: δ13C incremental sampling of G2N9821.

5.5 Holon and Payre mean and min-max strontium graphs

The following figures were created to represent the minimum and minimum maximum possible distances the individual animals could have moved in relation to the site. The Payre values are plotted in a temporal fashion to show changes in mobility overtime. The Holon values are plotted to compare species.

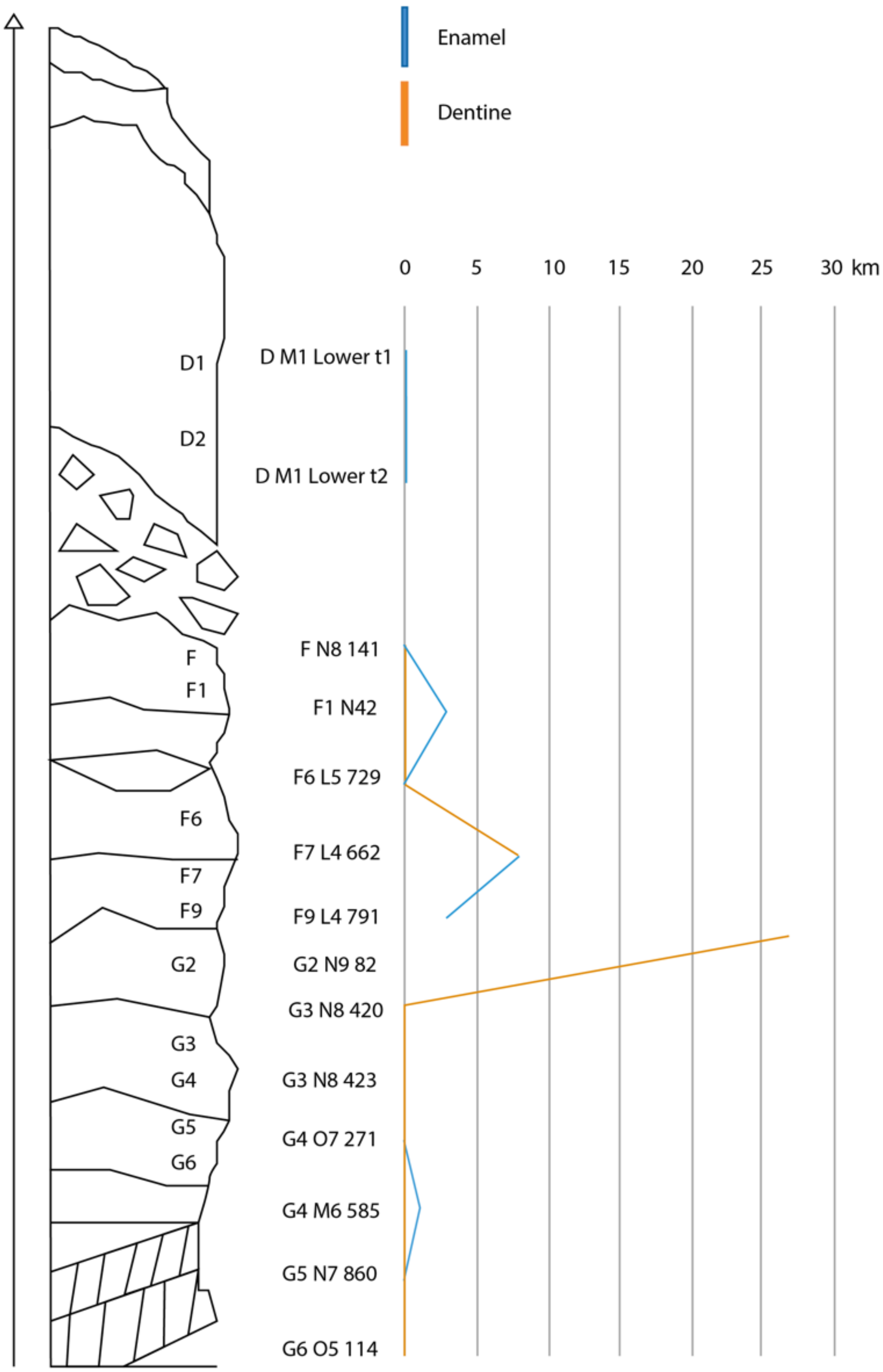

Figure 5. 35: Mean distance travelled by fauna from the site of Payre.

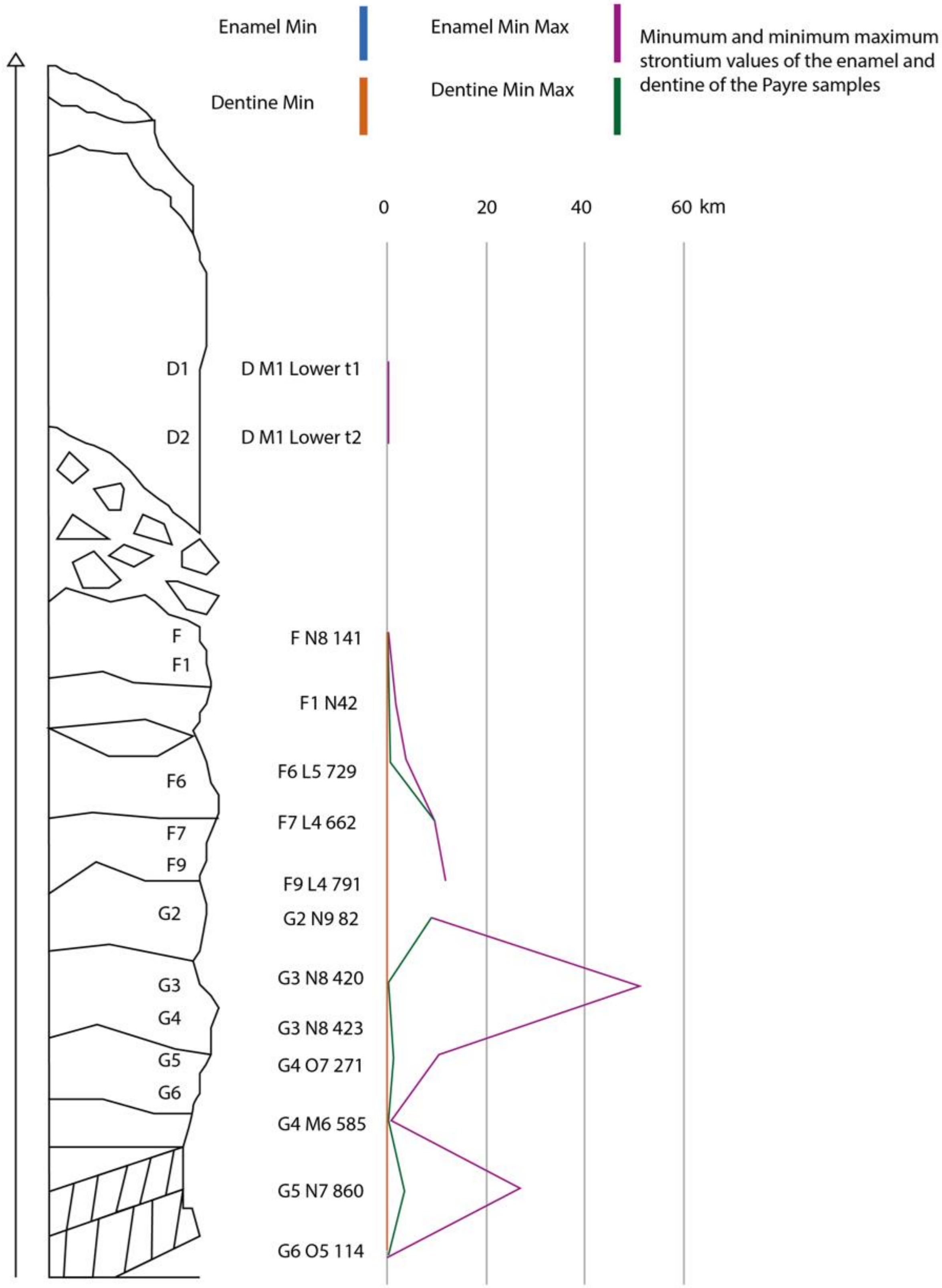

Figure 5. 36: The minimum and the maximum, minimum distances that the fauna could have travelled from the site of Payre.

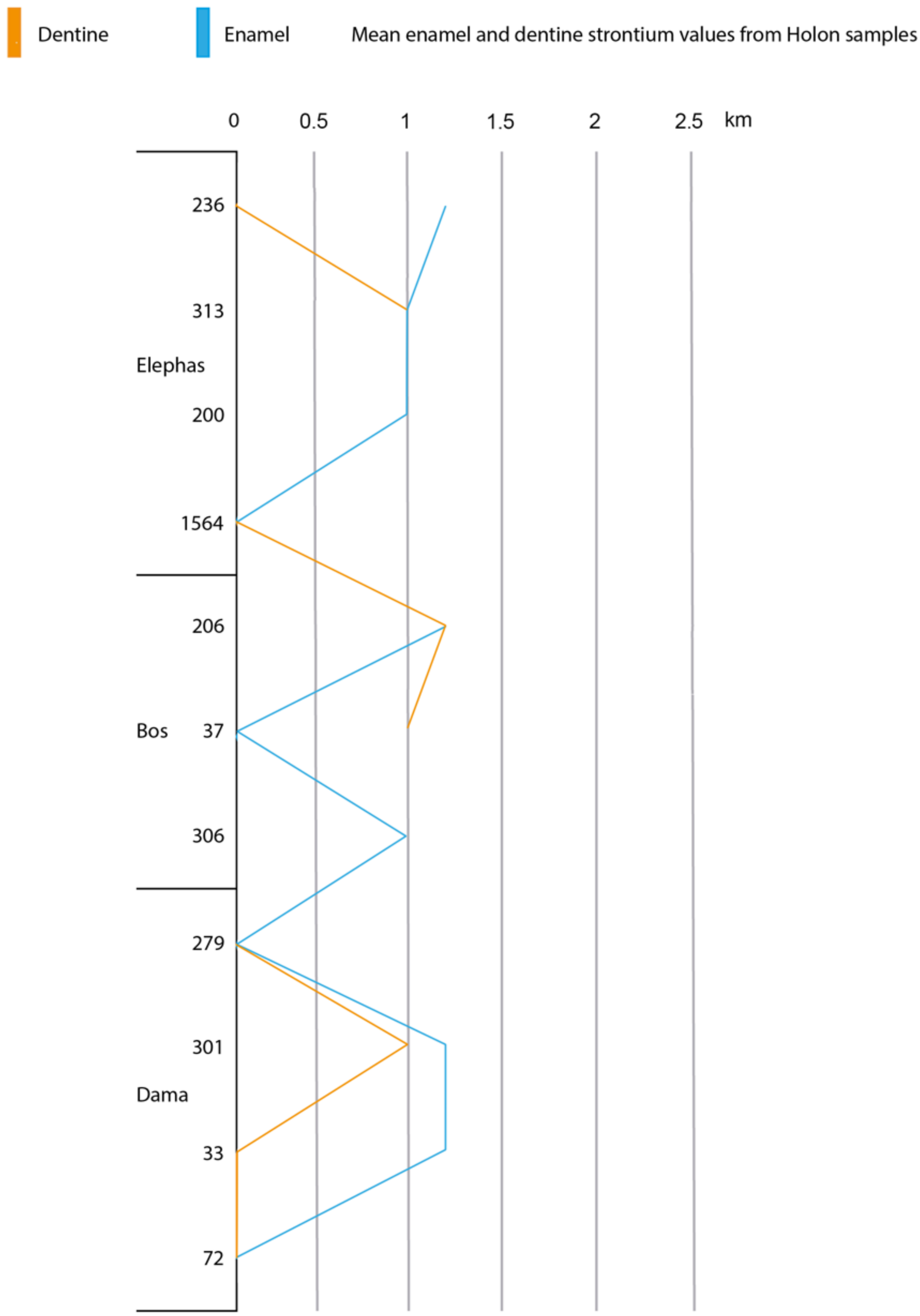

Figure 5. 37: Mean distance travelled by fauna from the site of Holon.

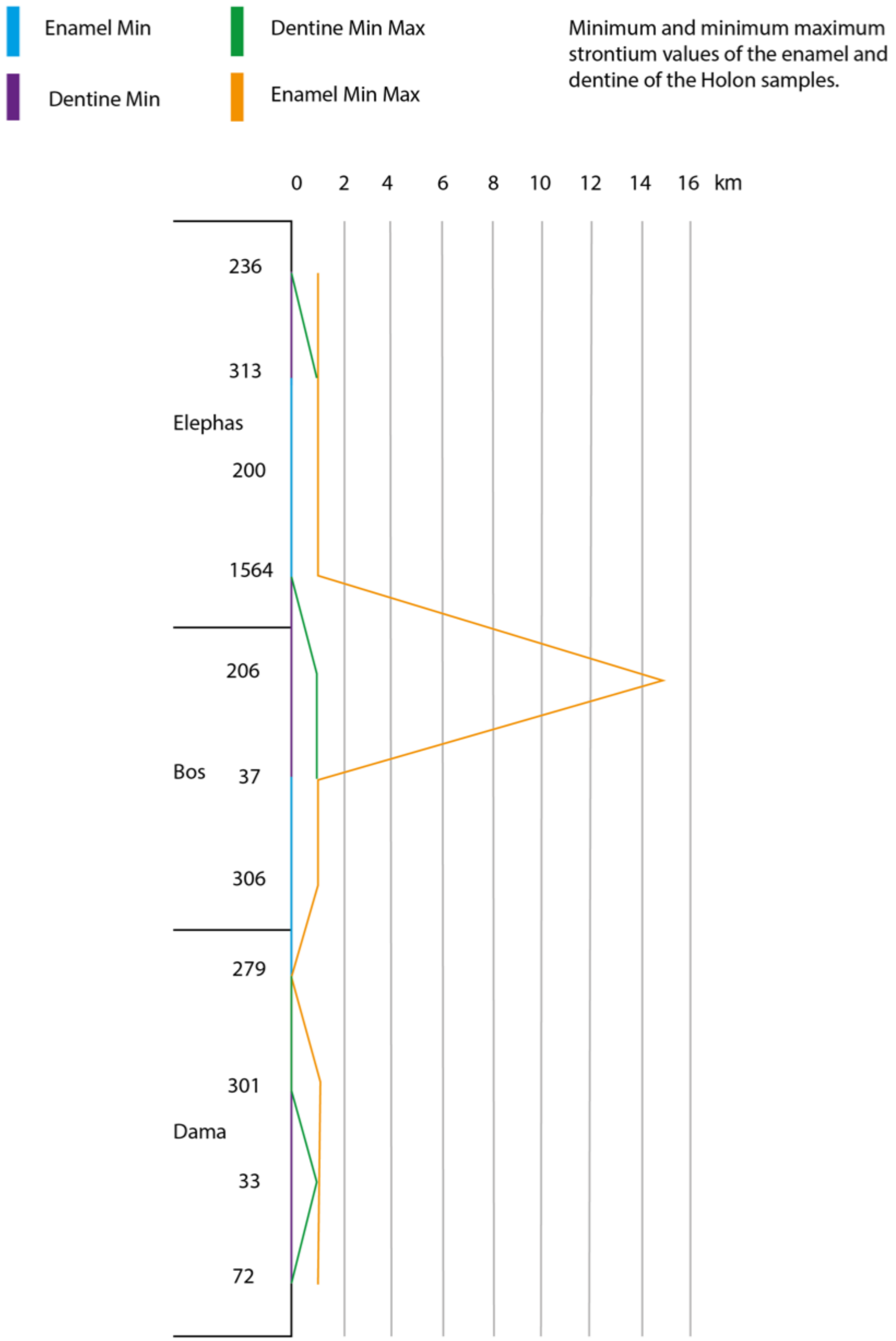

Figure 5. 38: The minimum and the maximum, minimum distances that the fauna could have travelled from the site of Holon.

Chapter Six: Discussion

The results of the stable isotope analysis of *Bos*, *Dama*, and *Palaeoloxodon* provide important insight into the mobility and diet of these prey as well as their changes in movement over time in relation to changing climate. Understanding the predation behaviours of early hominins such as *Homo erectus* and Neanderthals can be gained through examination of the diet and mobility of their prey and environment it was living in. As such, the application of this type of analysis to Palaeolithic archaeology is full of potential. The detailed analysis of each sample can be found in Appendix 2.

Comparison of *Bos Primigenius* mobility, diet and palaeo-environment at the two sites:

The strontium analysis of *Bos* from Holon and Payre show a vastly different range in mobility. The animals at Holon had a maximum range of 1.2 km from the site and showed little heterogeneity within the incremental sampling. These animals were only moving between the site and areas close by. Holon is located in an attractive area for fauna with a fluctuating freshwater marsh nearby (Horwitz and Chazan 2006) and the limited mobility of the animals suggests they did not need to be mobile to access resources. These samples date to the end of MIS 7 (Porat et al. 1999), which according to Cheddadi and Rossignol-Strick (1995) was when Israel was moving to a more arid climate, and the Mediterranean forest was being replaced by semi-desert vegetation. Under these circumstances access to water would have been even more attractive.

Payre however provides a different picture. The mobility of these animals changes systematically between the stratigraphic levels of the site, probably driven by variations in palaeoclimate. Figures 5.3 and 5.4 show this difference clearly, with the minimum distance of mobility changing from no movement in level D, to a minimum distance of 50km from the site in level G. Level D, as described by Moncel et al. (2009:1895) has a humid, temperate environment. The lack of mobility in level D (a mediterranean climate) suggests there was little need to migrate far for food or water. The environment here was still temperate in levels F and G, which was a forest environment (Reille et al. 1998; Reille and de Beaulieu 1990) however would have been cooler than the later period of level D. It is unsurprising then that there was a dramatic increase in mobility through time, with *Bos* in the earlier levels F and G showing greater mobility. The range of mobility in level G reached up to 51km from the site, far greater even than the maximum distance reached of 8km in layer F.

This analysis fits with earlier research performed using dental analysis, particularly that of Rivals et al. (2009:1074) who noted that the dietary habits of fauna around Payre were likely linked to the climate. During the colder season when dietary resources were limited, the fauna would have been moving further. The more arid climate in Holon, the increase in semi-desert vegetation and its location to a freshwater marsh likely all contributed to the lower level of mobility in the fauna compared to the fauna in Payre. The cooler (although still temperate) environment during MIS 7 that the Payre fauna (in levels G and F) lived in as well as the lack of freshwater so close to the site, suggest these animals were ranging further in order to find the necessary dietary resources.

The mobility of *Bos* at Holon is lower than that of some previous studies, Moffat (2013) found that the greatest distance was 7.6 km with a median value of 3.2 km. This may however reflect the location of the site and the access to ready sources of fresh water at Holon. Like Moffat (2013) however, the Israeli samples showed far less mobility than the French samples.

The $\delta^{13}C$ was similar between both sites, with both sets of fauna falling within the range of C_4 grasses. Despite the hot, dry conditions in the Israel region, modern Israel is dominated by C_3 grasses (61%) (Vogel et al. 1986). In regions which fall within the winter rainfall pattern of the mediterranean, this is to be expected (Vogel et al. 1986). Modern France is also dominated by C_3 plants (Bremond et al. 2012). However Bremond et al. (2012) point out that during and prior to the LGM there would have been a greater C_4 biomass. C_3 plants fall within a range of ~-20 to -37‰ (Kohn 2010) while C_4 vegetation have a threshold around 19.2% (Urban 2015). These samples (Table 5.3, 5.5) show a range of -9.20‰ to -14.54‰ (Payre) and -9.48‰ to -11.23‰ (Holon) which places

them within the range of a C_4 grass. Analysis was performed for $\delta^{13}C$ on 16 *Bos* or *Bison* from the Middle Palaeolithic site of Neumark-Nord 2, and the results showed much higher $\delta^{13}C$ in general and fell within the expected range for C_3 terrestrial animals (Britton et al 2012:172).
Analysis by Widga et al. (2010) who performed a study on modern Bison in the Great Plains showed that the bison were eating a combination of C_3 and C_4 grasses. C_4 grasses tend to grow in 'open and unshaded areas' (Andrews and Hixson 2014:270). The environment of Israel during this climatic period was moving toward an arid environment by the end of MIS 7, which the samples were identified as belonging to. Levels G and F at Payre were associated with changes in MIS 7 where steppe environments were more common. While studies such as Britton et al. (2012) indicated a higher level of C_3 vegetation in the same time-period in Germany, the climate in France during MIS 7 was clearly different or variable enough that C_4 vegetation was the most wide-spread, or easily accessible for the animals at Payre. The palaeoenvironment at Holon which was trending toward arid had a lot of open environment, perfect for C_4 grasses. Similarly to the $\delta^{13}C$ results, the $\delta^{18}O$ results were similar across the two sites (Table 5.3, 5.5).

Unfortunately in this study, the fractionation rate had not yet been worked out so the values can be compared against each other in context, but aren't very useful in a broader scale analysis of $\delta^{18}O$ values or palaeoenvironment when compared to other studies. In this case, the *Bos* at Holon show slightly lower $\delta^{18}O$ than at Payre. Because the ratio of oxygen isotopes is taken up into the enamel when the animal drinks, the ratio works as a proxy for palaeo-precipitation and palaeo-temperature (Aubert et al. 2011). In this case it suggests the temperatures at least for the end of MIS 7 were similar, but there was likely more precipitation around Payre than Holon.

Dama and *Palaeoloxodon* mobility, diet and palaeo-environment

The strontium analysis of the *Dama* and *Palaeoloxodon* at Holon both revealed a very low distance of mobility. The *Palaeoloxodon* had a maximum range of mobility from the site of 1.2 km, with the rest of the samples not moving further than 1 km from the site. The *Dama* was similar, with a maximum range of 1.2 km, and one sample not being mobile at all. *Palaeoloxodon antiquus* are primarily associated with more forested, wooded environments, however it has been found in more open contexts through Europe (Davies and Lister 2007:123). They appeared to have migrated through the Levant and into Europe however the evidence for the route of their migration or their mobility in general is limited (Davies and Lister 2007:123). *Dama dama* are considered to have a home range of 2km (Di Luzio 2005), and the animals at Holon are keeping well within that range. The low levels of mobility of these animals may be due to the same factors as the *Bos* in Holon, the location of the site in regard to fresh water in an increasingly arid climate. The $\delta^{13}C$ analysis (Table 5.3) shows the species are statistically indistinguishable from each other. Differences in $\delta^{13}C$ isotope values are often seen between species (Cerling and Harris 1999) although the reasons behind this remain debated (Britton et al. 2012:172). In this case however, the *Palaeoloxodon*, *Dama,* and the *Bos,* as discussed above all have very similar $\delta^{13}C$ values, suggesting that while there are different physiological factors that determine how carbon is incorporated into tissue between species, in this case C_4 grasses must have been the most abundant or appealing for all species. Rowland (2006) found that their $\delta^{13}C$ results for *Dama* were - 10 to -12‰ which matched these results. The $\delta^{18}O$ analysis (Table 5.3) was also strikingly similar, unsurprising perhaps given the location of fresh water near to the site. It appears likely the fauna would have been drinking the same water and would therefore have similar $\delta^{18}O_{bw}$ values.

Archaeological implications

The site of Payre was inhabited regularly by *H. neanderthalensis* populations during the more temperate climatic periods of MIS 8-7 to MIS 5 (Rivals et al. 2009:1070). The hunting of *Bos* likely took place for most of the year, but not during winter (Rivals et al. 2009:1072). The lower levels of mobility observed in level D correlate with a humid, temperate environment – a climate in which there was little need for *Bos* to range far for sources of food. Layers G and F however have periods of time associated with cooler, less temperate climates (Moncel et al. 2009; Reille et al. 1998; Reille and de Beaulieu 1990). It is in these levels that the mobility of the fauna increases dramatically, yet they still appear to pass the site. *H. neanderthalensis* are commonly accepted as being capable hunters (Bocherens et al. 2005; Hardy and Moncel 2011; Patau-Mathis 2000; Richards et al. 2000; Richards et al. 2008 and Villa and Lenoir 2006). The large array of fauna found at Payre beyond the samples analysed in this research suggests that Payre was a popular migratory area for many fauna, and the *H. neanderthalensis* appear to deliberately exploit this, so they have access to food regardless of season. The results in this thesis suggest that *H. nenderthalensis* are not only capable hunters, but they are good at strategically choosing locations where their prey will come to them.

H. erectus is primarily considered a scavenger (Isaac 1978; 1983; Binford 1981; Brain 1981; Blumenschine et al. 1994; Mitchell and Lane 2013). Primarily the debates that surround paint *H. erectus* predation behaviours argue they were a passive agent within the process of site formation, and that more often than not, the development of bone accumulations are the results of carnivores preying and *H. erectus* accessing this prey. Scavengers regularly minimize energy expenditure as a response to the uncertain availability of carrion (Ruxton and Houston 2004). As a result, most scavengers use an optimal searching strategy that maximises their encounter rate with resources (Lopez-Lopez et al. 2013). In the case of Holon, this strategy appears to have been to live near the water source where abundant non-mobile prey was available locally, particularly during the uncertain climatic conditions of MIS7 in Israel.

Conclusion

Using stable isotope analysis to investigate the lifeways of the fauna allows for more nuanced interpretation of sites. The sites of Payre and Holon were investigated, with 25 faunal teeth being analysed for their strontium, oxygen and carbon isotope composition. The Payre samples were then compared to the changing environment. A trend was seen with mobility increasing during the G layers and decreasing through to the D (the most modern) layers. The Holon samples were compared by species and all animals showed little range in mobility. The oxygen and carbon results were also examined over time but showed little change - the carbon values remained in the range for C_4 grasses across all layers.

When the early 'Man the Hunter' models were being developed, hunting became an indicator of intelligence and ability. However, this research suggests that the environment and climate were likely major factors in whether a hominin had to hunt or could scavenge successfully instead. The significant difference in the mobility of animals at the two sites is a clear indicator of this.

If hominin species are ignored, climate and vegetation differences are the best predictor of mobility. At Payre, mobility is highest in layer G (a forest environment) and decreases through to layer D (a mediterranean environment). At Holon the environment was semi-arid with a local water source, which is reflected in the low mobility of the prey. It is impossible to rigorously compare *H. erectus* to *H. neanderthalensis* prey mobility in the absence of two climate and landscape matched case studies. However, mobile species are less likely to die or be hunted by other species in a particular place, and so the low mobility at Holon may support the hypothesis that *H. erectus* are scavengers.

Using the mobility of fauna and the palaeoenvironment in which they lived as a lens to examine hominin predation behaviours is difficult, and perhaps at times tenuous. The environment and climate in which hominins lived likely had a huge impact on their ability or choice to hunt or scavenge, and differences in climate and vegetation are excellent predictors of prey mobility. It is clear in this research that the mobility behaviours of these prey correlate well with the expected hunting or scavenging behaviours of these hominins and adds nuance to the interpretation of these sites.

References

Andrews, P and S. Hixson Taxon-free methods of palaeoecology 2014 *Annales Zoologici Fennici* 51:269–284.

Antón, S.C. 2003 Natural history of Homo Erectus. *American Journal of Physical Anthropol*ogy 122:126–170.

Ardrey, R. 1961 *African genesis: A personal investigation into the animal origins and nature of man.* New York: Atheneum.

Ardrey, R. 1976 *The hunting hypothesis: A personal conclusion concerning the evolutionary nature of man.* New York: Atheneum.

Arppe, L., J.A. Karhu and S.L. Vartanyan 2009 Bioapatite $^{87}Sr/^{86}Sr$ of the last woolly mammoths: Implications for the isolation of Wrangel Island. *Geology* 37(4):347–350.

Aubert, M., I. S. Williams, K. Boljkovac, I. Moffat, M.H. Moncel, E. Dufour, R. Grun 2011 *In situ* oxygen isotope micro-analysis of faunal material and human teeth using a SHRIMP II: a new tool for palaeo-ecology and archaeology. *Journal of Archaeological Science* 39(2012):3184–3194.

Balasse, M 2002 Reconstruction dietary and environmental history from enamel isotopic analysis: time resolution of intra-tooth sequential sampling. *International Journal of Osteoarchaeology* 12(2002):155–165.

Beard, B.L. and C.M. Johnson 2000 Strontium isotope composition of skeletal material can determine the birth place and geographic mobility of humans and animals. *Journal of Forensic Science* 45(5):1049–1061.

Benson, A., L. Kinsley, M. Willmes, A. Defleur, H. Kokkonen, M. Mussi, R. Grun 2013 Laser ablation depth profiling of U-series and Sr isotope in human fossils. *Journal of Archaeological Science* 40(7):2991–3000.

Bentley, R.A., T.D. Price and E. Stephan 2004 Determining the `local' $^{87}Sr/^{86}Sr$ range for archaeological skeletons: A case study from Neolithic Europe. *Journal of Archaeological Science* 31(4):365–375.

Bentley, R.A. 2006 Strontium Isotopes from the earth to the archaeological skeleton: A review. *Journal of Archaeological Method and Theory* 13(3):135–187.

Bentley, R.A., H.R. Buckley, M. Spriggs, S. Bedford, C.J. Ottley, G.M. Nowell, C.G. Macpherson and D.G. Pearson 2007 Lapita migrants in the Pacific's oldest cemetery: Isotopic analysis at Teouma, Vanuatu. *American Antiquity* 72(4):645–656.

Bernard, A., V. Daux, C. Lecuyer, J.P. Brugal, D. Genty, K. Wainer, V. Gardien, F. Fourel, J. Aubert 2009 Pleistocene seasonal temperature variations recorded in the δ18O of *Bison priscus* teeth. *Earth and Planetary Science Letters* 283(2009):133–143.

Binford, L. R. 1981 Bones: *Ancient men and modern myths*. New York: Academic Press.
Binford, L. R., C. Kun Ho, J. S. Aigner, M.-H. Alimen, L. Alberto Borrero, C. Te-K'un, T. Chung, P. Goldberg, F. Ikawa-Smith, J. Luis Lanata, L. Zune, K. Luchterhand, R. Lee Lyman, G. Mengoni Gonalons, G. Pei, L. G. Straus, H. D. Yacobaccio and S. Yi 1985 Taphonomy at a Distance: Zhoukoudian, "The Cave Home of Beijing Man"? *Current Anthropology* 26(4):413–442.

Blum, J.D., E.H. Taliaferro, M.T. Weisse and R.T. Holmes 2000 Changes in Sr/Ca, Ba/Ca and $^{87}Sr/^{86}Sr$ ratios between trophic levels in two forest ecosystems in the northeastern U.S.A. *Biogeochemistry* 49(1):87–101.
Blumenschine, R. J 1988 Carcass consumption sequences and the archaeological distinction of scavenging and hunting. *Journal of Human Evolution* 15:639–659.
Blumenschine, R. J. 1991 Hominid carnivory and foraging strategies, and the socio-economic function of early archaeological sites. *Philosophical Transactions of the Royal Society London* 334: 211–221.
Blumenschine, R. J., J.A. Cavallo and S.D. Capaldo 1994 Competition for carcasses and early hominid behavioral ecology: A case study and a conceptual framework. *Journal of Human Evolution* 27:197–213.
Brain, C. K 1981 *The Hunters or the Hunted? An Introduction to African Cave Taphonomy.* University of Chicago Press.
Bryant, D.J., B. Luz and P. N Froelich 1994 Oxygen isotopic composition of fossil horse tooth phosphate as a record of continental palaeoclimate. *Palaeogeography, Palaeoclimatology, Palaeoecology* 107(1994):303–316.
Boehm, C. 1999 *Hierarchy in the forest: the evolution of egalitarian behaviour.* Cambridge: Harvard University.
Bocherens, H., D.B. Brinkmans, Y. Dauphin and A. Mariotti 1994 Microstructural and geochemical investigations on Late Cretaceous archosaur teeth from Alberta, Canada. *Canadian Journal of Earth Sciences* 31:783–792.
Bocherens, H., P.L. Koch, A. Mariotti, D. Geraads, J.-J. Jaeger 1996 Isotopic biogeochemistry (13C, 18O) of mammal enamel from African Pleistocene hominid sites: implications for the preservation of paleoclimatic isotopic signals. *Palios* 11:306–318.
Bocherens, H., D. Billiou, M. Patou-Mathis, M. Otte, D. Bonjean, M. Toussaint, A. Mariotti 1999 Palaeoenvironmental and paleodietary implications of isotopic biogeochemistry of late interglacial Neandertal and mammal

bones in Scladina Cave (Belgium). *Journal of Archaeological Science* 26:599–607.
Bocherens, H., D.G. Drucker, D. Billiou, M. Patou-Mathis, B. Vandermersch 2005 Isotopic evidence for diet and subsistence pattern of the Saint-Cesaire I Neanderthal: review and us of a multi-source mixing model. *Journal of Human Evolution* 49:71–87.
Bocherens, H., M.D.-Z. Bonilla, C. Daujeard, P. Fernandes, J.-P. Raynal, M.-H. Moncel 2016 Direct isotopic evidence for subsistence variability in Middle Pleistocene Neanderthals (Payre, southeastern France). *Quaternary Science Reviews* 154(2016):226–236.
Brain, C. K. 1981 *The hunters or the hunted.* Chicago: Chicago University Press.
Bremond, L., A. Boom and C. Favier 2012 Neotropical C_3/C_4 grass distributions – present, past and future. *Global Change Biology* 18(7):2324–2334.
Britton, K., V. Grimes, J. Dau and M.P. Richards 2009 Reconstructing faunal migrations using intra-tooth sampling and strontium and oxygen isotope analyses: A case study of modern caribou (Rangifer tarandus granti). *Journal of Archaeological Science* 36(5):1163–1172.
Britton, K., V. Grimes, L. Niven, T.E. Steele, S. McPherron, M. Soressi, T.E. Kelly, J. Jaubert, J.J. Hublin and M.P. Richards 2011 Strontium isotope evidence for migration in late Pleistocene rangifer: Implications for Neanderthal hunting strategies at the Middle Palaeolithic site of Jonzac, France. *Journal of Human Evolution* 61(2):176–185.
Britton, K., S. Gaudizinski-Windheuser, W. Roebroeks, L. Kindler, M. P. Richards 2012 Stable isotope analysis of well-preserved 120,000-year-old herbivore bone collagen from the Middle Palaeolithic site of Neumark-Nord 2, Germany reveals niche separation between bovids and equids. *Palaeogeography, Palaeoclimatology, Palaeoecology* 303:168–177.
Bryant, J.D., B. Luz and P.N. Froelich 1994 Oxygen isotopic composition of fossil horse tooth phosphate as a record of continental palaeoclimate. *Palaeogeography, Palaeoclimatology, Palaeoecology* 107:303–316.
Budd, P., A. Millard, C. Chenery, S. Lucy and C.A. Roberts 2004 Investigating population movement by stable isotope analysis: A report from Britain. *Antiquity* 78(299):127–141.
Bunn, H.T. and E.M. Kroll 1986 Systematic butchery by Plio-Pleistocene hominids at Olduvai Gorge, Tanzania. *Current Anthropology* 27:431–452.
Capo, R.C., B.W. Stewart and O.A. Chadwick 1998 Strontium isotopes as tracers of ecosystem processes: Theory and methods. *Geoderma* 82(1–3):197–225.

Callow, P and J. M Cornford 1986 La cotte de St Brelade 1961–1979. Excavations by C.B.M. McBurney. *GeoBooks Ed.*, Cambridge.
Cerling T.E and J.M. Harris 1999 Carbon isotope fractionation between diet and bioapatite in ungulate mammals and implications for ecological and paleoecological studies. *Oecologia* 120(3):347–363.
Chazan, M. 2007a Introduction, In M. Chazan and L.K. Horwitz (eds), Holon: *A Lower Paleolithic Site in Israel*, pp. 1–14, American School of Prehistoric Research, Cambridge.
Chazan, M. 2007b Lithic typology, In M. Chazan and L.K. Horwitz (eds), Holon: *A Lower Paleolithic Site in Israel,* pp. 43–59, American School of Prehistoric Research, Cambridge.
Chazan, M. 2007c Lithic technology, In M. Chazan and L.K. Horwitz (eds), Holon: *A Lower Paleolithic Site in Israel,* pp. 61–83, American School of Prehistoric Research, Cambridge.
Chazan, M. and L.K. Horwitz 2007 *Holon: A Lower Paleolithic site in Israel.* Cambridge: Peabody Museum of Archaeology and Ethnology, Harvard University.
Chazan, M. and L.K. Horwitz 2006 Finding the message in intricacy: The association of lithics and fauna on Lower Paleolithic multiple carcass sites. *Journal of Anthropological Archaeology* 25:436–447.
Chazan, M. and L.K. Horwitz (eds) 2007 *Holon: A Lower Paleolithic Site in Israel*, American School of Prehistoric Research, Cambridge.
Chazan, M., H. Monchot, N. Porat, A. Lister, P. Davies and L.K. Horwitz 2001 The Acheulian open-air-site from Holon (Israel): Preliminary results. *Earth and Planetary Sciences* 332:201-207
Cheddadi, R. and M. Rossignol-Strick 1995 Eastern Mediterranean Quaternary Paleoclimates from Pollen and Isotope Records of Marine Cores in the Nile Cone area. *Paleoceanography* 10(2):291–300
Dansgaard, W., S. Johnsen, H.B. Clausen, D. Dahl-Jensen, N. Gunderstrup, C.U. Hammer and H. Oeschger 1984 North Atlantic climatic events revealed by deep Greenland ice cores. In J.E. Hansen and T. Takahashi (eds), *Climate Processes and Climate Sensitivity*, pp. 288–298. Washington: American Geophysical Union.
Darwin, C. 1871 *The descent of man*. New York: Random House.
Davies, P and A. Lister 2007 Palaeoloxodon in *The Lower Paleolithic Site of Holon, Israel.*, (eds). Chazan, M and L. Horwitz., pp. 91-110. Harvard University: Cambridge Mass.
Dennell, R.W. 2003 Dispersal and colonisation, long and short chronologies: How continuous is the Early Pleistocene record for hominids outside East Africa? *Journal of Human Evolution* 45(6):421–440.

Dennell, R. and W. Roebroeks 2005 An Asian perspective on early human dispersal from Africa. *Nature* 438:1099–1104.
Discamps, E., J. Jaubert and F. Bachellerie 2011 Human choices and environmental constraints: Deciphering the variability of large game procurement from Mousterian to Aurignacian times (MIS 5–3) in southwestern France. *Quaternary Science Reviews* 30(19 20):2755–2775.
Di Luzio, P 2005 Uso dello spazio del Daino (*Dama dama* Linneus 1758) in ambiente mediterraneo. Thesis in Biological Science. Universita degli Studi di Roma “La Sapienza”.
Domínguez-Rodrigo, M. 2002 Hunting and scavenging by early humans: The state of the debate. *Journal of World Prehistory* 16(1):1–54.
Dominguez-Rodrigo, M., R.B. Egido and C.P. Egeland 2007 *Deconstructing Olduvai: A taphonomic study of the bed 1(I) sites* 2007. Netherlands: Springer.
Duthou, J.L., J.M. Cantagrel, J. Didier and Y. Vialette 1984 Palaeozoic granitoids from the French Massif Central; Age and origin studied by 87Rb–87Sr system. *Physics of the Earth and Planetary Interiors* 35(1-3):131–144.
Ecker, M., H. Bocherens, M.-A. Julien, F. Rivals, J.-P. Raynal, M.-H. Moncel 2013 Middle Pleistocene ecology and Neanderthal subsistence: Insights from stable isotope analysis in Payre (Ardeche, southeastern France). *Journal of Human Evolution* 65(2013):363–373.
El Albani, A., A. Meunier and F. Fursich. 2005 Unusual occurrence of glauconite in a shallow lagoonal environment (Lower Cretaceous, northern Aquitaine Basin, SW France). *Terra Nova* 17(6):537–544.
Ericson, J.E. 1985 Strontium isotope characterization in the study of prehistoric human ecology. *Journal of Human Evolution* 14(5):503–514.
Evans, J.A., C.A. Chenery and J. Montgomery 2012 A summary of strontium and oxygen isotope variation in archaeological human tooth enamel excavated from Britain. *Journal of Analytical Atomic Spectrometry* 27:754–764.
Evans, J.A., J. Montgomery and G. Wildman 2009 Isotope domain mapping of $^{87}Sr/^{86}Sr$ biosphere variation on the Isle of Skye, Scotland. *Journal of the Geological Society* 166(4):617–631.
Farrand, W.R. 2001 Sediments and stratigraphy in rockshelters and caves: A personal perspective on principles and pragmatics. Geoarchaeology: *An International Journal* 16(5):537–557.
Faure, G. and J.L. Powell 1972 *Strontium isotope geology*. Berlin: Springer-Verlag.
Feranec, R., N. Garcia, J.C. Diez, J.L. Arsuaga 2010 Understanding the ecology of mammalian carnivorans and herbivores from Valdegoba cave (Burgos,

northern Spain) through stable isotope analysis. *Palaeogeography, Palaeoclimatology, Palaeoecology.* 297(2):263–272.
Ferring, R., O. Oms, J. Agusti, F. Berna, M. Nioradze, T. Shlia, M. Tappen, A. Vekua, D. Zhvania and D. Lordkipanidze 2011 Earliest human occupations at Dmanisi (Georgian Caucasus) dated to 1.85-1.78 Ma. *Proceedings of the National Academy of Sciences* 108(26):10432–10436.
Frayer, D.W., M.H. Wolpoff, A.G. Thorne, F.H. Smith and G.G. Pope 1993 Theories of modern human origins: The paleontological test. *American Anthropologist* 95:14–50.
Fricke, H.C and J.R. O'Neil 1996 Inter-and intra-tooth variations in the oxygen isotope composition of mammalian tooth enamel phosphate: implications for palaeoclimatological and palaeobiological research. *Palaeogeography, Palaeoclimatology, Palaeoecology* 126(1996):91–99.
Gamble, C. 1986 *The Palaeolithic settlement of Europe*. Cambridge University: Cambridge.
Gamble, C. 1992 *The Palaeolithic settlement of Europe 2nd Ed.* Cambridge: Cambridge University Press.
Goldreich, Y 1995 The spatial distribution of annual rainfall in Israel – A review. *Theoretical and Applied Climatology* 50:45–59.
Goodall, J. 1963 My life among chimpanzees. *National Geographic* 124:272–308.
Goodall, J. 1986 *The chimpanzees of Gombe*. Cambridge: Harvard University Press.
Grootes, P.M., M. Stuiver, J.W.C, White, S. Johnsen, J. Jouzel 1993 Comparison of oxygen isotope records from the GISP2 and GRIP Greenland ice cores. *Nature* 366(1993):552–554.
Grün, R., M. Aubert, R. Joannes-Boyau and M.H. Moncel 2008 High resolution analysis of uranium and thorium concentration as well as U-series isotope distributions in a Neanderthal tooth from Payre (Ardeche, France) using laser ablation ICPMS. *Geochimica et Cosmochimica Acta* 72(21):5278–5290.
Hardy, B.L 2004 Neanderthal behavior and stone tool function at the Middle Palaeolithic site of La Quina, France. *Antiquity* 78(301):547–566.
Hatala, K. G., N.T. Roach, K.R. Ostrofsky, R.E. Wunderlich, H.L. Dingwall, B.A. Villmoare, D.J. Green, J.W.K. Harris, D.R. Braun and B.G. Richmond 2016 Footprints reveal direct evidence of group behavior and locomotion in *Homo Erectus. Scientific Reports* 6(28766):1–8.
Haviland, W.A., D. Walrath, H.E.L. Prins and B. McBride 2007 *Evolution and prehistory: The human challenge.* Belmont: Wadsworth publishing.

Higham, T., L.V. Golovanova, V.B. Doronichey 2011 Revised age of late Neanderthal occupation and the end of the Middle Palaeolithic in the northern Caucasus. *Proceedings of the National Academy of Sciences USA* 108(21):8611–8616.

Higham, T., K. Douka, R. Wood, C.B. Ramsey, F. Brock, L. Basell, M. Camps, A. Arrizabalaga, J. Baena, C. Barroso-Ruiz, C. Bergman, C. Boitard, P. Boitard, P. Boscato, M. Caparros, N.J. Conard, C. Draily, A. Froment, B. Galvan, P. Gambassini, A. Garcia-Morena, S. Grimaldi, P. Haesaerts, B. Holt, M.-J. Iriarte-Chiapusso, A. Jelinek, J.F. Jorda Pardo, J.-M. Maillo-Fernandez, A. Marom, J. Maroto, M. Menendez, L. Metz, E. Morin, A. Moroni, F. Negrino, E. Panagopoulou, M. Peresani, S. Pirson, M. de la Rasilla, J. Riel-Salvatore, A. Ronchitelli, D. Santamaria, P. Semal, L. Slimak, J. Soler, A. Villaluenga, R. Pinhasi, R. Jacobi 2014 The timing and spatiotemporal patterning of Neanderthal disappearance. *Nature* 512(7514):306–309.

Hoppe, K.A., P.L. Koch, R.W. Carlson and S.D. Webb 1999 Tracking mammoths and mastodons: Reconstruction of migratory behavior using strontium isotope ratios. *Geology* 27(5):439–442.

Horowitz, A. 1987 Travertines of the arid regions, oxygen isotope stages and Late Quaternary climates of Israel. *Quaternary Research* 27:103–105.

Horowitz, A. 1989 Continuous pollen diagrams for the last 3.5 m.y. from Israel: Vegetation, climate and correlation with the oxygen isotope record. *Palaeogeography, Palaeoclimatology, Palaeoecology* 72(0):63–78.

Horstwood, M.S.A., J.A. Evans and J. Montgomery 2008 Determination of Sr isotopes in calcium phosphates using laser ablation inductively coupled plasma mass spectrometry and their application to archaeological tooth enamel. *Geochimica et Cosmochimica Acta* 72(23):5659–5674.

Horwitz, L.K. and M. Chazan 2007 Holon in the context of the Levantine Lower Paleolithic 2007 in *Holon: A Lower Paleolithic Site in Israel*, American School of Prehistoric Research, Cambridge. Page 181.

Horwitz, L.K. and M. Chazan 2016 Taking a lèvy walk: Early hominin mobility in the Lower Paleolithic of the Southern Levant. In K.T. Lillios and M. Chazan (eds), *Fresh fields and pastures new: Papers presented in honor of Andrew M.T. Moore,* pp. 165–187.

Horwitz, L.K., M. Chazan, A. Lister, H. Monchot and N. Porat 2007 The Late Lower Paleolithic site of Holon, Israel: Subsistence, technology and chronology. *Journal of Anthropological Archaeology* 25, 436–447.

Horwitz, L.K. and H. Monchot 2002 Choice cuts: Hominid butchery activities at the Lower Paleolithic site of Holon, Israel. Proceedings of the fifth international symposium on the archaeozoology of southwestern Asia and adjacent areas “Archaeozoology of the Near East”.

Horwitz, L.K. and H. Monchot 2007 Sus, Hippopotamus, Bos and Gazella in The Lower Paleolithic Site of Holon, Israel., (eds). Chazan, M and L. Horwitz., pp. 91-110. Harvard University: Cambridge Mass.

Hublin, J.J. 2009 The origin of Neanderthals. *Proceedings of the National Academy of Sciences* 106(38):16022–16027.

Isaac, G. L. 1978 The food-sharing behavior of protohuman hominids. *Scientific American* 238:90–108.

Isaac, G. L. 1983 Bones in contention: Competing explanations for the juxtaposition of Early Pleistocene artifacts and faunal remains. In J. Clutton-Brock and C. Grigson (eds), *Animals and archaeology, hunters and their prey,* pp. 3–19. *British Archaeological Reports International Series* 163 Oxford.

Jelinek, J. 1978 Homo Erectus or Homo Sapiens? *Rec. Adv. Primatol* 3:419–429.

Johnsen, S. J., H.B. Clausen, W. Dansgaard, K. Fuhrer, N. Gundestrup, C.U. Hammer, P. Iversen, J. Jouzel, B. Stauffer, J.P. Steffensen 1992 Irregular glacial interstadials recorded in a new Greendland ice core. *Nature* 359(1992):311–313.

Julien, M.A., H. Bocherens, A. Burke, D.G. Drucker, M. Patou-Mathis, O. Krotava and S. Péan 2012 Were European steppe bison migratory? ^{18}O, ^{13}C and Sr intra-tooth isotopic variations applied to a palaeoethological reconstruction. *Quaternary International* 271:106–119.

Klein, R. 1999 *The Human career: Human biological and cultural origins.* Chicago: University of Chicago Press.

Koch, P.L., J. Heisinger, C. Moss, R.W. Carlson, M.L. Fogel and A.K. Behrensmeyer 1995 Isotopic tracking of change in diet and habitat use in African elephants. *Science* 267(5202):1340–1343.

Kohn, M.J., M.J. Schoeninger and J.W. Valley 1996 Variability in oxygen isotope compositions of herbivore teeth: Reflections of seasonality or developmental physiology. *Chemical Geology* 152:97–112.

Kohn, M.J., M.J Schoeninger, J.W. Valley 1998 Variability in herbivore tooth oxygen isotope compositions: reflections of seasonality or developmental physiology? *Geology* 152:97–112.

Kohn, M.J., M.P. McKay and J.L. Knight 2005 Dining in the Pleistocene – who's on the menu? *Geology* 33:649–652.

Kohn, M.J 2010 Carbon isotope compositions of terrestrial C3 plants as indicators of (paleo)ecology and (paleo)climate. *Proceedings of the National Academy of Sciences of the United States of America* 107(46):19691–19695.

Kuper, A. 1994 *The chosen primate. Human nature and cultural diversity*. Cambridge: Harvard University Press.

Lancaster, J.B. 1978 Carrying and sharing in human evolution. *Human Nature* 1:82–89.

Langway Jr, CC., H, Oeschger, W. Dansgaard (Eds.), 1985 Greenland Ice Core: Geophysics, geochemistry, and the environment. *Geophysical Monography, No. 33, American Geophysical Union,* Washington DC, pp118.

Laville, H., J.P. Rigaud and J. Sackett 1980 *Rockshelters of the Perigord: Geological stratigraphy and archaeological succession*. London: Academic Press.

Leakey, M.G., F. Spoor, M.C. Dean, C.S. Feibel, S.C. Anton, C. Kiarie and L.N. Leakey 2012 New fossils from Koobi For a in northern Kenya confirm taxonomic diversity in early Homo. *Nature* 488(7410):201–204.

Lee, R.B. and Y. De Vore 1968 *Man the hunter*. Chicago: Aldine.

Lee-Thorp, J. 2002 Two decades of progress towards understanding fossilization processes and isotopic signals in calcified tissue minerals. *Archaeometry* 44(3):435–446.

Lee-Thorp, J. and M. Sponheimer 2003 Three case studies used to reassess the reliability of fossil bone and enamel isotope signals for paleodietary studies. *Journal of Anthropological Archaeology* 22(2203):208–216.

Lopez-Lopez, P., J. Benavent-Corai, C. Garcia-Ripolles, V. Urios 2013 Scavengers on the Move: Behavioural Changes in Foraging Search Patterns during the Annual Cycle. *PLoS ONE* 8(1): e54352. https://doi.org/10.1371/journal.pone.0054352

Lordkipanidze, D., M.S. Ponce de Lèon, A. Margvelashvili, Y. Rak, G.P. Rightmire, A. Vekua and C.P.E. Zollikofer 2013 A complete skull from Dmanisi, Georgia, and the evolutionary biology of early Homo. *Science* 342(6156):326–331.

Lumley, H., S. Gregoire, D. Barsky, G. Batalla, S. Bailon, V. Belda, D. Briki, I. Byrne, E. Desclauz, K. El Guenouni, A. Fournier, S. A. Kacimi, F. Lacombat, M.A. Lumley, A.M. Moigne, J. Moutoussmy, C. Paunescu, C. Perenoud, V. Pois, J. Quiles, F. Rivals, T. Roger, A. Tetsu 2004 Habitat et mode de vie des chasseurs paleolithiques de la Caune de l'Arago (600 000–400 000 ans). *L'Anthropologie* 108:159–184.

Malinsky-Buller, A. 2014 Contextualizing Curational Strategies at the Late Lower Palaeolithic Site of Holon, Israel. *PaleoAnthropology* 2014:483–504.

Mellars, P. 1996 *The Neanderthal legacy: An archaeological perspective from Western Europe*. Princeton: Princeton University Press.

Mitchell, P. and P. Lane 2013 *The Oxford handbook of African archaeology.* Oxford: Oxford University Press.
Moffat, I. 2013 Spatially resolved strontium isotope micro-analysis of Lower and Middle Palaeolithic fauna from archaeological sites in Israel and Southern France. Unpublished PhD Thesis, The Australian National University.
Moncel, M.-H and M.G. Chacon 2007 Contributions to the understanding of Neanderthal technical behaviour during the end of OIS 6 and late interglacial (OIS 5) in Southern Europe: the lithic assemblage of upper level in the site of Payre (Rhone valley, Southeastern France). *Eurasian Prehistory* 5:21–45.
Moncel, M.-H and S. Condemi 1996 Decouverte de dents humaines dans le site Paleolithique moyen de Payre (Ardeche, France). *Comptes Rendus de l'Academi des Sciences* 322:251–257.
Moncel, M.-H. and S. Condemi 1997 Des restes humains dans le site Paleolithique moyed ancient de Payre (Ardeche): dents et parietal. Nouvelles decouvertes de 1996. *BSPF* 96(2):168–171.
Moncel, M.-H and S. Condemi 2007 The human remains of the site of Payre (S-E France, MIS 7-5). Remarks on stratigraphic position and interest. *Anthropologie* 45(1):19–29.
Moncel, M.-H., E. Debard, E. Desclaux, J.-M. Dubois, F. Lamarque, M. Patou-Mathis, P. Vilette 2002 Le cadre de vie des hommes du Paleolithique moyen (stades isotopiques 6 et 5) dans le site de Payre (Rompon Ardeche):d'une grott a un abri-sous-roche effondre. *Bulletin de la Societe Prehistorique Francaise* 99:249–275.
Moncel, M.-H L'exploitation de 'lespace et la moilite des groups humains au travers des assemblages lithiques a la fin du Pleistocene moyen et au debut du Pleistocene superieur. La moyenne vallee du Rhone entre Drome et Ardeche. *BAR International Series 1184 Oxford.*
Moncel, M.-H., C. Daujeard, E. Cregut-Bonnoure, P. Fernandez, M. Faure, C. Guerin 2004 L'occupation de la grotte de Saint-Marcel (Ardeche, France) au Paleolithique moyen: strategie d'exploitation de l'environment et type d'occupation de la grotte. L'exemble ds couches I, j et j'. *BSPF* 101(2):257–304.
Moncel, M.-H., M.G. Chacon, A. Coudenneau, P. Fernandes 2009 Points and convergent tools in the European Early Middle Palaeolithic of Payre (SE, France). *Journal of Archaeological Science* 36(2009):1892–1909.
Moncel, M.-H and F. Rivals 2011 On the Question of Short-Term Neanderthal Site Occupations: Payre, France (MIS8-7), and Taubach/Weimar Germany (MIS 5). *Journal of Anthropological Research* 67(1):47–75.

Monchot, H. and L.K. Horwitz 2007 Taxon Representation and Age and Sex Distributions in The Lower Paleolithic Site of Holon, Israel., (eds). Chazan, M and L. Horwitz., pp. 91-110. Harvard University: Cambridge Mass.

Monchot, H., M. Chazan and L.K. Horwitz 2012. Testing the spatial association of lithic and faunal remains: A case study from the Lower Palaeolithic site of Holon (Israel). In K. Seetah and B. Gravina (eds), *Bones for Tools – Tools for Bones: the Interplay Between Objects and Objectives* (McDonald Institute Monographs.) Cambridge: McDonald Institute for Archaeological Research, 25–38.

Montgomery, J. 2010 Passports from the past: Investigating human dispersals using strontium isotope analysis of tooth enamel. *Annals of Human Biology* 37(3):325–346.

Mounier, A., F. Marchal and S. Condemi 2009 Is Homo heidelbergensis a distinct species? New insights on the Mauer mandible. *Journal of Human Evolution* 56(3):219-246.

O'Connell, J. F., K. Hawkes, K.D. Lupo and N. Blurton Jones 2002. Male strategies and Plio-Pleistocene archaeology. *Journal of Human Evolution* 43:831–872.

Paton, C., J. Hellstrom, B. Paul, J. Woodhead, J. Hergt 2011 Iolite: Freeware for the visualisation and processing of mass spectrometric data. *Journal of Analytical Atomic Spectrometry* 26(12):2508–2518.

Pellegrini, M., R.E. Donahue, C. Chenery, J. Evans, J. Lee-Thorp, J. Montgomery and M. Mussi 2008 Faunal migration in late-glacial central Italy: Implications for human resource exploitation. *Rapid Communications in Mass Spectrometry* 22(11):1714–1726.

Pellegrini, M., J.A. Lee-Thorp and R.E. Donahue 2011 Exploring the variation of the $\delta^{18}O_p$ and $\delta^{18}O_c$ relationship in enamel increments. *Palaeogeography, Palaeoclimatology, Palaeoecology* 310(2011):71–83.

Pollard, M., C. Batt, B. Stern and S.M.M. Young 2007 *Analytical chemistry in archaeology*. Cambridge: Cambridge University Press.

Pomeral, C. 1980 *Geology of France with Twelve Itineraries.* Paris: Masson.

Potts, R. 1982 Lower Pleistocene site formation and hominid activities at Olduvai Gorge, Tanzania. PhD Dissertation, Harvard University, Cambridge.

Porat, N., L.P. Zhou, M. Chazan, T. Noy and L.K. Horwitz 1999 Dating the Lower Paleolithic open-air site of Holon, Israel by luminescence and ESR techniques. *Quaternary Research* 51(3):328–341.

Price, T.D., J.H. Burton and R.A. Bentley 2002 The characterization of biologically available strontium isotope ratios for the study of prehistoric migration. *Archaeometry* 44(1):117–135.
Reille, M. and J.L. de Beaulieu 1990 Pollen analysis of a long upper Pleistocene continental sequence in a Velay maar (Massif Central, France). *Palaeogeography, Palaeoclimatology, Palaeoecology* 80(1):35–48.
Reille, M., V.R. Andrieu, J.L. de Beaulieu, P. Guenet and C. Goeury 1998 A long pollen record from Lac du Bouchet, Massif Central, France: For the period ca. 325 TO 100 ka BP (OIS 9c to OIS 5e). *Quaternary Science Reviews* 17(12):1107–1123.
Richards, M.P., G. Taylor, T. Steele, S.P. McPherron, M. Soressi, J. Jaubert, J. Orschiedt, J.B. Mallye, W. Rendu and J.J. Hublin 2008 Isotopic dietary analysis of a Neanderthal and associated fauna from the site of Jonzac (Charente-Maritime), France. *Journal of Human Evolution* 55(1):179–185.
Rivals, F., M.-H. Moncel, M. Patou-Mathis 2009 Seasonality and intra-site variation of Neanderthal occupations in the Middle Palaeolithic locality of Payre (Ardeche, France) using dental wear analyses. *Journal of Archaeological Science* 36(2009):1070–1078.
Rose, L. and F. Marshall 1996 Meat eating, hominid sociality, and home bases revisited. *Current Anthropology* 37:307–338.
Rowland, J. C. 2006 Inter-and intra-tooth isotopic variations in mammalian tooth enamel from Western Israel: implications for palaeoenvironmental and palaeoclimate change over the past 350kyr. MSc University of Arizona.
Ruxton, G.D., D.C. Houston 2004 Obligate vertebrate scavengers must be large soaring fliers. *Journal of Theoretical Biology* 228(3):431–436.
Schick, K. and N. Toth 1993 *Making silent stones speak*. New York: Simon and Schuster.
Schweissing, M.M. and G. Grupe 2003 Tracing migration events in man and cattle by stable strontium isotope analysis of appositionally grown mineralized tissue. *International Journal of Osteoarchaeology* 13:96–103.
Shimron, A.E. and H.J. Zwart 1970 The occurrence of low pressure metamorphism in the Precambrian of the Middle East and North East Africa. *Geologie En Mijnbouw* 49:369–374.
Shackleton, N.J. and N.D. Opdyke 1973 Oxygen isotope and palaeomagnetic stratigraphy of Equatorial Pacific core V28–238: Oxygen isotope temperatures and ice volume on a 105 and 106 year time scale. *Quaternary Research* 3(1):39–55.

Shackleton, N.J. and N.D. Opdyke 1976 Oxygen isotope and paleomagnetic stratigraphy of Pacific core V28–238: Late Pliocene to Latest Pleistocene. Memoir (Geological Society of America) 145:449–464.

Sharma, S., M.M. Joachimski, H. J. Tobschall, I.G. Singh, D.P. Tewari and R. Tewari 2004 Oxygen isotopes of bovid teeth as archives of paleoclimate variations in archaeological deposits of the Ganga plain, India. *Quaternary Research* 62(2004):19–28.

Shea, J.J. 2007 Behavioral differences between Middle and Upper Paleolithic Homo sapiens in the East Mediterranean Levant: The roles of intraspecific competition and dispersal from Africa. *Journal of Anthropological Research* 63(4):449–488.

Sillen, A., G. Hall, S. Richardson and R. Armstrong 1998 $^{87}Sr/^{86}Sr$ ratios in modern and fossil food-webs of the Sterkfontein Valley: Implications for early hominid habitat preference. *Geochimica et Cosmochimica Acta* 62(14):2463–2473.

Sips, A.J.A.M., W.J.F. van der Vijgh, R. Barto and J.C. Netelenbos 1996 Intestinal absorption of strontium chloride in healthy volunteers: Pharmacokinetics and reproducibility. *British Journal of Clinical Pharmacology* 41(6):543–549.

Slovak, N.M., A. Paytan and B.A. Wiegand 2009 Reconstructing middle horizon mobility patterns on the coast of Peru through strontium isotope analysis. *Journal of Archaeological Science* 36(1):157–165.

Sneh, A., Y. Bartov, T. Weissbrod and M. Rosensaft 1998. *Geological Map of Israel 1:200,000, Sheet 1,2,3,4.* Geological Survey of Israel.

Sponheimer, M. and J. Lee-Thorp 1999. Isotopic evidence for the diet of an early hominid Australopithecus Africanus. *Science* 283:368–370.

Spötl, C and Vennemann, T. W 2003 Continuous-flow isotope ratio mass spectrometric analysis of carbonate minerals. *Rapid Communications in Mass Spectrometry* 17: 1004-1006.

Stringer, C and C. Gamble 1993 *In Search of the Neanderthals: Solving the puzzle of human origins.* London: Thames and Hudson.

Trickett, M.A., P. Budd, J. Montgomery and J. Evans 2003 An assessment of solubility profiling as a decontamination procedure for the $^{87}Sr/^{86}Sr$ analysis of archaeological human skeletal tissue. *Applied Geochemistry* 18(5):653–658.

Urban, M. A 2015 *Evolution and ecology of C4 grasses: insights from carbon isotope analysis of grass pollen grains.* Unpublished PhD thesis, School of Integrative Biology, University of Illinois.

Vaks, A., M. Bar-Matthews, A. Ayalon, A. Matthews, A. Frumkin, U. Dayan, L. Halicz, A. Almogi-Labin and B. Schilman 2006 Paleoclimate and location of the border between Mediterranean climate region and the Saharo-Arabian Desert as revealed by speleothems from the northern Negev Desert, Israel. *Earth and Planetary Science Letters* 249(3–4):384–399.

Villa, P., P. Boscato, F. Rabaldo, F. Ronchitelli 2009 Stone tools for the hunt: points with impact scars from a Middle Palaeolithic site in southern Italy. *Journal of Archaeological Science* 36(3):850–859.

Villa, P and M. Lenoir 2006 Hunting weapons of the Middle Stone Age and the Middle Palaeolithic: spear points from Sibudu, Rose Cottage and Bouheben. *Southern African Humanities* 18(1):89–122.

Vogel, J. C., A. Fuls and A. Danin 1986 Geographical and environmental distribution of C3 and C4 grasses in the Sinai, Negev and Judean Deserts. *Oecologia* 70:258–265.

Vogel, J.C., B. Eglington and J.M. Auret 1990 Isotope fingerprints in elephant bone and ivory. *Nature* 346(6286):747–749.

Webb, T., III, and P. J. Bartlein (1992). Global changes during the last 3 million years: Climatic controls and biotic responses. *Annual Reviews of Ecology and Systematics* 23, 141-173.

Weidenreich, F. 1943 The "Neanderthal Man" and the ancestors of "Homo Sapiens". *American Anthropologist* 45:39–48.

White, W.M. 2015 *Isotope geochemistry* Hoboken, United States: Wiley-Blackwell.

White, T.D. and P.A. Folkens 2005 *The human bone manual*. California: Elsevier Press.

Widga, C., J.D. Walker and L.D. Stockli 2010 Middle Holocene bison diet and mobility in the eastern Great Plains (USA) based on $\delta^{13}C$, $\delta^{18}O$ and $^{87}Sr/^{86}Sr$ analyses of tooth enamel carbonate. *Quaternary Research* 73(3):449–463.

Willmes, M., L. McMorrow, L. Kinsley, R. A. Armstrong, M. Aubert, S. Eggins, C. Falgueres, B. Maureille, I. Moffat, R. Grun 2014 The IRHUM (Isotopic Reconstruction of Human Migration) database – bioavailable strontium isotope ratios for geochemical fingerprinting in France. *Earth System Science Data* 6(1):117–122.

Yizraeli, T. 1967 A lower Paleolithic site at Holon, Israel. *Exploration Journal* 17:144–152.

Yamori, W., K. Hikosaka, D.A. Way 2014 Temperature response of photosynthesis in C3, C4 and CAM plants: temperature acclimation and temperature adaptation. *Pubmed* 119(1-2):101–117.

Zumdahl, S.S. 1997 *Chemistry*. Boston: Houghton Mifflin.

Appendices

Appendix One: Sample details and MatLab algorithm

Holon Samples

Specimen HN#236, season 1970, Sq. 6, bn#35 *Elephas* tooth fragment

Specimen HN#313, season 1970, Sq. 3, Level 3, *Elephas* tooth fragment

Specimen HN# 200, season1970, Square 9-11 m, *Elephas* tooth fragment

Specimen HN#1564, no data, *Elephas* tooth fragment

Specimen HN#206, 20.8.1964, bn# 278, *Bos* upper molar 1/2

Specimen HN#37, no data, *Bos* upper left probably molar 2

Specimen HN#306, 1970, Square 3, Bone # 41, height 67.90, *Bos* upper molar fragment

Specimen HN#279, season 1963, *Dama* fallow deer lower M1/2

Specimen HN#301, season 1970, Sq. 34, height 4-6, *Dama* fallow deer lower M3

Specimen HN# 33, season 11-8-1964, *Dama* fallow deer lower M3

Specimen HN#72, season 1970, Sq. 21, surface 8-10 ½, *Dama* fallow deer lower M3

These samples were provided by Dr Liora Kolska, from the National Natural History Collections in the Hebrew University of Jerusalem, Israel.

Payre Samples

D collection Bertrand M1lower (t1)

D collection Bertrand M1lower (t2)

F N8 141 M1lower

F1 N4 2 M2lower

F6 L5 729 M3lower

F7 L4 662 P4lower

F9 L4 791 M2lower

G2 N9 83

G3 N8 420 P4upper

G3 N8 423 M3lower

G4 585 M2lower

G4 O7 271 M3lower

G5 N7 860 M1-M2lower

G6 O5 114 P4lower

Data files were imported in the algorithm. The 'input' data file were the processed strontium values and the 'reference' file was the collected strontium values for the country.

E.g.

INPUT FILE

G6O5114_Enam_1 0.71081 0.00045
G6O5114_Enam_2 0.71069 0.0006
G6O5114_Enam_3 0.71066 0.00058
G6O5114_Dent_1 0.70953 0.00039
G6O5114_Dent_2 0.70956 0.00061
G6O5114_Dent_3 0.70909 0.00032
G5N7860_Enam_1 0.70652 0.00059
G5N7860_Enam_2 0.707 0.0011
G5N7860_Enam_3 0.70675 0.0008
G5N7860_Enam_4 0.70616 0.00019
G5N7860_Enam_5 0.706 0.00012
G5N7860_Enam_6 0.70621 0.00032
G5N7860_Enam_7 0.70621 0.0003
G5N7860_Enam_8 0.70618 0.00033
G5N7860_Enam_9 0.70603 0.00028

Table A.1. 1 Example of input file.

REFERENCE FILE

FS008-2	Sand, clay, gravel, pebble	0,7085590	0,000011
FS011-1	Limestone, marl, clay, sand	0,708584	0,000011
FS016-1	Marl, limestone, clay	0,707727	0,000010

FS018-1	Limestone, marl, clay, sand	0,708161	0,000011
SS001F	Limestone, marl, clay, sand	0,708985	0,000013
F12R	Marl, limestone, clay	0,707368	0,000029
F16R	Limestone, marl	0,707681	0,000028
F1R	Marl, limestone, clay	0,707326	0,000031
F23R1	Marl, limestone, clay	0,707129	0,000023
F23R2	Marl, limestone, clay	0,707071	0,000029
F24R	Marl, limestone, clay	0,707250	0,000033
F25R	Marl, limestone, clay	0,708990	0,000185
F27R	Basanite, hawaiite, tephra	0,708079	0,000028
F2R	Marl, limestone, clay	0,707237	0,000031
F40R	Limestone, marl	0,707617	0,000008
F4R	Limestone, marl, clay, sand	0,707478	0,000025

Table A.1. 2 Example of reference file.

Three different filters were applied with a different 'acceptance' range of matching values.
1st "Wide"
2nd "Medium"
3rd "Narrow"

The output file would then provide the geological ranges that the value of each spot would match – depending on the filter applied.

OUTPUT FILE

M6_G4_585_En_1	gm	0.708090	0.000420	0.708079	0.000028
M6_G4_585_En_1	c1	0.708090	0.000420	0.708056	0.000037
M6_G4_585_En_2	gm	0.707870	0.000170	0.701799	0.006234
M6_G4_585_En_2	m	0.707870	0.000170	0.707768	0.000269
M6_G4_585_En_3	gm	0.707906	0.000099	0.701799	0.006234
M6_G4_585_En_3	m	0.707906	0.000099	0.707768	0.000269
M6_G4_585_En_4	gm	0.707970	0.000140	0.701799	0.006234
M6_G4_585_En_4	m	0.707970	0.000140	0.707768	0.000269
M6_G4_585_En_4	q3	0.707970	0.000140	0.707968	0.000023
M6_G4_585_En_5	gm	0.707960	0.000480	0.701799	0.006234
M6_G4_585_En_5	m	0.707960	0.000480	0.707768	0.000269
M6_G4_585_En_5	q3	0.707960	0.000480	0.707968	0.000023
M6_G4_585_En_6	gm	0.707894	0.000140	0.701799	0.006234
M6_G4_585_En_6	m	0.707894	0.000140	0.707768	0.000269
M6_G4_585_En_7	gm	0.708029	0.000270	0.701799	0.006234
M6_G4_585_En_7	c1	0.708029	0.000270	0.708056	0.000037
M6_G4_585_En_7	m	0.708029	0.000270	0.707768	0.000269
M6_G4_585_En_7	c1	0.708029	0.000270	0.708039	0.000012
M6_G4_585_En_7	q3	0.708029	0.000270	0.708016	0.000031

Table A.1. 3: Example of at output file.

MatLab algorithm

```
clc; clear all; close force all;

% Reading Optimum File
[filename1,pathname]=uigetfile('*.txt','Select Input File');
mes_in1=fullfile(pathname, filename1);
input=importdata(mes_in1);

% Reading Observed File
[filename2,pathname]=uigetfile('*.txt','Select Reference File');
mes_in2=fullfile(pathname, filename2);
refer=importdata(mes_in2);

% Create a "RangeBar" of Input data
for i=1:length(input.data(:,2))
   input.data(i,3)=input.data(i,1)-input.data(i,2);    % min INPUT value
   input.data(i,4)=input.data(i,1)+input.data(i,2);    % max INPUT value
end

% Create a "RangeBar" of Reference data
for i=1:length(refer.data(:,2))
   refer.data(i,3)=refer.data(i,1)-refer.data(i,2);    % min REFERENCE value
   refer.data(i,4)=refer.data(i,1)+refer.data(i,2);    % max REFERENCE value
end

%%%%%%%%%%%%%%%%%%%%%%
% FILTER 1 - Wide
%%%%%%%%%%%%%%%%%%%%%%
k=0;j=0;i=0;                               % k compared data indicator
for i=1:length(input.data(:,1))              % i Input Data
   for j=1:length(refer.data(:,1))            % j Reference Data
      if input.data(i,4)>=refer.data(j,3) && ...
            input.data(i,3)<=refer.data(j,4)
         k=k+1;
         comp.textdata(k,1)=(input.textdata(i));    % k Compared Data
         comp.textdata(k,2)=(refer.textdata(j));
         comp.data(k,1)=(input.data(i,1));
         comp.data(k,2)=(input.data(i,2));
         comp.data(k,3)=(refer.data(j,1));
         comp.data(k,4)=(refer.data(j,2));
      end
   end
end

% %%%%%%%%%%%%%%%%%%%%%%%%%
% % % FILTER 2 - Medium
% %%%%%%%%%%%%%%%%%%%%%%%%%
% k=0;j=0;i=0;                               % k compared data indicator
% for i=1:length(input.data(:,1))              % i Input Data
%    for j=1:length(refer.data(:,1))            % j Reference Data
%       if input.data(i,1)>=refer.data(j,3) && ...
%             input.data(i,1)<=refer.data(j,4)
%          k=k+1;
```

```
%           comp.textdata(k,1)=(input.textdata(i));     % k Compared Data
%           comp.textdata(k,2)=(refer.textdata(j));
%           comp.data(k,1)=(input.data(i,1));
%           comp.data(k,2)=(input.data(i,2));
%           comp.data(k,3)=(refer.data(j,1));
%           comp.data(k,4)=(refer.data(j,2));
%        end
%     end
% end

% %%%%%%%%%%%%%%%%%%%%%%%
% % % FILTER 3 - Narrow
% %%%%%%%%%%%%%%%%%%%%%%%
% k=0;j=0;i=0;                          % k compared data indicator
% for i=1:length(input.data(:,1))               % i Input Data
%     for j=1:length(refer.data(:,1))            % j Reference Data
%        if input.data(i,3)>=refer.data(j,3) && ...
%              input.data(i,4)<=refer.data(j,4)
%           k=k+1;
%           comp.textdata(k,1)=(input.textdata(i));     % k Compared Data
%           comp.textdata(k,2)=(refer.textdata(j));
%           comp.data(k,1)=(input.data(i,1));
%           comp.data(k,2)=(input.data(i,2));
%           comp.data(k,3)=(refer.data(j,1));
%           comp.data(k,4)=(refer.data(j,2));
%        end
%     end
% end

count=length(filename1)-4;   %Removing file extension
str0=filename1(1:count);
    filename3=[str0,'_',filename2];
   fid1=fopen(filename3,'wt');
   for c=1:k
    fprintf(fid1,'%s\t %s\t %0.6f %0.6f\t %0.6f %0.6f\n',...
       char(comp.textdata(c,1)),char(comp.textdata(c,2)),...
        comp.data(c,1),comp.data(c,2),...
        comp.data(c,3),comp.data(c,4));
   end
   fclose(fid1);

   disp '  comparison_file .... Ready'
   disp(filename3)
```

Figure A.1. 1: MatLab algorithm used.

Appendix Two: detailed analysis of results

Four *Palaeoloxodon sp.* specimens from Holon were analysed in this study. The fragments of teeth came from stratum C of the excavation.

Figure A.2. 1: Sample 236.

Sample 236 had 67 enamel spots and 23 dentine spots collected during the strontium analysis. The mean enamel and dentine values for this sample are statistically distinguishable, with the dentine matching the site location strontium value, but the enamel showing values different from the geological unit, indicating that the sample would have been at minimum 1.2 km from site at some point during amelogenesis. The strontium value of the site correlates to a quaternary red sand and loam "hamra" (clay, silt and sand) sediment. Incremental sampling of the enamel and dentine showed some statistically distinguishable values between the enamel and dentine, but on the whole, the enamel spots remained statistically indistinguishable from each other, likewise with the dentine. What can be determined from this sample is that it is unlikely to have been local due to the low incidence of site correlation with the strontium values along the tooth and would have spent the majority of its amelogenesis approximately 1.2 km from the site, with a value corresponding to a quaternary alluvium sediment (gravel, sand and clay).

Figure A.2. 2: Sample 313.

Sample 313 had 40 enamel spots and 18 dentine spots collected during sampling. The mean values showed a significant difference between the enamel and the dentine strontium values. The dentine mean value correlated to the site geology, while the enamel matching a quaternary calcareous sandstone "kurkar" (clay, silt, sand) geology, located 1 km away. The incremental sampling of this sample indicated that this animal was non local and remained outside the site location for the majority of its amelogenesis. Of the 40 enamel spots analysed, 17 showed that the animal visited the site location, or another geology that was the same as the site. This also indicates the animal was mobile throughout amelogenesis.

Figure A.2. 3: Sample 200.

Sample 200 only had the enamel sampled due to problems accessing viable dentine. Forty spots were analysed. The mean value of this sample placed it at a minimum distance of 1 km from the site, with a strontium value correlating to a calcareous sandstone “kurkar” (clay, silt, sand) geology. The incremental sampling showed a reasonable level of heterogeneity. Of the 40 spots analysed, 10 showed evidence that the animal would have been moving into the site or into a geology that matched that of the site. The remaining 30 indicated it was mainly staying 1km from the site, however moving through several geologies, including a quaternary alluvium (gravel, sand and clay) geology.

Figure A.2. 4: Sample 1564.

Sample 1565 had 75 enamel and 73 dentine spots sampled. The mean enamel and dentine values for this sample were statistically indistinguishable and both correlated to the site geology. The incremental sampling showed heterogeneity within the enamel during amelogenesis, 61 of the spots correlated to the site geology, with a remaining 14 indicated movement up to 1 km from the site, into both calcareous sandstone “kurkar” (clay, silt, sand) and red sand and loam “hamra” (clay, silt and sand) geologies. The level of mobility compared to the other *palaeoloxodon sp.* samples appears less however.

Bos primigenius

Three *Bos primigenius* samples from Holon (stratum C) and 14 from Payre were analysed. The *Bos* samples from Payre were found in layers D, F and G.

Figure A.2. 5: Sample 206.

Sample 206 was an upper molar, either 1 or 2. 83 enamel and 83 dentine spots were analysed. The enamel and dentine mean values for this sample were different from the site geology, and correlated with an alluvium gravel, sand and clay geology 1.2 km away. The incremental sampling of this specimen showed 23 spots correlating with the site geology, and the remainder moving between calcareous sandstone “kurkar” (clay, silt, sand) and red sand and loam “hamra” (clay, silt and sand) geologies 1km from the site. Spot 41 correlated with a geology located a minimum of 15km from the site, known as the Bina Formation (turonian carbonates: limestone, marl, dolostone). The dentine was far more homogenous with 23 incidences of strontium values correlating to geologies outside the site, primarily to the same calcareous sandstone “kurkar” (clay, silt, sand) and red sand and loam “hamra” (clay, silt and sand) geologies. Overall this sample showed a high degree of mobility during amelogenesis and does not appear local to the site.

Figure A.2. 6: Sample 37.

Sample 37 was an upper left molar, likely number 2. This sample had 41 enamel and 52 dentine spots analysed. The mean values for the enamel and dentine were statistically indistinguishable and correlated with the site geology. There was very little heterogeneity in the enamel values, and limited mobility. The enamel spots showed evidence of only one mobility event, with the animal moving to either a “kurkar” (clay, silt, sand) or a red sand and loam “hamra” (clay, silt and sand) geology approximately 1 km from the site. The dentine also showed some out of the site geology to the same areas, 1 km away, however this specimen appears to be local to the site, with limited mobility.

Figure A.2. 7: Sample 306.

Sample 306 was a fragment of an upper molar. This sample had 68 enamel spots collected, but no dentine spots due to issues finding viable dentine to sample. The mean value of 306 placed it 1 km from the site, in a calcareous sandstone “kurkar” (clay, silt, sand) geology. The incremental sampling suggested a high level of mobility, moving between the site geology, the quaternary sand dunes 0.5 km away, and calcareous sandstone “kurkar” (clay, silt, sand) and red sand and loam “hamra” (clay, silt and sand) geologies approximately 1 km from the site. The distance of mobility however, was quite low.

Figure A.2. 8: Sample DM1t1.

Sample D M1 (t1) was a lower 1st molar. For this analysis, 38 enamel and 38 dentine spots were sampled. The mean enamel and dentine values both correlated with the site geology; Upper Jurassic, marl, limestone and clay. The incremental sampling also showed that the sample likely stayed either only within the site geology or moved to geologies that shared the same strontium value and are therefore indistinguishable from the site. This animal appears to be local to the site and remained at the site during amelogenesis.

Figure A.2. 9: Sample DM1t2.

Sample D M1 (t2) was also a lower 1st molar. Due to difficulty sampling dentine, only the enamel was analysed for this sample. 54 spots were sampled, and the mean values of those spots indicated a correlation with the site geology. The incremental sampling was mostly statistically indistinguishable and every spot correlated with the site geology, suggesting this animal was not mobile, although it is possible the animal was moving to a geology further away which had the same strontium value as the site location.

Figure A.2. 10: Sample FN8141.

Sample FN8141 was a lower 1st molar. There were 78 enamel and 20 dentine spots analysed. The mean values of both enamel and dentine correlated with the site geology. The incremental sampling appeared to show a greater level of heterogeneity between the dentine and enamel, however the minimum possible geology which matched the spot values for the enamel and dentine all correlated to the site geology. This animal was local to the site and not mobile during amelogenesis.

Figure A.2. 11: Sample F1N42.

Sample F1N42 was a lower 2nd molar and had 80 enamel and 66 dentine spots analysed. The mean dentine value correlated with the site geology, however the mean enamel value correlated with two geologies, both 3km away. One, a Holocene sand, clay, gravel and pebble geology and the other a Lower Cretaceous marl, sandstone, shale and limestone geology. The incremental sampling showed a more nuanced picture, with the majority of the animals time during amelogenesis being spent between the site geology and a Middle Jurassic, limestone, marl and dolomite geology 1 km from the site. The animal may have been local to the site but was mobile during amelogenesis.

Figure A.2. 12: Sample F6L5729.

Sample F6L5729 was a 3rd lower molar. 28 enamel and 14 dentine spots were analysed for this sample. The mean value for dentine and enamel were statistically distinguishable and appeared to indicate a fair degree of variation. However, both values correlated to the site geology. The incremental sampling also showed continuously statistically distinguishable values for the enamel and dentine, but primarily both had values staying within the site geology. The enamel did however indicate that at one point during amelogenesis, this animal made its way to a Holocene sand, clay, gravel and shingle geology, 3 km from the site. Regarding heterogeneity within the enamel values, they are mostly homogenous and show very little mobility. This animal was probably local, and didn't move much during amelogenesis, despite the trip 3 km away.

Figure A.2. 13: Sample F7L4662.

Sample F7L4662 was a lower incisor and had 38 enamel and 41 dentine spots analysed. The mean value for both enamel and dentine correlated with a geology 8km from the site: Oligocene, Miocene - basanite, hawaiite and tephra geology. The incremental sampling for this sample showed a strong correlation between the enamel and the dentine. Primarily this animal remained sessile within this geology 8 km away however at one point the enamel and dentine indicate the animal moved into the site location, or at least into a geology that had the same strontium value as the site. This animal was not local to the site and was not very mobile at all during amelogenesis.

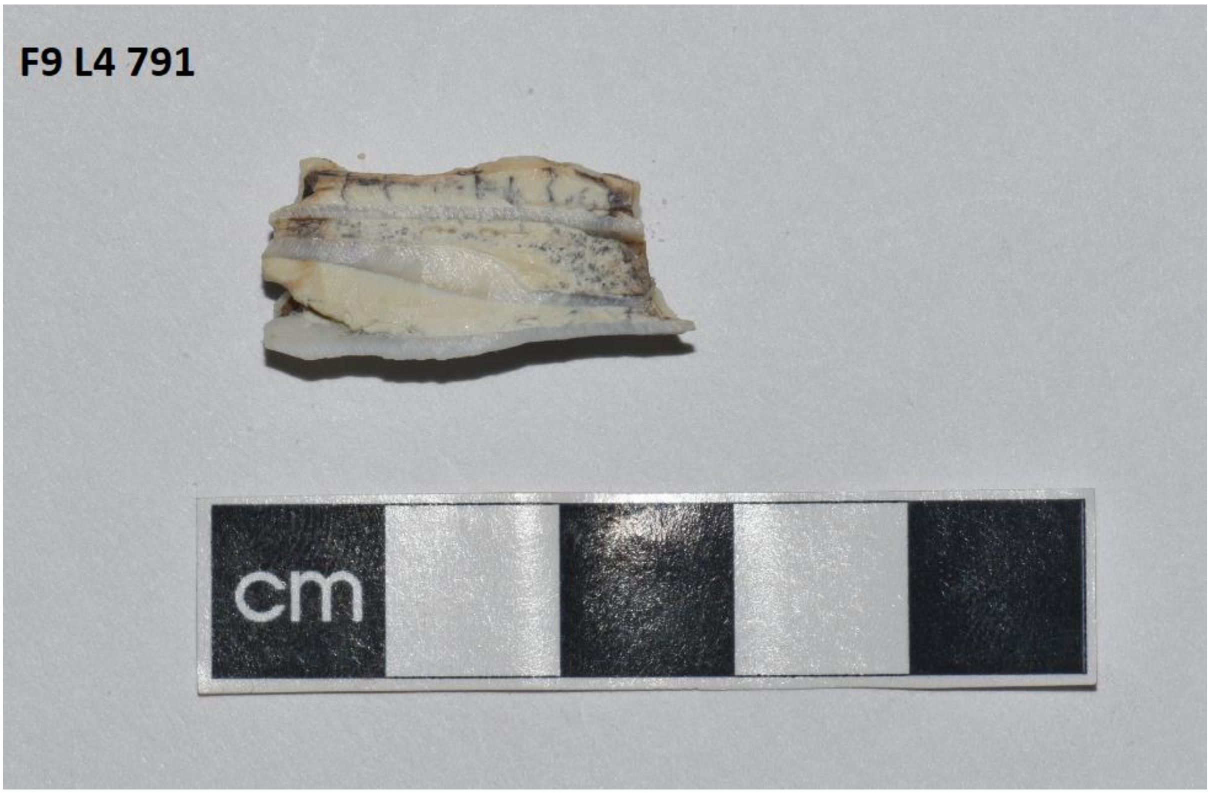

Figure A.2. 14: Sample F9L4791.

Sample F9L4791 was a lower 2nd molar. There were 37 enamel spots sampled for this tooth, however no dentine was able to be sampled. The mean value for the enamel correlated with a geology 3km away: a Dinatien, Namurien and Westphalien – monzogranite and granodiorite geology. The incremental sampling however showed that while this animal may have been moving in and out of the site geology and the geology 3km away, it was also moving as far as 10 km from the site to a Namurien, Westphalien and Stephanien – monzogranite and granodiorite geology. This animal was not local and was quite mobile during amelogenesis.

Figure A.2. 15: Sample G2N982.

Sample G2N982 had 45 enamel and 49 dentine spots analysed. The mean values for the enamel and dentine were quite different and neither correlated with the site geology. The enamel correlated to a Lower Jurassic, marl, limestone and dolomite geology located 9 km from the site. The mean value for the dentine correlated to an Upper Cretaceous, limestone, marl, clay and sand geology, 27 km from the site. The incremental sampling was quite interesting; most of the enamel spots has several potential geological matches and most of them matched with the site geology or the site 9km away. However, a number matched only with the site 9km away, suggesting this animal spent much of its time during amelogenesis there. The dentine too showed a similar pattern. While we must choose the minimum possible distance to represent the mobility of the animal, it is clearer in this situation that while spot values may correlate with the site location, it is more accurate to suggest much of the animals amelogenesis was spent elsewhere and this animal is not local.

Figure A.2. 16: Sample G3N8420.

Sample G3N8420 was an upper incisor and had 9 enamel and 19 dentine spots analysed. The mean enamel value did not correlate to any mapped geologies in France, however the mean minimum distance for the dentine did correlate to the site geology. The incremental sampling showed a large range of mobility with strontium values correlating to a geology 51 km away (Namurien, Westphalien, Stephanien – monzogranite, granodiorite). Other geologies this animal moved through during amelogenesis included the site geology, and a Middle-Upper Pleistocene, clay, sand, gravel and shingle geology 6 km from the site. This animal wouldn't have been local to the site and showed evidence of mobility during amelogenesis.

Figure A.2. 17: Sample G3N8423.

Sample G3N8423 was a lower 3rd molar. There were 58 enamel and 30 dentine spots collected for this sample. Like the other G3 sample, the mean enamel value did not match any strontium values from the French mapping study. The mean dentine value correlated to the site geology. The incremental sampling of the enamel provided a clearer view, indicating that the animal was moving in and out of the site geology during amelogenesis, ranging to 10 km away (a Namurien, Westphalien and Stephanien – monzogranite and granodiorite geology). The animal was also moving in and out of a Middle-Upper Triassic – dolomite, marl and evaporite geology 6 km from the site as well as a Dinantien, Namurien, Westphalien – monzogranite, granodiorite geology 3 km from the site. This animal was probably not local to the site and was very mobile during amelogenesis.

Figure A.2. 18: Sample G4M5585.

Sample G4M6585 was a lower 2nd molar and had 34 enamel and 28 dentine spots collected during analysis. The mean values of the enamel and dentine both correlated to the site geology. The incremental sampling showed that the animal was primarily staying within the site geology, but was frequently moving 1 km away into a Middle Jurassic, limestone and marl geology. This animal was probably local to the site, but mobile during amelogenesis, with a small range.

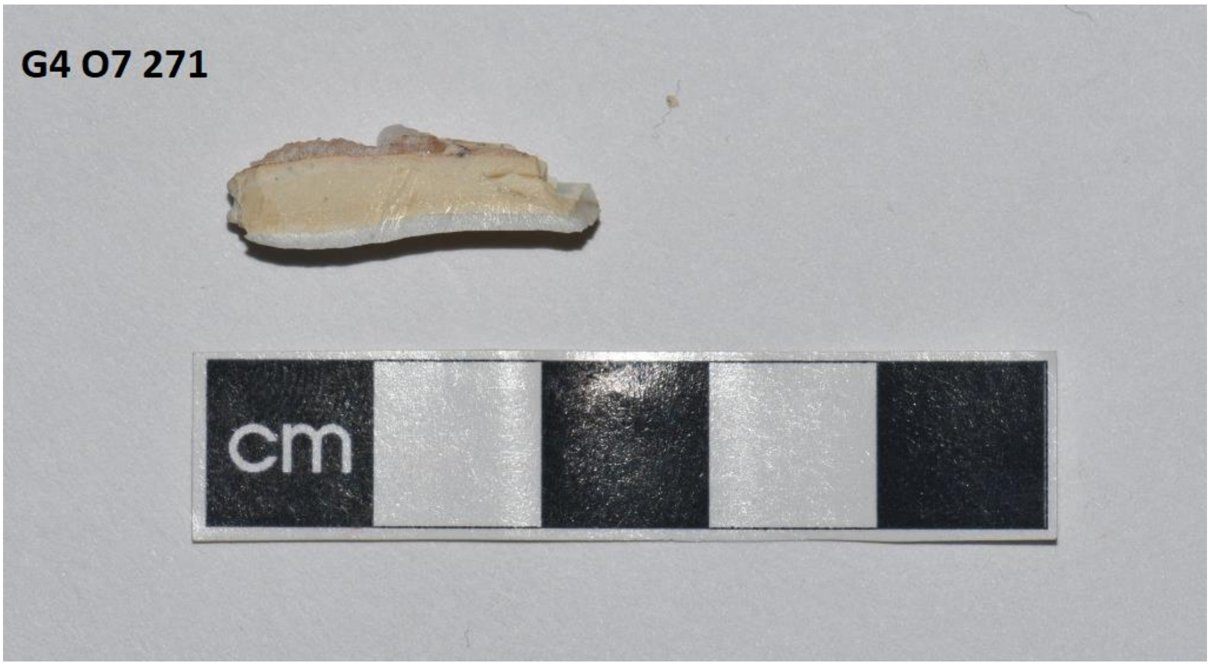

Figure A.2. 19 Sample G4O7271.

Sample G4O7271 was a lower 3rd molar. 47 enamel and 41 dentine spots were analysed. The mean value of the enamel correlated with a geology 1 km from the site (Middle Jurassic, limestone and marl) and the mean dentine value correlated with the site. The incremental sampling showed a wide range of mobility, with spot values correlating to a geology 27 km from the site (Upper Cretaceous, limestone, marl, clay, sand) and evidence of movement through geologies, 3 km, 6 km and 9km away as well as the site geology (respectively: Holocene – sand, clay, gravel, pebble; Lower Jurassic – marl, limestone, dolomite; Upper Brioverien, Cambrian – anatectic orthogneisses). This animal wasn't local to the site and showed mobility during amelogenesis.

Sample G5N7860 was a lower 1st or 2nd molar and had 84 enamel and 76 dentine spots sampled. The mean values for both the enamel and dentine correlated with the site geology. The incremental sampling shows an animal that is mobile during amelogenesis, ranging to 8 km from the site (Oligocene, Miocene – basanite, hawaiite, tephra). The sample values also correlate with site geology suggesting the animal was local to the site but was likely moving between these areas during amelogenesis.

Figure A.2. 20: Sample G6O5114..

Sample G6 O5 114 was a lower incisor, and 3 enamel and 3 dentine spots were collected. The minimum possible geology that correlated with the mean value for both the dentine and enamel was the site geology. The incremental sampling also indicated that the minimum possible geology that the sample values could match to the site geology. This suggests this animal was local to the site and was not mobile during amelogenesis.

Four *Dama cf. mesopotamica* samples from the site of Holon were analysed.

Figure A.2. 21: Sample 279.

Sample 279 had 14 enamel and 12 dentine spots collected. Both the mean value for the enamel and dentine correlated with the site geology. The incremental sampling also showed every spot correlating to the site geology, indicating that this animal was both local, and apparently sessile during amelogenesis. Considering the geology of Israel, it is possible however the animal could have been moving to areas that had a value the same as the site geology and this would not be visible to us.

Figure A.2. 22: Sample 301.

Sample 301 had 21 enamel and 14 dentine spots analysed. The mean values for the dentine and enamel were both different from the site geology. The enamel value correlated with a geology 1.2 km from the site (Quaternary, alluvium – gravel, sand, clay). The dentine value correlated with a geology 1 km from the site (Quaternary, Calcareous Sandstone “kurkar” – clay, silt, sand). The incremental sampling showed that the animal was mobile during amelogenesis, with values correlating to a geology 1.2 km from the site (Quaternary, alluvium – gravel, sand, clay) as well as the site geology. These results suggest this animal was not local to the site, but was mobile during amelogenesis.

Figure A.2. 23: Sample 33.

Sample 33 had 20 enamel spots and 28 dentine spots collected for strontium analysis. The mean value for the dentine matched the site geology. The mean value for the enamel correlated with a Quaternary alluvium (gravel, sand and clay) geology, 1.2 km from the site. The incremental sampling of the enamel and dentine both indicated spots with values that correlate to the site geology and the alluvium geology 1.2 km from the site. This animal was likely not local to the site and was also mobile during amelogenesis.

Figure A.2. 24: Sample 72.

Sample 72 had 26 enamel and 23 dentine spots analysed. The mean values for the enamel and dentine both correlated to the site geology. The incremental sampling however showed that several enamel spot values correlated with a Quaternary alluvium (gravel, sand and clay) geology, 1.2 km from the site. The dentine correlated only with the site geology. This animal may have been local to the site, but it also shows evidence of being mobile during amelogenesis.

Appendix Three: tables showing strontium values for each spot

Holon

279

Spot	Material	87Sr/86Sr	87Sr/86Sr error σ^2
1	Enamel	0.70848	0.00011
2	Enamel	0.708477	0.000097
3	Enamel	0.708484	0.000091
4	Enamel	0.70856	0.00036
5	Enamel	0.70865	0.00012
6	Enamel	0.70845	0.00015
7	Enamel	0.708512	0.000083
8	Enamel	0.708461	0.000092
9	Enamel	0.70855	0.00041
10	Enamel	0.708619	0.000085

11	Enamel	0.70864	0.00029
12	Enamel	0.70857	0.0001
13	Enamel	0.70855	0.00011
14	Enamel	0.70854	0.00014

Table A.3. 1 Sample 279 enamel values.

Spot	Material	87Sr/86Sr	87Sr/86Sr error σ²
1	Dentine	0.708594	0.00006
2	Dentine	0.70864	0.00025
3	Dentine	0.70863	0.00011
4	Dentine	0.70878	0.00005
5	Dentine	0.70869	0.00015
6	Dentine	0.70855	0.00012
7	Dentine	0.7085	0.00016
8	Dentine	0.70853	0.00014
9	Dentine	0.70869	0.00012
10	Dentine	0.708578	0.000067
11	Dentine	0.70866	0.00013
12	Dentine	0.70835	0.00023
13	Dentine	0.708485	0.000096
14	Dentine	0.70845	0.0001
15	Dentine	0.70826	0.00014
16	Dentine	0.70835	0.00015
17	Dentine	0.70829	0.00027
18	Dentine	0.70847	0.00016
19	Dentine	0.70845	0.00012
20	Dentine	0.70837	0.00023
21	Dentine	0.70851	0.00023
22	Dentine	0.70843	0.00013
23	Dentine	0.70864	0.00024
24	Dentine	0.70845	0.00014
25	Dentine	0.70838	0.00012
26	Dentine	0.70847	0.00022
27	Dentine	0.70817	0.00016
28	Dentine	0.7083	0.00044

Table A.3. 2: Sample 279 dentine values.

33

Spot	Material	87Sr/86Sr	87Sr/86Sr error σ²
1	Enamel	0.70818	0.00014
2	Enamel	0.70829	0.00018
3	Enamel	0.70817	0.00075

4	Enamel	0.708444	0.00008
5	Enamel	0.70831	0.00026
6	Enamel	0.70848	0.00013
7	Enamel	0.70838	0.00039
8	Enamel	0.70846	0.00023
9	Enamel	0.7086	0.00037
10	Enamel	0.708332	0.000087
11	Enamel	0.70836	0.00013
12	Enamel	0.70831	0.00015
13	Enamel	0.70842	0.00015
14	Enamel	0.70837	0.00014
15	Enamel	0.70832	0.0001
16	Enamel	0.70831	0.00016
17	Enamel	0.70836	0.00018
18	Enamel	0.70843	0.00036
19	Enamel	0.70843	0.00011
20	Enamel	0.7085	0.000091

Table A.3. 3: Sample 33 enamel values.

Spot	Material	87Sr/86Sr	87Sr/86Sr error σ^2
1	Dentine	0.708594	0.00006
2	Dentine	0.70864	0.00025
3	Dentine	0.70863	0.00011
4	Dentine	0.70878	0.00005
5	Dentine	0.70869	0.00015
6	Dentine	0.70855	0.00012
7	Dentine	0.7085	0.00016
8	Dentine	0.70853	0.00014
9	Dentine	0.70869	0.00012
10	Dentine	0.708578	0.000067

11	Dentine	0.70866	0.00013
12	Dentine	0.70835	0.00023
13	Dentine	0.708485	0.000096
14	Dentine	0.70845	0.0001
15	Dentine	0.70826	0.00014
16	Dentine	0.70835	0.00015
17	Dentine	0.70829	0.00027
18	Dentine	0.70847	0.00016
19	Dentine	0.70845	0.00012
20	Dentine	0.70837	0.00023
21	Dentine	0.70851	0.00023
22	Dentine	0.70843	0.00013
23	Dentine	0.70864	0.00024
24	Dentine	0.70845	0.00014
25	Dentine	0.70838	0.00012
26	Dentine	0.70847	0.00022
27	Dentine	0.70817	0.00016
28	Dentine	0.7083	0.00044

Table A.3. 4: Sample 33 dentine values..

37

Spot	Material	87Sr/86Sr	87Sr/86Sr error σ²
1	Enamel	0.7088	0.00014
2	Enamel	0.70871	0.00023
3	Enamel	0.70871	0.00029
4	Enamel	0.70888	0.00049
5	Enamel	0.7087	0.00051
6	Enamel	0.70847	0.00039
7	Enamel	0.70871	0.00045
8	Enamel	0.7086	0.00018

9	Enamel	0.70864	0.00013
10	Enamel	0.70881	0.00022
11	Enamel	0.70862	0.00024
12	Enamel	0.70861	0.00013
13	Enamel	0.708577	0.000097
14	Enamel	0.70873	0.00021
15	Enamel	0.70861	0.00016
16	Enamel	0.70873	0.0002
17	Enamel	0.70854	0.00024
18	Enamel	0.70829	0.00028
19	Enamel	0.70876	0.00032
20	Enamel	0.70836	0.00027
21	Enamel	0.70856	0.00014
22	Enamel	0.70866	0.00029
23	Enamel	0.70861	0.00024
24	Enamel	0.70894	0.0004
25	Enamel	0.70853	0.00024
26	Enamel	0.70872	0.00016
27	Enamel	0.7086	0.00017
28	Enamel	0.7086	0.0002
29	Enamel	0.70855	0.00017
30	Enamel	0.70856	0.00017
31	Enamel	0.70882	0.00052
32	Enamel	0.70863	0.00017
33	Enamel	0.70868	0.00014
34	Enamel	0.70886	0.00013
35	Enamel	0.70873	0.00017
36	Enamel	0.70875	0.00017
37	Enamel	0.70877	0.00019

38	Enamel	0.70879	0.00023
39	Enamel	0.70867	0.0002
40	Enamel	0.70884	0.00033
41	Enamel	0.70862	0.00012

Table A.3. 5: Sample 37 enamel values.

Spot	Material	87Sr/86Sr	87Sr/86Sr error σ²
1	Dentine	0.70861	0.00036
2	Dentine	0.70879	0.00025
3	Dentine	0.70871	0.00024
4	Dentine	0.70882	0.00031
5	Dentine	0.70855	0.00037
6	Dentine	0.7087	0.00011
7	Dentine	0.70861	0.00024
8	Dentine	0.70877	0.00012
9	Dentine	0.70889	0.00038
10	Dentine	0.7087	0.00014
11	Dentine	0.70889	0.00027
12	Dentine	0.7088	0.00017
13	Dentine	0.70875	0.00027
14	Dentine	0.70847	0.00039
15	Dentine	0.708762	0.000091
16	Dentine	0.70854	0.00029
17	Dentine	0.70863	0.00037
18	Dentine	0.70865	0.0002
19	Dentine	0.70863	0.0002
20	Dentine	0.70866	0.00013
21	Dentine	0.70864	0.00018
22	Dentine	0.70875	0.00013
23	Dentine	0.70874	0.00016

24	Dentine	0.70876	0.00011
25	Dentine	0.70895	0.00012
26	Dentine	0.7087	0.000087
27	Dentine	0.70866	0.0001
28	Dentine	0.70853	0.00019
29	Dentine	0.70875	0.00012
30	Dentine	0.70885	0.00014
31	Dentine	0.70875	0.00018
32	Dentine	0.70889	0.00016
33	Dentine	0.708773	0.000096
34	Dentine	0.70881	0.00026
35	Dentine	0.70859	0.00015
36	Dentine	0.70877	0.00031
37	Dentine	0.70856	0.00014
38	Dentine	0.70878	0.00027
39	Dentine	0.70876	0.00015
40	Dentine	0.70859	0.00019
41	Dentine	0.70881	0.00017
42	Dentine	0.70866	0.00015
43	Dentine	0.70875	0.00023
44	Dentine	0.70861	0.00013
45	Dentine	0.7087	0.00017
46	Dentine	0.70862	0.0004
47	Dentine	0.70874	0.00016
48	Dentine	0.708635	0.000076
49	Dentine	0.70871	0.00012
50	Dentine	0.70873	0.00016
51	Dentine	0.70873	0.00015
52	Dentine	0.70872	0.00013

Table A.3. 6: Sample 37 dentine values.

72

Spot	Material	87Sr/86Sr	87Sr/86Sr error σ²
1	Enamel	0.7087	0.00017
2	Enamel	0.70864	0.00015
3	Enamel	0.70845	0.00022
4	Enamel	0.708616	0.000089
5	Enamel	0.70848	0.00022
6	Enamel	0.70868	0.00019
7	Enamel	0.70853	0.00012
8	Enamel	0.7085	0.00036
9	Enamel	0.70848	0.00011
10	Enamel	0.7085	0.00011
11	Enamel	0.70866	0.00016
12	Enamel	0.708526	0.00009
13	Enamel	0.7087	0.00022
14	Enamel	0.70861	0.00013
15	Enamel	0.7086	0.00051
16	Enamel	0.70854	0.00017
17	Enamel	0.70848	0.0001
18	Enamel	0.708444	0.000093
19	Enamel	0.70829	0.00029
20	Enamel	0.70841	0.00011
21	Enamel	0.70835	0.00013
22	Enamel	0.70839	0.00018
23	Enamel	0.70866	0.00034
24	Enamel	0.70851	0.00013
25	Enamel	0.70845	0.00014
26	Enamel	0.70857	0.00016

Spot	Material	87Sr/86Sr	87Sr/86Sr error σ²
1	Dentine	0.70856	0.00029
2	Dentine	0.708474	0.000084
3	Dentine	0.7086	0.00039
4	Dentine	0.708532	0.000079
5	Dentine	0.70851	0.00012
6	Dentine	0.7086	0.00018
7	Dentine	0.70849	0.00011
8	Dentine	0.70863	0.00019
9	Dentine	0.7086	0.00024
10	Dentine	0.70847	0.00018
11	Dentine	0.70861	0.00014
12	Dentine	0.708549	0.000072
13	Dentine	0.70858	0.00024
14	Dentine	0.708573	0.000044
15	Dentine	0.708567	0.000088
16	Dentine	0.70864	0.00015
17	Dentine	0.70846	0.00014
18	Dentine	0.70843	0.00032
19	Dentine	0.708442	0.000074
20	Dentine	0.70851	0.0003
21	Dentine	0.708637	0.000087
22	Dentine	0.70856	0.0002
23	Dentine	0.70859	0.0002

Table A.3. 7: Sample 72 enamel and dentine values.

200

Spot	Material	87Sr/86Sr	87Sr/86Sr error σ²

1	Enamel	0.70927	0.00014
2	Enamel	0.70929	0.00011
3	Enamel	0.70932	0.00029
4	Enamel	0.709111	0.000081
5	Enamel	0.70915	0.00011
6	Enamel	0.70915	0.0003
7	Enamel	0.709176	0.000083
8	Enamel	0.70907	0.00022
9	Enamel	0.709139	0.00007
10	Enamel	0.70914	0.00015
11	Enamel	0.70919	0.000067
12	Enamel	0.70925	0.00013
13	Enamel	0.709388	0.00009
14	Enamel	0.70929	0.00012
15	Enamel	0.70917	0.00022
16	Enamel	0.70943	0.00023
17	Enamel	0.70922	0.00015
18	Enamel	0.70911	0.0005
19	Enamel	0.70918	0.00012
20	Enamel	0.70921	0.00012
21	Enamel	0.70916	0.00019
22	Enamel	0.70934	0.000066
23	Enamel	0.70905	0.00015
24	Enamel	0.70919	0.00022
25	Enamel	0.70919	0.00012
26	Enamel	0.7093	0.00012
27	Enamel	0.70906	0.00011
28	Enamel	0.70908	0.00012
29	Enamel	0.70903	0.00011

30	Enamel	0.70904	0.00023
31	Enamel	0.70928	0.0002
32	Enamel	0.70927	0.00023
33	Enamel	0.70927	0.00024
34	Enamel	0.70926	0.00011
35	Enamel	0.70917	0.00014
36	Enamel	0.70922	0.00014
37	Enamel	0.70937	0.00017
38	Enamel	0.7093	0.0002
39	Enamel	0.70926	0.00011
40	Enamel	0.70921	0.00019

Table A.3. 8: Sample 200 enamel values.

206

Spot	Material	87Sr/86Sr	87Sr/86Sr error σ²
1	Enamel	0.70859	0.00056
2	Enamel	0.70855	0.00046
3	Enamel	0.70858	0.00079
4	Enamel	0.70824	0.00013
5	Enamel	0.708175	0.000084
6	Enamel	0.70805	0.00021
7	Enamel	0.70804	0.00013
8	Enamel	0.70829	0.00042
9	Enamel	0.70812	0.00016
10	Enamel	0.70837	0.00023
11	Enamel	0.70818	0.0001
12	Enamel	0.70825	0.00039
13	Enamel	0.70809	0.00018
14	Enamel	0.70813	0.00027
15	Enamel	0.70838	0.0003

16	Enamel	0.70865	0.00098
17	Enamel	0.70831	0.00027
18	Enamel	0.70821	0.00015
19	Enamel	0.70834	0.00065
20	Enamel	0.7078	0.00046
21	Enamel	0.70797	0.00054
22	Enamel	0.70762	0.00035
23	Enamel	0.70786	0.0003
24	Enamel	0.70849	0.00062
25	Enamel	0.7081	0.00025
26	Enamel	0.70808	0.00053
27	Enamel	0.70799	0.0002
28	Enamel	0.70816	0.00013
29	Enamel	0.70798	0.00024
30	Enamel	0.70806	0.00044
31	Enamel	0.70793	0.00024
32	Enamel	0.7078	0.00022
33	Enamel	0.70787	0.00023
34	Enamel	0.70784	0.00019
35	Enamel	0.70789	0.0002
36	Enamel	0.70794	0.00013
37	Enamel	0.70824	0.00034
38	Enamel	0.7079	0.00019
39	Enamel	0.70792	0.00021
40	Enamel	0.70813	0.00064
41	Enamel	0.70712	0.00041
42	Enamel	0.70774	0.00021
43	Enamel	0.70788	0.00022
44	Enamel	0.70804	0.00071

45	Enamel	0.70755	0.00045
46	Enamel	0.70772	0.00028
47	Enamel	0.70788	0.00017
48	Enamel	0.70768	0.00017
49	Enamel	0.70752	0.00017
50	Enamel	0.70788	0.00035
51	Enamel	0.70809	0.00091
52	Enamel	0.70771	0.00031
53	Enamel	0.70781	0.00015
54	Enamel	0.70769	0.00011
55	Enamel	0.7077	0.00016
56	Enamel	0.7077	0.00015
57	Enamel	0.70833	0.00013
58	Enamel	0.70844	0.00014
59	Enamel	0.708297	0.000098
60	Enamel	0.70842	0.00016
61	Enamel	0.70827	0.00017
62	Enamel	0.70833	0.00016
63	Enamel	0.70827	0.00023
64	Enamel	0.70839	0.00014
65	Enamel	0.70837	0.00021
66	Enamel	0.70814	0.00018
67	Enamel	0.70837	0.00021
68	Enamel	0.70759	0.00016
69	Enamel	0.70757	0.00016
70	Enamel	0.70746	0.00025
71	Enamel	0.70755	0.00023
72	Enamel	0.70787	0.00018
73	Enamel	0.70756	0.00016

74	Enamel	0.7078	0.00047
75	Enamel	0.70762	0.00016
76	Enamel	0.70793	0.00059
77	Enamel	0.70767	0.00029
78	Enamel	0.70775	0.00015
79	Enamel	0.70791	0.00033
80	Enamel	0.70776	0.0002
81	Enamel	0.70783	0.00012
82	Enamel	0.70779	0.00014
83	Enamel	0.70788	0.00011

Table A.3. 9: Sample 206 enamel values.

206

Spot	Material	87Sr/86Sr	87Sr/86Sr error σ^2
1	Dentine	0.708538	0.000098
2	Dentine	0.70828	0.00026
3	Dentine	0.7084	0.00022
4	Dentine	0.70839	0.00012
5	Dentine	0.70829	0.00023
6	Dentine	0.70838	0.00012
7	Dentine	0.7084	0.00034
8	Dentine	0.70849	0.00024
9	Dentine	0.7084	0.00013
10	Dentine	0.70842	0.00016
11	Dentine	0.708443	0.000096
12	Dentine	0.70847	0.00016
13	Dentine	0.70855	0.00023
14	Dentine	0.7085	0.00028
15	Dentine	0.7084	0.00014
16	Dentine	0.70845	0.00031

17	Dentine	0.70842	0.00043
18	Dentine	0.70829	0.00029
19	Dentine	0.70828	0.00032
20	Dentine	0.70838	0.00013
21	Dentine	0.70838	0.00015
22	Dentine	0.70839	0.0001
23	Dentine	0.70829	0.00021
24	Dentine	0.70842	0.00025
25	Dentine	0.70836	0.00012
26	Dentine	0.70835	0.00016
27	Dentine	0.70845	0.00016
28	Dentine	0.70841	0.00015
29	Dentine	0.708465	0.000087
30	Dentine	0.70842	0.00011
31	Dentine	0.70843	0.00022
32	Dentine	0.70857	0.00013
33	Dentine	0.70835	0.00013
34	Dentine	0.70843	0.00015
35	Dentine	0.70837	0.00015
36	Dentine	0.70836	0.00011
37	Dentine	0.708344	0.000094
38	Dentine	0.70872	0.00065
39	Dentine	0.70838	0.00011
40	Dentine	0.70836	0.0004
41	Dentine	0.70835	0.00015
42	Dentine	0.70829	0.00078
43	Dentine	0.7084	0.00024
44	Dentine	0.70851	0.00015
45	Dentine	0.708364	0.000096

46	Dentine	0.70834	0.00015
47	Dentine	0.7085	0.00042
48	Dentine	0.70843	0.00017
49	Dentine	0.70836	0.00014
50	Dentine	0.70835	0.00016
51	Dentine	0.708348	0.000082
52	Dentine	0.70826	0.00023
53	Dentine	0.708315	0.000094
54	Dentine	0.7088	0.00054
55	Dentine	0.70826	0.00012
56	Dentine	0.70823	0.00012
57	Dentine	0.70832	0.00025
58	Dentine	0.70836	0.000099
59	Dentine	0.70835	0.00015
60	Dentine	0.70838	0.00015
61	Dentine	0.70845	0.00011
62	Dentine	0.7085	0.00023
63	Dentine	0.70862	0.00028
64	Dentine	0.70839	0.00016
65	Dentine	0.70824	0.00016
66	Dentine	0.708527	0.000074
67	Dentine	0.70835	0.00014
68	Dentine	0.70834	0.0001
69	Dentine	0.70831	0.0001
70	Dentine	0.70839	0.00031
71	Dentine	0.708295	0.00009
72	Dentine	0.70836	0.00013
73	Dentine	0.70842	0.00013
74	Dentine	0.708371	0.00006

75	Dentine	0.70849	0.00019
76	Dentine	0.70832	0.00015
77	Dentine	0.70847	0.00014
78	Dentine	0.70833	0.00011
79	Dentine	0.70851	0.00012
80	Dentine	0.70827	0.00017
81	Dentine	0.70835	0.00062
82	Dentine	0.70843	0.00016
83	Dentine	0.708426	0.000077

Table A.3. 10: Sample 206 dentine values.

236

Spot	Material	87Sr/86Sr	87Sr/86Sr error σ^2
1	Enamel	0.70897	0.00019
2	Enamel	0.708701	0.000089
3	Enamel	0.70877	0.00046
4	Enamel	0.708761	0.000075
5	Enamel	0.70884	0.00033
6	Enamel	0.708793	0.000056
7	Enamel	0.70875	0.00019
8	Enamel	0.7089	0.00021
9	Enamel	0.70872	0.00018
10	Enamel	0.70867	0.00043
11	Enamel	0.70882	0.00011
12	Enamel	0.70886	0.00053
13	Enamel	0.7089	0.00014
14	Enamel	0.70869	0.00021
15	Enamel	0.70888	0.00018
16	Enamel	0.70879	0.00016
17	Enamel	0.70891	0.00023

18	Enamel	0.708759	0.000089
19	Enamel	0.70881	0.00054
20	Enamel	0.708934	0.000079
21	Enamel	0.70887	0.00021
22	Enamel	0.70877	0.000085
23	Enamel	0.70885	0.00038
24	Enamel	0.70894	0.00019
25	Enamel	0.70901	0.00025
26	Enamel	0.70883	0.0002
27	Enamel	0.70878	0.00013
28	Enamel	0.70875	0.00012
29	Enamel	0.70872	0.00011
30	Enamel	0.70871	0.00039
31	Enamel	0.708706	0.000078
32	Enamel	0.7086	0.00014
33	Enamel	0.708705	0.000076
34	Enamel	0.70874	0.00011
35	Enamel	0.70874	0.00013
36	Enamel	0.708682	0.000076
37	Enamel	0.70886	0.00041
38	Enamel	0.70875	0.00014
39	Enamel	0.70882	0.00027
40	Enamel	0.70881	0.00014
41	Enamel	0.708739	0.000076
42	Enamel	0.70891	0.00024
43	Enamel	0.708895	0.000064
44	Enamel	0.708788	0.000067
45	Enamel	0.70878	0.000075
46	Enamel	0.70877	0.00015

47	Enamel	0.708895	0.000074
48	Enamel	0.70872	0.00014
49	Enamel	0.708742	0.000092
50	Enamel	0.708727	0.000067
51	Enamel	0.708735	0.000084
52	Enamel	0.708746	0.00006
53	Enamel	0.708876	0.000069
54	Enamel	0.70876	0.00045
55	Enamel	0.70882	0.00013
56	Enamel	0.70882	0.00041
57	Enamel	0.708915	0.00007
58	Enamel	0.70893	0.00033
59	Enamel	0.708837	0.000092
60	Enamel	0.70872	0.00011
61	Enamel	0.708871	0.000071
62	Enamel	0.70879	0.00013
63	Enamel	0.70885	0.0001
64	Enamel	0.70871	0.00012
65	Enamel	0.70886	0.00021
66	Enamel	0.70895	0.00033
67	Enamel	0.7089	0.00015

Table A.3. 11: Sample 236 enamel values.

Spot	**Material**	**87Sr/86Sr**	**87Sr/86Sr error σ²**
1	Dentine	0.708704	0.000093
2	Dentine	0.70859	0.00012
3	Dentine	0.70865	0.00011
4	Dentine	0.70865	0.00011
5	Dentine	0.70867	0.00011
6	Dentine	0.70872	0.00007

7	Dentine	0.70873	0.0001
8	Dentine	0.708716	0.000078
9	Dentine	0.70867	0.00031
10	Dentine	0.70853	0.00024
11	Dentine	0.70873	0.00022
12	Dentine	0.708726	0.000079
13	Dentine	0.708646	0.000095
14	Dentine	0.70866	0.00013
15	Dentine	0.70861	0.0001
16	Dentine	0.70863	0.00017
17	Dentine	0.70867	0.00013
18	Dentine	0.70871	0.0001
19	Dentine	0.70869	0.00017
20	Dentine	0.70866	0.00018
21	Dentine	0.70863	0.00016
22	Dentine	0.70861	0.00012
23	Dentine	0.70863	0.0001

Table A.3. 12: Sample 236 dentine values.

301

Spot	**Material**	**87Sr/86Sr**	**87Sr/86Sr error σ^2**
1	Enamel	0.70839	0.00011
2	Enamel	0.70844	0.00053
3	Enamel	0.70849	0.00031
4	Enamel	0.708347	0.00017
5	Enamel	0.70849	0.00023
6	Enamel	0.708264	0.00022
7	Enamel	0.70839	0.00018
8	Enamel	0.70841	0.00016

9	Enamel	0.70825	0.00063
10	Enamel	0.70833	0.00016
11	Enamel	0.70832	0.00024
12	Enamel	0.70832	0.00036
13	Enamel	0.708312	0.00016
14	Enamel	0.708277	0.00047
15	Enamel	0.70819	0.00011
16	Enamel	0.70813	0.00011
17	Enamel	0.708126	0.00018
18	Enamel	0.708265	0.00017
19	Enamel	0.70826	0.00045
20	Enamel	0.708467	0.0003
21	Enamel	0.708402	0.00029

Table A.3. 13: Sample 301 enamel values.

Spot	**Material**	**87Sr/86Sr**	**87Sr/86Sr error σ²**
1	Dentine	0.70851	0.0003
2	Dentine	0.708547	0.00014
3	Dentine	0.70843	0.00027
4	Dentine	0.708412	0.00034
5	Dentine	0.708409	0.00013
6	Dentine	0.708478	0.00033
7	Dentine	0.708473	9.70E-05
8	Dentine	0.708492	0.00037
9	Dentine	0.708507	0.00014
10	Dentine	0.708483	0.00031
11	Dentine	0.708418	0.00012
12	Dentine	0.708446	0.0002
13	Dentine	0.708476	0.00022
14	Dentine	0.708427	0.00011

Table A.3. 14: Sample 301 dentine values.

306

Spot	Material	87Sr/86Sr	87Sr/86Sr error σ²
1	Enamel	0.7093	0.00012
2	Enamel	0.70926	0.00016
3	Enamel	0.70936	0.00047
4	Enamel	0.70913	0.0002
5	Enamel	0.70922	0.00042
6	Enamel	0.709	0.0007
7	Enamel	0.70915	0.00037
8	Enamel	0.70936	0.0002
9	Enamel	0.7093	0.00021
10	Enamel	0.70933	0.00015
11	Enamel	0.70936	0.00056
12	Enamel	0.70944	0.00013
13	Enamel	0.70938	0.00037
14	Enamel	0.70936	0.00016
15	Enamel	0.70938	0.00024
16	Enamel	0.70931	0.00028
17	Enamel	0.7094	0.00022
18	Enamel	0.70948	0.00029
19	Enamel	0.70933	0.00019
20	Enamel	0.70956	0.00054
21	Enamel	0.70917	0.00031
22	Enamel	0.70945	0.00021
23	Enamel	0.70929	0.00012
24	Enamel	0.70929	0.00027
25	Enamel	0.7093	0.00044
26	Enamel	0.70962	0.00021

27	Enamel	0.7094	0.00029
28	Enamel	0.70962	0.00015
29	Enamel	0.70918	0.00045
30	Enamel	0.70943	0.00022
31	Enamel	0.70948	0.00014
32	Enamel	0.70931	0.00026
33	Enamel	0.70953	0.00014
34	Enamel	0.70942	0.00024
35	Enamel	0.70958	0.00014
36	Enamel	0.70971	0.00015
37	Enamel	0.70937	0.00016
38	Enamel	0.70934	0.00016
39	Enamel	0.70934	0.00021
40	Enamel	0.70941	0.00017
41	Enamel	0.70935	0.00031
42	Enamel	0.70932	0.00019
43	Enamel	0.70912	0.00017
44	Enamel	0.70916	0.0002
45	Enamel	0.70928	0.00021
46	Enamel	0.70931	0.00018
47	Enamel	0.70951	0.00024
48	Enamel	0.70939	0.00018
49	Enamel	0.70931	0.00015
50	Enamel	0.70922	0.00039
51	Enamel	0.7093	0.00027
52	Enamel	0.70946	0.00015
53	Enamel	0.70947	0.00023
54	Enamel	0.70938	0.00011
55	Enamel	0.70936	0.00054

56	Enamel	0.70919	0.00018
57	Enamel	0.70916	0.00021
58	Enamel	0.70923	0.00031
59	Enamel	0.70932	0.00013
60	Enamel	0.70919	0.00038
61	Enamel	0.70904	0.00039
62	Enamel	0.70915	0.00015
63	Enamel	0.70901	0.00022
64	Enamel	0.70923	0.00016
65	Enamel	0.70903	0.00016
66	Enamel	0.70913	0.00058
67	Enamel	0.70913	0.00018
68	Enamel	0.70912	0.00046

Table A.3. 15: Sample 306 enamel values.

313

Spot	Material	87Sr/86Sr	87Sr/86Sr error σ^2
1	Enamel	0.70924	0.00015
2	Enamel	0.70927	0.00014
3	Enamel	0.709244	0.000091
4	Enamel	0.70913	0.00017
5	Enamel	0.70916	0.000078
6	Enamel	0.70918	0.00011
7	Enamel	0.70915	0.00022
8	Enamel	0.709107	0.000078
9	Enamel	0.70915	0.00016
10	Enamel	0.70912	0.00017
11	Enamel	0.70929	0.00032
12	Enamel	0.70932	0.000099
13	Enamel	0.70927	0.00015

14	Enamel	0.7094	0.00014
15	Enamel	0.70928	0.00012
16	Enamel	0.70947	0.00017
17	Enamel	0.70936	0.00012
18	Enamel	0.70936	0.00026
19	Enamel	0.70942	0.00012
20	Enamel	0.70919	0.00019
21	Enamel	0.70937	0.0003
22	Enamel	0.7094	0.00015
23	Enamel	0.70941	0.00013
24	Enamel	0.70942	0.00017
25	Enamel	0.70938	0.00013
26	Enamel	0.70937	0.00017
27	Enamel	0.70931	0.00012
28	Enamel	0.70929	0.00026
29	Enamel	0.709297	0.000087
30	Enamel	0.70934	0.00022
31	Enamel	0.709343	0.000075
32	Enamel	0.70922	0.00016
33	Enamel	0.70922	0.0003
34	Enamel	0.70926	0.00016
35	Enamel	0.70928	0.00027
36	Enamel	0.70922	0.00014
37	Enamel	0.709278	0.00009
38	Enamel	0.709276	0.000097
39	Enamel	0.70918	0.00034
40	Enamel	0.70926	0.00017

Table A.3. 16: Sample 313 enamel values.

Spot	**Material**	**87Sr/86Sr**	**87Sr/86Sr error σ^2**

1	Dentine	0.708689	0.000078
2	Dentine	0.70877	0.00012
3	Dentine	0.70882	0.00016
4	Dentine	0.708692	0.000094
5	Dentine	0.70885	0.00022
6	Dentine	0.70884	0.00014
7	Dentine	0.708745	0.000083
8	Dentine	0.708686	0.000076
9	Dentine	0.70859	0.00023
10	Dentine	0.70828	0.00049
11	Dentine	0.70868	0.00013
12	Dentine	0.7088	0.0003
13	Dentine	0.70881	0.0001
14	Dentine	0.70876	0.00017
15	Dentine	0.7088	0.00018
16	Dentine	0.70873	0.00011
17	Dentine	0.70883	0.00013
18	Dentine	0.70867	0.00016

Table A.3. 17: Sample 313 dentine values.

1564

Spot	Material	87Sr/86Sr	87Sr/86Sr error σ^2
1	Enamel	0.70873	0.00042
2	Enamel	0.70863	0.00013
3	Enamel	0.70852	0.00021
4	Enamel	0.70845	0.00022
5	Enamel	0.70842	0.00033
6	Enamel	0.70844	0.00012
7	Enamel	0.70827	0.00025
8	Enamel	0.708516	0.000091

9	Enamel	0.70839	0.00018
10	Enamel	0.70826	0.00036
11	Enamel	0.70839	0.00039
12	Enamel	0.70857	0.00044
13	Enamel	0.70814	0.00025
14	Enamel	0.70844	0.00031
15	Enamel	0.70831	0.00017
16	Enamel	0.70843	0.00045
17	Enamel	0.70829	0.00031
18	Enamel	0.70843	0.00049
19	Enamel	0.70839	0.00021
20	Enamel	0.70837	0.00016
21	Enamel	0.70812	0.00011
22	Enamel	0.70855	0.00011
23	Enamel	0.70823	0.00022
24	Enamel	0.70864	0.00019
25	Enamel	0.70864	0.00015
26	Enamel	0.70863	0.00027
27	Enamel	0.70847	0.00018
28	Enamel	0.70863	0.00032
29	Enamel	0.70832	0.00024
30	Enamel	0.70857	0.00019
31	Enamel	0.70855	0.00016
32	Enamel	0.70826	0.00015
33	Enamel	0.70851	0.00026
34	Enamel	0.708313	0.000087
35	Enamel	0.70842	0.00012
36	Enamel	0.70851	0.00013
37	Enamel	0.70864	0.00012

38	Enamel	0.70821	0.00018
39	Enamel	0.70815	0.00013
40	Enamel	0.70823	0.00022
41	Enamel	0.7085	0.00023
42	Enamel	0.7084	0.00016
43	Enamel	0.70856	0.00017
44	Enamel	0.7084	0.00012
45	Enamel	0.70848	0.00024
46	Enamel	0.70832	0.00018
47	Enamel	0.70833	0.00012
48	Enamel	0.7085	0.00011
49	Enamel	0.7084	0.00012
50	Enamel	0.70829	0.00015
51	Enamel	0.70842	0.00011
52	Enamel	0.70827	0.00011
53	Enamel	0.70856	0.00012
54	Enamel	0.70859	0.00011
55	Enamel	0.708692	0.000081
56	Enamel	0.70868	0.0001
57	Enamel	0.70879	0.00011
58	Enamel	0.7087	0.00014
59	Enamel	0.70874	0.00011
60	Enamel	0.70871	0.000099
61	Enamel	0.70871	0.00032
62	Enamel	0.70866	0.00013
63	Enamel	0.708692	0.000084
64	Enamel	0.70877	0.00014
65	Enamel	0.70866	0.00011
66	Enamel	0.70861	0.0001

67	Enamel	0.70859	0.00012
68	Enamel	0.70871	0.00013
69	Enamel	0.708654	0.000096
70	Enamel	0.70856	0.00012
71	Enamel	0.70846	0.00015
72	Enamel	0.70869	0.00011
73	Enamel	0.70883	0.00013
74	Enamel	0.70858	0.00012
75	Enamel	0.708642	0.00008

Table A.3. 18: Sample 1564 enamel values.

Spot	**Material**	**87Sr/86Sr**	**87Sr/86Sr error σ²**
1	Dentine	0.70856	0.0002
2	Dentine	0.7084	0.00015
3	Dentine	0.70855	0.00018
4	Dentine	0.70859	0.00016
5	Dentine	0.70858	0.00014
6	Dentine	0.708555	0.000095
7	Dentine	0.7085	0.00013
8	Dentine	0.708434	0.00007
9	Dentine	0.70862	0.00032
10	Dentine	0.70853	0.0001
11	Dentine	0.70856	0.00011
12	Dentine	0.70833	0.00028
13	Dentine	0.708611	0.000077
14	Dentine	0.70854	0.0001
15	Dentine	0.70852	0.00023
16	Dentine	0.70855	0.00036
17	Dentine	0.70845	0.00015
18	Dentine	0.70844	0.00014

19	Dentine	0.70841	0.00013
20	Dentine	0.70846	0.00016
21	Dentine	0.7085	0.0001
22	Dentine	0.708539	0.000088
23	Dentine	0.70841	0.00025
24	Dentine	0.70862	0.0001
25	Dentine	0.70848	0.0003
26	Dentine	0.70838	0.00019
27	Dentine	0.70846	0.00015
28	Dentine	0.70842	0.0003
29	Dentine	0.708539	0.000085
30	Dentine	0.70868	0.00017
31	Dentine	0.70849	0.00011
32	Dentine	0.70846	0.00015
33	Dentine	0.70849	0.00014
34	Dentine	0.70852	0.00012
35	Dentine	0.70857	0.00024
36	Dentine	0.70881	0.00049
37	Dentine	0.70848	0.00026
38	Dentine	0.70855	0.00014
39	Dentine	0.70856	0.00017
40	Dentine	0.70842	0.00029
41	Dentine	0.70877	0.00043
42	Dentine	0.7084	0.00028
43	Dentine	0.70858	0.00013
44	Dentine	0.7085	0.00029
45	Dentine	0.70848	0.00014
46	Dentine	0.70871	0.00032
47	Dentine	0.70857	0.0001

48	Dentine	0.70861	0.00025
49	Dentine	0.70841	0.00012
50	Dentine	0.7085	0.00012
51	Dentine	0.70849	0.00012
52	Dentine	0.70857	0.00013
53	Dentine	0.70862	0.00019
54	Dentine	0.70863	0.00014
55	Dentine	0.70868	0.00014
56	Dentine	0.70849	0.00024
57	Dentine	0.70865	0.00027
58	Dentine	0.70858	0.00017
59	Dentine	0.70873	0.00036
60	Dentine	0.70858	0.00012
61	Dentine	0.70859	0.00015
62	Dentine	0.70866	0.00019
63	Dentine	0.70866	0.00017
64	Dentine	0.70859	0.00027
65	Dentine	0.7085	0.00016
66	Dentine	0.70868	0.00018
67	Dentine	0.7085	0.00018
68	Dentine	0.708385	0.00009
69	Dentine	0.70845	0.00015
70	Dentine	0.70853	0.00021
71	Dentine	0.70845	0.00018
72	Dentine	0.708577	0.000089
73	Dentine	0.70848	0.00015

Table A.3. 19: Sample 1564 dentine values.

Payre

G6 O5 114

Spot	**Material**	**$^{87}Sr/^{86}Sr$**	**$^{87}Sr/^{86}Sr$ σ^2 error**
1	Enamel	0.71081	0.00045
2	Enamel	0.71069	0.0006
3	Enamel	0.71066	0.00058

Table A.3. 20: Sample G6O5114 enamel values.

Spot	**Material**	**$^{87}Sr/^{86}Sr$**	**$^{87}Sr/^{86}Sr$ σ^2 error**
1	Dentine	0.70953	0.00039
2	Dentine	0.70956	0.00061
3	Dentine	0.70909	0.00032

Table A.3. 21: Sample G6O5114 dentine values.

G5 N7 860

Spot	**Material**	**$^{87}Sr/^{86}Sr$**	**$^{87}Sr/^{86}Sr$ error σ^2**
1	Enamel	0.70652	0.00059
2	Enamel	0.707	0.0011
3	Enamel	0.70675	0.0008
4	Enamel	0.70616	0.00019
5	Enamel	0.706	0.00012
6	Enamel	0.70621	0.00032
7	Enamel	0.70621	0.0003
8	Enamel	0.70618	0.00033
9	Enamel	0.70603	0.00028
10	Enamel	0.70615	0.00043
11	Enamel	0.70609	0.0001
12	Enamel	0.70637	0.00026
13	Enamel	0.70633	0.00018
14	Enamel	0.70674	0.00041
15	Enamel	0.70705	0.00055

16	Enamel	0.70704	0.00028
17	Enamel	0.70712	0.0003
18	Enamel	0.70732	0.0007
19	Enamel	0.70691	0.00048
20	Enamel	0.70668	0.00029
21	Enamel	0.70707	0.00083
22	Enamel	0.70679	0.00046
23	Enamel	0.70676	0.00028
24	Enamel	0.70677	0.00039
25	Enamel	0.70743	0.00087
26	Enamel	0.706597	0.000097
27	Enamel	0.70712	0.00055
28	Enamel	0.70741	0.00075
29	Enamel	0.70701	0.00026
30	Enamel	0.70743	0.00065
31	Enamel	0.70717	0.00033
32	Enamel	0.70707	0.00027
33	Enamel	0.70707	0.0002
34	Enamel	0.70722	0.00039
35	Enamel	0.70714	0.00083
36	Enamel	0.70714	0.00055
37	Enamel	0.70697	0.00026
38	Enamel	0.70749	0.00082
39	Enamel	0.70753	0.00046
40	Enamel	0.70807	0.00065
41	Enamel	0.70819	0.00088
42	Enamel	0.70829	0.00078
43	Enamel	0.7078	0.00028
44	Enamel	0.70767	0.00062

45	Enamel	0.70765	0.00023
46	Enamel	0.708	0.00053
47	Enamel	0.70828	0.00034
48	Enamel	0.70827	0.00057
49	Enamel	0.7084	0.00032
50	Enamel	0.70817	0.0003
51	Enamel	0.70868	0.00069
52	Enamel	0.70836	0.00015
53	Enamel	0.70834	0.00044
54	Enamel	0.70832	0.00024
55	Enamel	0.70847	0.0003
56	Enamel	0.70833	0.00047
57	Enamel	0.70855	0.00034
58	Enamel	0.70862	0.0004
59	Enamel	0.70838	0.00021
60	Enamel	0.70874	0.00052
61	Enamel	0.70856	0.00036
62	Enamel	0.70852	0.00049
63	Enamel	0.70882	0.00049
64	Enamel	0.70888	0.0006
65	Enamel	0.7087	0.00025
66	Enamel	0.70895	0.00029
67	Enamel	0.70884	0.00024
68	Enamel	0.70898	0.00024
69	Enamel	0.70926	0.00035
70	Enamel	0.7095	0.00069
71	Enamel	0.70962	0.00015
72	Enamel	0.71015	0.00064
73	Enamel	0.71086	0.00086

74	Enamel	0.71056	0.0006
75	Enamel	0.71014	0.00018
76	Enamel	0.71021	0.0002
77	Enamel	0.71038	0.00033
78	Enamel	0.71048	0.00041
79	Enamel	0.71032	0.00036
80	Enamel	0.70998	0.00036
81	Enamel	0.71028	0.00042
82	Enamel	0.71047	0.00069
83	Enamel	0.71039	0.00021
84	Enamel	0.71067	0.00069

Table A.3. 22: Sample G5N7860 enamel values.

Spot	Material	87Sr/86Sr	87Sr/86Sr error σ^2
1	Dentine	0.7069	0.00022
2	Dentine	0.70744	0.00016
3	Dentine	0.70792	0.00062
4	Dentine	0.70708	0.00042
5	Dentine	0.70716	0.00037
6	Dentine	0.70738	0.00033
7	Dentine	0.70724	0.00016
8	Dentine	0.70789	0.00082
9	Dentine	0.70748	0.00049
10	Dentine	0.70721	0.00016
11	Dentine	0.70723	0.00024
12	Dentine	0.70739	0.00025
13	Dentine	0.70779	0.00066
14	Dentine	0.70747	0.00033
15	Dentine	0.70728	0.00026
16	Dentine	0.70769	0.00066

17	Dentine	0.70762	0.00078
18	Dentine	0.70727	0.00045
19	Dentine	0.70762	0.00065
20	Dentine	0.70693	0.00042
21	Dentine	0.70727	0.00033
22	Dentine	0.70685	0.00034
23	Dentine	0.7075	0.00055
24	Dentine	0.70733	0.00062
25	Dentine	0.70771	0.00081
26	Dentine	0.70767	0.00079
27	Dentine	0.70737	0.00019
28	Dentine	0.70745	0.0005
29	Dentine	0.70732	0.00023
30	Dentine	0.70758	0.0004
31	Dentine	0.70711	0.00024
32	Dentine	0.7073	0.00032
33	Dentine	0.70725	0.00051
34	Dentine	0.70691	0.00023
35	Dentine	0.70738	0.00055
36	Dentine	0.70774	0.00074
37	Dentine	0.70759	0.00047
38	Dentine	0.70712	0.00067
39	Dentine	0.70709	0.00042
40	Dentine	0.70742	0.0004
41	Dentine	0.7081	0.0011
42	Dentine	0.70732	0.00049
43	Dentine	0.70719	0.00029
44	Dentine	0.70687	0.00062
45	Dentine	0.70728	0.00051

46	Dentine	0.70758	0.00073
47	Dentine	0.70796	0.0006
48	Dentine	0.70811	0.00095
49	Dentine	0.7074	0.0014
50	Dentine	0.70665	0.00054
51	Dentine	0.70656	0.00025
52	Dentine	0.70665	0.00016
53	Dentine	0.70686	0.00032
54	Dentine	0.70745	0.00071
55	Dentine	0.70777	0.00057
56	Dentine	0.70758	0.00017
57	Dentine	0.70795	0.00044
58	Dentine	0.70798	0.00026
59	Dentine	0.70778	0.00029
60	Dentine	0.70783	0.00039
61	Dentine	0.70748	0.00017
62	Dentine	0.70708	0.00016
63	Dentine	0.70726	0.00047
64	Dentine	0.70744	0.00053
65	Dentine	0.70752	0.00036
66	Dentine	0.70826	0.00072
67	Dentine	0.70822	0.00012
68	Dentine	0.70871	0.00064
69	Dentine	0.70844	0.00061
70	Dentine	0.70836	0.00062
71	Dentine	0.70813	0.00021
72	Dentine	0.70848	0.00031
73	Dentine	0.70845	0.00028
74	Dentine	0.70864	0.00016

75	Dentine	0.70899	0.00025
76	Dentine	0.70924	0.00062

Table A.3. 23: Sample G5N7860 dentine values.

G4 O7 271

Spot	Material	87Sr/86Sr	87Sr/86Sr error σ^2
1	Enamel	0.71041	0.00014
2	Enamel	0.71049	0.00011
3	Enamel	0.71031	0.00011
4	Enamel	0.70996	0.0003
5	Enamel	0.71026	0.00012
6	Enamel	0.71032	0.00021
7	Enamel	0.710193	0.000092
8	Enamel	0.7102	0.00026
9	Enamel	0.71009	0.00018
10	Enamel	0.71064	0.00023
11	Enamel	0.71096	0.00017
12	Enamel	0.710894	0.000087
13	Enamel	0.710787	0.000083
14	Enamel	0.71068	0.00027
15	Enamel	0.71073	0.00011
16	Enamel	0.71056	0.00012
17	Enamel	0.71064	0.00013
18	Enamel	0.71056	0.000068
19	Enamel	0.71079	0.00016
20	Enamel	0.71107	0.00016
21	Enamel	0.71113	0.00036
22	Enamel	0.710905	0.00005
23	Enamel	0.71068	0.00035
24	Enamel	0.71059	0.00012

25	Enamel	0.71045	0.00024
26	Enamel	0.71052	0.00034
27	Enamel	0.7106	0.00013
28	Enamel	0.71051	0.00018
29	Enamel	0.71078	0.00012
30	Enamel	0.71097	0.00017
31	Enamel	0.71083	0.00048
32	Enamel	0.711003	0.000058
33	Enamel	0.71094	0.00011
34	Enamel	0.71106	0.00011
35	Enamel	0.71098	0.00056
36	Enamel	0.71114	0.00013
37	Enamel	0.7111	0.00031
38	Enamel	0.71119	0.00014
39	Enamel	0.71113	0.00013
40	Enamel	0.71113	0.00016
41	Enamel	0.71105	0.00013
42	Enamel	0.71038	0.00012
43	Enamel	0.71045	0.0001
44	Enamel	0.70995	0.00013
45	Enamel	0.709898	0.000077
46	Enamel	0.71025	0.00011
47	Enamel	0.710654	0.000091

Table A.3. 24: Sample G4 O7 271 enamel values.

Spot	Material	87Sr/86Sr	87Sr/86Sr error σ^2
1	Dentine	0.70909	0.00037
2	Dentine	0.70886	0.00021
3	Dentine	0.7081	0.0011

4	Dentine	0.70842	0.00065
5	Dentine	0.70869	0.00036
6	Dentine	0.7088	0.00015
7	Dentine	0.7088	0.00021
8	Dentine	0.70905	0.00019
9	Dentine	0.70926	0.00036
10	Dentine	0.70937	0.00024
11	Dentine	0.70934	0.00019
12	Dentine	0.70956	0.00013
13	Dentine	0.7096	0.00011
14	Dentine	0.70952	0.00043
15	Dentine	0.70951	0.00016
16	Dentine	0.70901	0.00017
17	Dentine	0.70895	0.00031
18	Dentine	0.70882	0.00014
19	Dentine	0.70877	0.00019
20	Dentine	0.70876	0.00018
21	Dentine	0.70865	0.00017
22	Dentine	0.70886	0.00016
23	Dentine	0.70885	0.00019
24	Dentine	0.70909	0.00022
25	Dentine	0.70917	0.00017
26	Dentine	0.70907	0.00021
27	Dentine	0.70923	0.00011
28	Dentine	0.70936	0.00014
29	Dentine	0.70994	0.00019
30	Dentine	0.710107	0.000095
31	Dentine	0.71048	0.00034
32	Dentine	0.71056	0.00012

33	Dentine	0.71063	0.00013
34	Dentine	0.710546	0.000095
35	Dentine	0.71038	0.00021
36	Dentine	0.71054	0.0002
37	Dentine	0.71017	0.00015
38	Dentine	0.71057	0.0002
39	Dentine	0.71039	0.00011
40	Dentine	0.71007	0.00032
41	Dentine	0.710155	0.000093

Table A.3. 25: Sample G4 O7 271 dentine values.

G4 M6 585

Spot	**Material**	**87Sr/86Sr**	**87Sr/86Sr error σ²**
1	Enamel	0.70809	0.00042
2	Enamel	0.70787	0.00017
3	Enamel	0.707906	9.90E-05
4	Enamel	0.70797	0.00014
5	Enamel	0.70796	0.00048
6	Enamel	0.707894	0.00014
7	Enamel	0.708029	0.00027
8	Enamel	0.707995	0.00021
9	Enamel	0.70798	0.00023
10	Enamel	0.70802	0.00028
11	Enamel	0.70777	0.00022
12	Enamel	0.70768	0.00053
13	Enamel	0.70774	0.00027
14	Enamel	0.70766	0.00054
15	Enamel	0.70761	0.00039

16	Enamel	0.707591	0.00028
17	Enamel	0.70756	0.00023
18	Enamel	0.707537	0.00012
19	Enamel	0.707674	0.00049
20	Enamel	0.707609	0.00018
21	Enamel	0.70758	0.00015
22	Enamel	0.707689	0.00028
23	Enamel	0.7075	0.0002
24	Enamel	0.707465	0.00043
25	Enamel	0.70749	0.00023
26	Enamel	0.707502	0.00055
27	Enamel	0.70745	0.00016
28	Enamel	0.70732	0.00018
29	Enamel	0.70746	0.00013
30	Enamel	0.707406	0.00011
31	Enamel	0.70734	0.00044
32	Enamel	0.70775	0.00014
33	Enamel	0.7079	0.00041
34	Enamel	0.70839	0.00016

Table A.3. 26: Sample G4 M6 585 enamel values.

Spot	Material	87Sr/86Sr	87Sr/86Sr error σ^2
1	Dentine	0.70846	0.00028
2	Dentine	0.70842	0.00023
3	Dentine	0.7083	0.00032
4	Dentine	0.709003	0.0002
5	Dentine	0.70823	0.00022
6	Dentine	0.70828	0.00028
7	Dentine	0.70829	0.0016

8	Dentine	0.70897	0.00027
9	Dentine	0.70937	0.00031
10	Dentine	0.70958	0.00026
11	Dentine	0.70968	0.00019
12	Dentine	0.70939	0.00011
13	Dentine	0.709511	0.00018
14	Dentine	0.70959	0.00033
15	Dentine	0.70957	8.70E-05
16	Dentine	0.70951	0.00024
17	Dentine	0.70957	0.00036
18	Dentine	0.709528	0.00053
19	Dentine	0.70955	0.00023
20	Dentine	0.709468	0.0005
21	Dentine	0.70955	0.00016
22	Dentine	0.70923	0.0002
23	Dentine	0.70938	0.00026
24	Dentine	0.709447	0.00016
25	Dentine	0.709482	0.00021
26	Dentine	0.709328	0.0002
27	Dentine	0.70898	0.00037
28	Dentine	0.708716	0.0002

Table A.3. 27: Sample G4 M6 585 dentine values.

G3 N8 423

Spot	**Material**	**87Sr/86Sr**	**87Sr/86Sr error σ²**
1	Enamel	0.71518	0.0004
2	Enamel	0.71552	0.00066
3	Enamel	0.71543	0.00061
4	Enamel	0.71593	0.00058

5	Enamel	0.71551	0.00053
6	Enamel	0.71578	0.00026
7	Enamel	0.71572	0.00051
8	Enamel	0.71572	0.00026
9	Enamel	0.71575	0.00016
10	Enamel	0.71553	0.00042
11	Enamel	0.71577	0.00038
12	Enamel	0.71553	0.00035
13	Enamel	0.71598	0.00025
14	Enamel	0.71595	0.00042
15	Enamel	0.71617	0.00042
16	Enamel	0.71552	0.00027
17	Enamel	0.71577	0.00038
18	Enamel	0.71577	0.00045
19	Enamel	0.71589	0.0006
20	Enamel	0.71628	0.00043
21	Enamel	0.71639	0.00037
22	Enamel	0.71601	0.00031
23	Enamel	0.71606	0.00024
24	Enamel	0.71628	0.00019
25	Enamel	0.71584	0.00038
26	Enamel	0.71603	0.00038
27	Enamel	0.71647	0.00057
28	Enamel	0.71608	0.00035
29	Enamel	0.71591	0.00051
30	Enamel	0.71612	0.00041
31	Enamel	0.71611	0.0005
32	Enamel	0.71628	0.00027
33	Enamel	0.7162	0.00056

34	Enamel	0.71529	0.00048
35	Enamel	0.71563	0.00042
36	Enamel	0.71574	0.00016
37	Enamel	0.71559	0.00027
38	Enamel	0.71584	0.00039
39	Enamel	0.71583	0.00053
40	Enamel	0.71537	0.0007
41	Enamel	0.71575	0.00061
42	Enamel	0.71567	0.00077
43	Enamel	0.71562	0.00072
44	Enamel	0.71562	0.00069
45	Enamel	0.71601	0.00065
46	Enamel	0.71562	0.00053
47	Enamel	0.71526	0.00029
48	Enamel	0.71552	0.0005
49	Enamel	0.71553	0.00064
50	Enamel	0.71609	0.00045
51	Enamel	0.71551	0.00064
52	Enamel	0.7158	0.00048
53	Enamel	0.71603	0.00047
54	Enamel	0.71634	0.00039
55	Enamel	0.71616	0.00062
56	Enamel	0.71582	0.00061
57	Enamel	0.71615	0.00063
58	Enamel	0.71566	0.00043

Table A.3. 28: Sample G3 N8 423 enamel values.

Spot	**Material**	**87Sr/86Sr**	**87Sr/86Sr error σ²**
1	Dentine	0.71427	0.00049

2	Dentine	0.71491	0.00052
3	Dentine	0.7118	0.0032
4	Dentine	0.71533	0.0007
5	Dentine	0.71511	0.00076
6	Dentine	0.7154	0.001
7	Dentine	0.71437	0.00052
8	Dentine	0.71283	0.00056
9	Dentine	0.7167	0.0056
10	Dentine	0.7117	0.0089
11	Dentine	0.7119	0.0019
12	Dentine	0.7127	0.0035
13	Dentine	0.7112	0.0049
14	Dentine	0.7153	0.0013
15	Dentine	0.7113	0.0035
16	Dentine	0.71536	0.00072
17	Dentine	0.7141	0.0011
18	Dentine	0.7112	0.0039
19	Dentine	0.7069	0.0032
20	Dentine	0.71398	0.0007
21	Dentine	0.7145	0.001
22	Dentine	0.7096	0.0026
23	Dentine	0.7116	0.0066
24	Dentine	0.7118	0.0038
25	Dentine	0.71552	0.00042
26	Dentine	0.71402	0.00046
27	Dentine	0.71393	0.00073
28	Dentine	0.71389	0.00037
29	Dentine	0.7144	0.00036
30	Dentine	0.7132	0.0013

Table A.3. 29: Sample G3 N8 423 dentine values.

G3 N8 420

Spot	Material	87Sr/86Sr	87Sr/86Sr error σ²
1	Enamel	0.71361	0.00017
2	Enamel	0.71358	0.00042
3	Enamel	0.71353	0.00036
4	Enamel	0.71359	0.00039
5	Enamel	0.71363	0.00023
6	Enamel	0.71385	0.0012
7	Enamel	0.7126	0.0003
8	Enamel	0.71319	0.00065
9	Enamel	0.71361	0.00025

Table A.3. 30: Sample G3 N8 420 enamel values.

Spot	Material	87Sr/86Sr	87Sr/86Sr error σ²
1	Dentine	0.71035	0.0004
2	Dentine	0.71038	0.00037
3	Dentine	0.70998	0.00057
4	Dentine	0.70999	0.00044
5	Dentine	0.71006	0.00065
6	Dentine	0.71043	0.00056
7	Dentine	0.71006	0.00033
8	Dentine	0.71005	0.00073
9	Dentine	0.71009	0.00025
10	Dentine	0.71006	0.00048
11	Dentine	0.71026	0.00041
12	Dentine	0.71002	0.00048
13	Dentine	0.71012	0.00082

14	Dentine	0.71018	0.00024
15	Dentine	0.71038	0.00096
16	Dentine	0.71101	0.00025
17	Dentine	0.71108	0.00039
18	Dentine	0.71078	0.00023

Table A.3. 31: Sample G3 N8 420 dentine values.

G2 N9 82

Spot	Material	87Sr/86Sr	87Sr/86Sr error σ²
1	Enamel	0.71456	0.0003
2	Enamel	0.71454	0.00028
3	Enamel	0.71463	0.00034
4	Enamel	0.71435	0.00058
5	Enamel	0.7145	0.00019
6	Enamel	0.71469	0.00027
7	Enamel	0.71466	0.00019
8	Enamel	0.71454	0.00025
9	Enamel	0.71434	0.00052
10	Enamel	0.7144	0.00028
11	Enamel	0.71428	0.00029
12	Enamel	0.71447	0.00025
13	Enamel	0.71442	0.00027
14	Enamel	0.71493	0.00044
15	Enamel	0.71459	0.00019
16	Enamel	0.71436	0.00026
17	Enamel	0.71472	0.00019
18	Enamel	0.71441	0.00074
19	Enamel	0.71494	0.00049
20	Enamel	0.71466	0.00065

21	Enamel	0.71445	0.00023
22	Enamel	0.71411	0.00046
23	Enamel	0.71449	0.00054
24	Enamel	0.71405	0.00059
25	Enamel	0.71381	0.00044
26	Enamel	0.71425	0.00041
27	Enamel	0.71395	0.00035
28	Enamel	0.71418	0.00033
29	Enamel	0.71413	0.0005
30	Enamel	0.71434	0.00024
31	Enamel	0.71435	0.00032
32	Enamel	0.71405	0.00032
33	Enamel	0.71415	0.0002
34	Enamel	0.71415	0.00031
35	Enamel	0.71425	0.00017
36	Enamel	0.71428	0.00015
37	Enamel	0.71427	0.00028
38	Enamel	0.71431	0.0002
39	Enamel	0.71428	0.00022
40	Enamel	0.71418	0.00011
41	Enamel	0.71431	0.00047
42	Enamel	0.71413	0.00027
43	Enamel	0.71423	0.00032
44	Enamel	0.71433	0.00024
45	Enamel	0.7142	0.00022

Table A.3. 32: Sample G2 N9 82 enamel values.

Spot	Material	87Sr/86Sr	87Sr/86Sr error σ^2
1	Dentine	0.71087	0.00014
2	Dentine	0.71102	0.00015

3	Dentine	0.7109	0.00035
4	Dentine	0.71077	0.0002
5	Dentine	0.71067	0.00031
6	Dentine	0.71089	0.00033
7	Dentine	0.71084	0.00026
8	Dentine	0.71062	0.00026
9	Dentine	0.71074	0.0004
10	Dentine	0.71069	0.00054
11	Dentine	0.7103	0.00035
12	Dentine	0.71072	0.00023
13	Dentine	0.7105	0.00029
14	Dentine	0.71087	0.00034
15	Dentine	0.71064	0.00028
16	Dentine	0.71109	0.00023
17	Dentine	0.71082	0.00042
18	Dentine	0.71087	0.00018
19	Dentine	0.71065	0.00017
20	Dentine	0.71068	0.00047
21	Dentine	0.71088	0.0003
22	Dentine	0.71084	0.0003
23	Dentine	0.71108	0.0003
24	Dentine	0.71108	0.00033
25	Dentine	0.71084	0.00025
26	Dentine	0.71086	0.00022
27	Dentine	0.71063	0.00056
28	Dentine	0.71112	0.00045
29	Dentine	0.71057	0.00065
30	Dentine	0.71099	0.00043
31	Dentine	0.71109	0.00038

32	Dentine	0.71153	0.00039
33	Dentine	0.71124	0.00042
34	Dentine	0.7106	0.00044
35	Dentine	0.71096	0.00035
36	Dentine	0.71107	0.00061
37	Dentine	0.71126	0.00051
38	Dentine	0.71104	0.00039
39	Dentine	0.711	0.00022
40	Dentine	0.71117	0.00042
41	Dentine	0.71084	0.00079
42	Dentine	0.71107	0.00025
43	Dentine	0.71092	0.00048
44	Dentine	0.71101	0.00028
45	Dentine	0.71063	0.00028
46	Dentine	0.71089	0.00032
47	Dentine	0.71121	0.00061
48	Dentine	0.71102	0.00021
49	Dentine	0.71097	0.00041

Table A.3. 33: Sample G2 N9 82 dentine values.

F9 L4 791

Spot	Material	87Sr/86Sr	87Sr/86Sr error σ^2
1	Enamel	0.71591	0.00021
2	Enamel	0.71561	0.00016
3	Enamel	0.7157	0.00011
4	Enamel	0.7158	0.00015
5	Enamel	0.71547	0.00022
6	Enamel	0.71538	0.00025
7	Enamel	0.71537	0.00024
8	Enamel	0.71511	0.00039

9	Enamel	0.71544	0.00017
10	Enamel	0.71551	0.00014
11	Enamel	0.71566	0.00014
12	Enamel	0.71536	0.00025
13	Enamel	0.71464	0.00034
14	Enamel	0.71474	0.00037
15	Enamel	0.71488	0.00033
16	Enamel	0.71482	0.00021
17	Enamel	0.71485	0.00061
18	Enamel	0.71512	0.00019
19	Enamel	0.71541	0.00029
20	Enamel	0.71511	0.00022
21	Enamel	0.71528	0.00023
22	Enamel	0.71585	0.00022
23	Enamel	0.71558	0.00027
24	Enamel	0.71588	0.00015
25	Enamel	0.71528	0.00018
26	Enamel	0.71441	0.00023
27	Enamel	0.71508	0.00017
28	Enamel	0.7158	0.00033
29	Enamel	0.71587	0.00022
30	Enamel	0.71581	0.00022
31	Enamel	0.71563	0.00053
32	Enamel	0.7157	0.00026
33	Enamel	0.71584	0.00033
34	Enamel	0.71572	0.00017
35	Enamel	0.71577	0.0002
36	Enamel	0.71577	0.00026
37	Enamel	0.71552	0.00017

Table A.3. 34: Sample F9 L4 791 enamel values.

F7 L4 662

Spot	Material	87Sr/86Sr	87Sr/86Sr error σ^2
1	Enamel	0.70737	0.00035
2	Enamel	0.70679	0.00028
3	Enamel	0.70657	0.00014
4	Enamel	0.7066	0.00011
5	Enamel	0.70653	0.00044
6	Enamel	0.70668	0.00014
7	Enamel	0.70654	0.00023
8	Enamel	0.70657	0.00017
9	Enamel	0.7064	0.00015
10	Enamel	0.70655	0.0002
11	Enamel	0.70645	0.00023
12	Enamel	0.70627	0.00026
13	Enamel	0.70627	0.0001
14	Enamel	0.70631	0.00024
15	Enamel	0.70624	0.00015
16	Enamel	0.70631	0.00042
17	Enamel	0.70641	0.00012
18	Enamel	0.70644	0.00028
19	Enamel	0.70637	0.00016
20	Enamel	0.70629	0.00018
21	Enamel	0.70651	0.00022
22	Enamel	0.70635	0.00024
23	Enamel	0.70637	0.00026
24	Enamel	0.70619	0.00017
25	Enamel	0.70614	0.00024
26	Enamel	0.70644	0.00039

27	Enamel	0.70597	0.00013
28	Enamel	0.70614	0.00027
29	Enamel	0.70614	0.00014
30	Enamel	0.70617	0.00023
31	Enamel	0.70626	0.00018
32	Enamel	0.70619	0.00021
33	Enamel	0.706	0.00032
34	Enamel	0.706	0.00018
35	Enamel	0.70598	0.00036
36	Enamel	0.70575	0.00027
37	Enamel	0.70567	0.00027
38	Enamel	0.7058	0.00019

Table A.3. 35: Sample F7 L4 662 enamel values.

Spot	Material	87Sr/86Sr	87Sr/86Sr error σ^2
1	Dentine	0.70648	0.0005
2	Dentine	0.70629	0.00015
3	Dentine	0.70633	0.00021
4	Dentine	0.70652	0.00018
5	Dentine	0.70611	0.00015
6	Dentine	0.70624	0.00013
7	Dentine	0.706231	0.000099
8	Dentine	0.70628	0.00011
9	Dentine	0.70634	0.00014
10	Dentine	0.70614	0.00015
11	Dentine	0.70618	0.0002
12	Dentine	0.70602	0.00013
13	Dentine	0.70601	0.0004
14	Dentine	0.70606	0.0001
15	Dentine	0.70617	0.00017

16	Dentine	0.70615	0.00013
17	Dentine	0.70626	0.00032
18	Dentine	0.70608	0.00013
19	Dentine	0.70626	0.00017
20	Dentine	0.70626	0.00011
21	Dentine	0.70639	0.00012
22	Dentine	0.70629	0.00013
23	Dentine	0.70634	0.00014
24	Dentine	0.706308	0.000091
25	Dentine	0.70625	0.0001
26	Dentine	0.70641	0.00018
27	Dentine	0.70642	0.00016
28	Dentine	0.70661	0.00011
29	Dentine	0.70644	0.00021
30	Dentine	0.706504	0.00005
31	Dentine	0.70629	0.00014
32	Dentine	0.70656	0.00012
33	Dentine	0.70677	0.00033
34	Dentine	0.70668	0.00014
35	Dentine	0.70662	0.00015
36	Dentine	0.706574	0.000095
37	Dentine	0.70639	0.00011
38	Dentine	0.70632	0.00014
39	Dentine	0.70624	0.00013
40	Dentine	0.70612	0.00015
41	Dentine	0.70614	0.00041

Table A.3. 36: Sample F7 L4 662 dentine values.

F6 L5 729

Spot	Material	87Sr/86Sr	87Sr/86Sr error σ²

1	Enamel	0.71084	0.00059
2	Enamel	0.7108	0.00049
3	Enamel	0.71059	0.00033
4	Enamel	0.71068	0.0014
5	Enamel	0.71089	0.00065
6	Enamel	0.71087	0.00028
7	Enamel	0.71083	0.00062
8	Enamel	0.71069	0.00023
9	Enamel	0.711	0.0008
10	Enamel	0.71107	0.00023
11	Enamel	0.71103	0.00061
12	Enamel	0.71111	0.00024
13	Enamel	0.71074	0.00055
14	Enamel	0.71074	0.00023
15	Enamel	0.71066	0.0003
16	Enamel	0.71059	0.00031
17	Enamel	0.71084	0.0008
18	Enamel	0.71051	0.00032
19	Enamel	0.71054	0.00084
20	Enamel	0.710583	0.00032
21	Enamel	0.71044	0.00042
22	Enamel	0.710594	0.0002
23	Enamel	0.71058	0.00044
24	Enamel	0.71084	0.00032
25	Enamel	0.71073	0.00032
26	Enamel	0.71097	0.00036
27	Enamel	0.71084	0.00018
28	Enamel	0.71078	0.00064

Table A.3. 37: Sample F6 L5 729 enamel values.

Spot	Material	87Sr/86Sr	87Sr/86Sr error σ²
1	Dentine	0.70851	0.0003
2	Dentine	0.708547	0.00014
3	Dentine	0.70843	0.00027
4	Dentine	0.708412	0.00034
5	Dentine	0.708409	0.00013
6	Dentine	0.708478	0.00033
7	Dentine	0.708473	9.70E-05
8	Dentine	0.708492	0.00037
9	Dentine	0.708507	0.00014
10	Dentine	0.708483	0.00031
11	Dentine	0.708418	0.00012
12	Dentine	0.708446	0.0002
13	Dentine	0.708476	0.00022
14	Dentine	0.708427	0.00011

Table A.3. 38: Sample F6 L5 729 dentine values.

F1 N4 2

Spot	Material	87Sr/86Sr	87Sr/86Sr error σ²
1	Enamel	0.70811	0.00017
2	Enamel	0.7083	0.0002
3	Enamel	0.70815	0.00021
4	Enamel	0.70807	0.00048
5	Enamel	0.70821	0.00017
6	Enamel	0.70826	0.00037
7	Enamel	0.7082	0.0002
8	Enamel	0.70815	0.0002
9	Enamel	0.70811	0.00057
10	Enamel	0.70831	0.00036
11	Enamel	0.70811	0.00026

12	Enamel	0.70798	0.00022
13	Enamel	0.70828	0.0004
14	Enamel	0.70819	0.00048
15	Enamel	0.70795	0.00019
16	Enamel	0.70802	0.00038
17	Enamel	0.70799	0.00024
18	Enamel	0.70802	0.00024
19	Enamel	0.70827	0.0003
20	Enamel	0.70839	0.00043
21	Enamel	0.70823	0.00022
22	Enamel	0.70821	0.00023
23	Enamel	0.70813	0.00058
24	Enamel	0.70838	0.00036
25	Enamel	0.70829	0.00038
26	Enamel	0.70821	0.00019
27	Enamel	0.7082	0.00032
28	Enamel	0.70841	0.00034
29	Enamel	0.70807	0.0003
30	Enamel	0.70834	0.00026
31	Enamel	0.70834	0.00052
32	Enamel	0.70785	0.00066
33	Enamel	0.70823	0.00051
34	Enamel	0.70864	0.00097
35	Enamel	0.70823	0.00062
36	Enamel	0.70823	0.00045
37	Enamel	0.70794	0.0003
38	Enamel	0.70839	0.00053
39	Enamel	0.70803	0.00024
40	Enamel	0.70817	0.00018

41	Enamel	0.70802	0.00022
42	Enamel	0.70842	0.00053
43	Enamel	0.70808	0.00027
44	Enamel	0.70814	0.00059
45	Enamel	0.70821	0.00021
46	Enamel	0.7081	0.00036
47	Enamel	0.70813	0.00039
48	Enamel	0.70806	0.00056
49	Enamel	0.70837	0.00028
50	Enamel	0.70794	0.00023
51	Enamel	0.70814	0.00055
52	Enamel	0.70816	0.00057
53	Enamel	0.70825	0.00094
54	Enamel	0.70788	0.00014
55	Enamel	0.70821	0.0002
56	Enamel	0.70771	0.00023
57	Enamel	0.7078	0.00037
58	Enamel	0.70816	0.00026
59	Enamel	0.70811	0.00038
60	Enamel	0.70848	0.00062
61	Enamel	0.70807	0.00022
62	Enamel	0.70831	0.00029
63	Enamel	0.70809	0.00022
64	Enamel	0.70801	0.00017
65	Enamel	0.70805	0.00019
66	Enamel	0.70808	0.00026
67	Enamel	0.70826	0.0004
68	Enamel	0.70815	0.00027
69	Enamel	0.7081	0.00017

70	Enamel	0.70791	0.00015
71	Enamel	0.70796	0.00023
72	Enamel	0.70815	0.00031
73	Enamel	0.70788	0.00027
74	Enamel	0.70819	0.00048
75	Enamel	0.70795	0.00027
76	Enamel	0.70801	0.0002
77	Enamel	0.708	0.00023
78	Enamel	0.7081	0.00065
79	Enamel	0.70799	0.00032
80	Enamel	0.70843	0.00063

Table A.3. 39: Sample F1 N4 2 enamel values.

Spot	**Material**	**87Sr/86Sr**	**87Sr/86Sr error σ²**
1	Dentine	0.7087	0.00035
2	Dentine	0.70851	0.00022
3	Dentine	0.7086	0.00032
4	Dentine	0.70834	0.00059
5	Dentine	0.70862	0.00041
6	Dentine	0.70853	0.0004
7	Dentine	0.70839	0.00023
8	Dentine	0.70843	0.00037
9	Dentine	0.7087	0.00016
10	Dentine	0.70855	0.00062
11	Dentine	0.70852	0.00018
12	Dentine	0.7085	0.00034
13	Dentine	0.70839	0.00026
14	Dentine	0.70849	0.0003
15	Dentine	0.70842	0.00021
16	Dentine	0.7083	0.00013

17	Dentine	0.7086	0.00044
18	Dentine	0.70861	0.00081
19	Dentine	0.70837	0.00028
20	Dentine	0.70815	0.0002
21	Dentine	0.70811	0.00056
22	Dentine	0.70777	0.00029
23	Dentine	0.70786	0.00018
24	Dentine	0.70761	0.00019
25	Dentine	0.70767	0.0006
26	Dentine	0.70772	0.00019
27	Dentine	0.70747	0.00036
28	Dentine	0.70757	0.00016
29	Dentine	0.70745	0.00026
30	Dentine	0.70764	0.00014
31	Dentine	0.70762	0.00038
32	Dentine	0.70786	0.00023
33	Dentine	0.70802	0.00035
34	Dentine	0.70786	0.00021
35	Dentine	0.70796	0.00022
36	Dentine	0.70766	0.0002
37	Dentine	0.70816	0.00017
38	Dentine	0.70855	0.00034
39	Dentine	0.70841	0.00018
40	Dentine	0.70834	0.00053
41	Dentine	0.7084	0.00026
42	Dentine	0.70825	0.00014
43	Dentine	0.70828	0.00034
44	Dentine	0.70827	0.00023
45	Dentine	0.70853	0.00046

46	Dentine	0.708451	8.80E-05
47	Dentine	0.70879	0.00057
48	Dentine	0.70839	0.00018
49	Dentine	0.70842	0.00016
50	Dentine	0.70844	0.00016
51	Dentine	0.70874	0.00024
52	Dentine	0.70846	0.00021
53	Dentine	0.70853	0.00016
54	Dentine	0.70857	0.00021
55	Dentine	0.70844	0.00019
56	Dentine	0.70849	0.00021
57	Dentine	0.70836	0.00022
58	Dentine	0.7089	0.001
59	Dentine	0.70848	0.00027
60	Dentine	0.70864	0.00052
61	Dentine	0.70887	0.00046
62	Dentine	0.70843	0.00026
63	Dentine	0.70855	0.00025
64	Dentine	0.7085	0.00019
65	Dentine	0.70842	0.00023
66	Dentine	0.70823	0.00027

Table A.3. 40: Sample F1 N4 2 dentine values.

F N8 141

Spot	Material	87Sr/86Sr	87Sr/86Sr error σ²
1	Enamel	0.7094	0.00034
2	Enamel	0.7097	0.00031
3	Enamel	0.70953	0.00039
4	Enamel	0.7095	0.00028
5	Enamel	0.70932	0.00078

6	Enamel	0.70956	0.00029
7	Enamel	0.70936	0.00044
8	Enamel	0.70928	0.00085
9	Enamel	0.71012	0.00054
10	Enamel	0.7096	0.00046
11	Enamel	0.70962	0.00069
12	Enamel	0.70964	0.0002
13	Enamel	0.70982	0.0005
14	Enamel	0.70922	0.00061
15	Enamel	0.71017	0.00045
16	Enamel	0.71016	0.00055
17	Enamel	0.70941	0.00042
18	Enamel	0.70961	0.00045
19	Enamel	0.70971	0.00037
20	Enamel	0.70987	0.00031
21	Enamel	0.70954	0.00062
22	Enamel	0.70983	0.00082
23	Enamel	0.70941	0.00092
24	Enamel	0.70916	0.00062
25	Enamel	0.70944	0.00036
26	Enamel	0.70969	0.00024
27	Enamel	0.7096	0.00026
28	Enamel	0.70957	0.00037
29	Enamel	0.71005	0.00062
30	Enamel	0.70934	0.00041
31	Enamel	0.70926	0.00043
32	Enamel	0.70969	0.00061
33	Enamel	0.70951	0.00051
34	Enamel	0.70958	0.00056

35	Enamel	0.70972	0.00048
36	Enamel	0.70905	0.00046
37	Enamel	0.70918	0.00031
38	Enamel	0.70942	0.00048
39	Enamel	0.70944	0.00029
40	Enamel	0.70955	0.00026
41	Enamel	0.70978	0.00017
42	Enamel	0.70952	0.00027
43	Enamel	0.70968	0.00029
44	Enamel	0.70954	0.00022
45	Enamel	0.70949	0.00046
46	Enamel	0.70936	0.00022
47	Enamel	0.70946	0.00025
48	Enamel	0.70961	0.00023
49	Enamel	0.70943	0.00021
50	Enamel	0.70944	0.00037
51	Enamel	0.70959	0.00018
52	Enamel	0.70977	0.00027
53	Enamel	0.70962	0.00016
54	Enamel	0.70952	0.00035
55	Enamel	0.7095	0.00032
56	Enamel	0.70986	0.00042
57	Enamel	0.70984	0.00027
58	Enamel	0.70953	0.00015
59	Enamel	0.70965	0.00044
60	Enamel	0.70959	0.00044
61	Enamel	0.70953	0.00038
62	Enamel	0.70959	0.00031
63	Enamel	0.70939	0.0002

64	Enamel	0.70987	0.00049
65	Enamel	0.70977	0.00043
66	Enamel	0.70942	0.00038
67	Enamel	0.70964	0.00018
68	Enamel	0.70946	0.0003
69	Enamel	0.70951	0.00035
70	Enamel	0.70938	0.0004
71	Enamel	0.70976	0.00034
72	Enamel	0.70958	0.00085
73	Enamel	0.70942	0.00071
74	Enamel	0.7092	0.00035
75	Enamel	0.71001	0.00052
76	Enamel	0.70968	0.00024
77	Enamel	0.70948	0.00023
78	Enamel	0.70917	0.00017

Table A.3. 41: Sample F N8 141 enamel values.

Spot	Material	87Sr/86Sr	87Sr/86Sr error σ^2
1	Dentine	0.709	0.0002
2	Dentine	0.70884	0.00057
3	Dentine	0.70908	0.00019
4	Dentine	0.70884	0.00019
5	Dentine	0.70865	0.00036
6	Dentine	0.70888	0.00019
7	Dentine	0.70903	0.00073
8	Dentine	0.70901	0.00035
9	Dentine	0.70878	0.00024
10	Dentine	0.70944	0.00082
11	Dentine	0.70882	0.00026
12	Dentine	0.70955	0.00075

13	Dentine	0.70885	0.00021
14	Dentine	0.70874	0.00023
15	Dentine	0.70876	0.00031
16	Dentine	0.70878	0.00018
17	Dentine	0.70912	0.00025
18	Dentine	0.70908	0.00044
19	Dentine	0.7089	0.00021
20	Dentine	0.70882	0.00016

Table A.3. 42: Sample F N8 141 dentine values.

D M1 Lower (t1)

Spot	Material	87Sr/86Sr	87Sr/86Sr error σ^2
1	Enamel	0.70823	0.00034
2	Enamel	0.70823	0.00017
3	Enamel	0.708209	6.20E-05
4	Enamel	0.70811	0.00035
5	Enamel	0.708	0.0005
6	Enamel	0.70828	0.00019
7	Enamel	0.70835	0.00024
8	Enamel	0.70842	0.00021
9	Enamel	0.70843	0.00021
10	Enamel	0.70872	0.00019
11	Enamel	0.70869	0.00026
12	Enamel	0.70827	0.00038
13	Enamel	0.70841	0.00035
14	Enamel	0.70841	0.00019
15	Enamel	0.70876	0.0008
16	Enamel	0.70782	0.00085
17	Enamel	0.70809	0.00048
18	Enamel	0.70835	0.00042

19	Enamel	0.70802	0.00036
20	Enamel	0.70766	0.00026
21	Enamel	0.70756	0.00026
22	Enamel	0.70827	0.00031
23	Enamel	0.7072	0.0014
24	Enamel	0.7075	0.0048
25	Enamel	0.70716	0.00025
26	Enamel	0.7072	0.0011
27	Enamel	0.70727	0.00034
28	Enamel	0.70731	0.00019
29	Enamel	0.70707	0.00016
30	Enamel	0.70786	0.00076
31	Enamel	0.71016	0.00018
32	Enamel	0.7088	0.00022
33	Enamel	0.70881	0.00028
34	Enamel	0.70855	0.00016
35	Enamel	0.70832	0.00016
36	Enamel	0.70789	0.00014
37	Enamel	0.70894	0.00018
38	Enamel	0.70951	0.00038

Table A.3. 43: Sample D M1 Lower (t1) enamel values.

Spot	**Material**	**87Sr/86Sr**	**87Sr/86Sr error σ^2**
1	Dentine	0.70876	0.00024
2	Dentine	0.70908	0.00014
3	Dentine	0.70938	0.00028
4	Dentine	0.7091	0.00044
5	Dentine	0.70875	0.00015
6	Dentine	0.70876	0.00035
7	Dentine	0.70899	0.00023

8	Dentine	0.70908	0.00026
9	Dentine	0.70938	0.00013
10	Dentine	0.70943	0.00033
11	Dentine	0.70902	0.00035
12	Dentine	0.70945	0.00017
13	Dentine	0.70896	0.00055
14	Dentine	0.70895	0.00018
15	Dentine	0.70942	0.00032
16	Dentine	0.70952	0.00014
17	Dentine	0.70938	0.00031
18	Dentine	0.70949	0.00017
19	Dentine	0.70914	0.00023
20	Dentine	0.70897	0.00041
21	Dentine	0.70904	0.00018
22	Dentine	0.70964	0.00018
23	Dentine	0.70954	0.00018
24	Dentine	0.70955	0.00032
25	Dentine	0.70972	0.00017
26	Dentine	0.70968	0.00029
27	Dentine	0.7097	0.00024
28	Dentine	0.70938	0.00024
29	Dentine	0.70922	0.00016
30	Dentine	0.70933	0.0002
31	Dentine	0.70961	0.00018
32	Dentine	0.70955	0.00015
33	Dentine	0.70948	0.0005
34	Dentine	0.70995	0.00026
35	Dentine	0.7096	0.00016
36	Dentine	0.70869	0.00028

37	Dentine	0.70892	0.00018
38	Dentine	0.70921	0.00016

Table A.3. 44: Sample D M1 Lower (t1) dentine values.

D M1 Lower (t2)

Spot	Material	87Sr/86Sr	87Sr/86Sr error σ²
1	Enamel	0.70957	0.0011
2	Enamel	0.70942	0.00035
3	Enamel	0.70939	0.00012
4	Enamel	0.70936	0.00065
5	Enamel	0.709309	0.00026
6	Enamel	0.7093	0.00045
7	Enamel	0.70933	0.00033
8	Enamel	0.70919	0.00069
9	Enamel	0.70925	0.00023
10	Enamel	0.70937	0.00053
11	Enamel	0.709284	0.00026
12	Enamel	0.70924	0.00024
13	Enamel	0.70942	0.00034
14	Enamel	0.709361	0.00018
15	Enamel	0.709253	0.00074
16	Enamel	0.70925	0.00014
17	Enamel	0.70931	0.00074
18	Enamel	0.7093	0.00022
19	Enamel	0.70928	0.00018
20	Enamel	0.709235	0.00032
21	Enamel	0.70936	0.00016
22	Enamel	0.70918	0.00068
23	Enamel	0.7093	0.00043
24	Enamel	0.70913	0.00081

25	Enamel	0.70923	0.00031
26	Enamel	0.70927	0.00055
27	Enamel	0.7091	0.00022
28	Enamel	0.70906	0.00055
29	Enamel	0.709076	0.0002
30	Enamel	0.7091	0.00029
31	Enamel	0.70914	0.00029
32	Enamel	0.708987	0.0004
33	Enamel	0.70906	0.00033
34	Enamel	0.708953	0.00016
35	Enamel	0.70891	0.00055
36	Enamel	0.708839	0.00014
37	Enamel	0.708924	0.00021
38	Enamel	0.708969	0.00012
39	Enamel	0.70914	0.00052
40	Enamel	0.7091	0.00019
41	Enamel	0.709107	0.00033
42	Enamel	0.709135	0.00018
43	Enamel	0.70916	0.0003
44	Enamel	0.709075	0.00017
45	Enamel	0.709103	0.00013
46	Enamel	0.70918	0.00029
47	Enamel	0.70914	0.00014
48	Enamel	0.709187	0.00065
49	Enamel	0.709128	0.00014
50	Enamel	0.709172	0.00037
51	Enamel	0.709139	0.00014
52	Enamel	0.709161	0.00016
53	Enamel	0.70919	0.00024

54	Enamel	0.709233	9.80E-05

Table A.3. 45: Sample D M1 Lower (t2) enamel values.